HAMILTONIAN SHOCKS AND OTHER SINGULAR FRONTS IN HYPERBOLIC SYSTEMS OF CONSERVATION LAWS

Russell Arnold

A dissertation submitted to the faculty at the University of North Carolina at Chapel Hill in partial fulfillment of the requirements for the degree of Doctor of Philosophy in the Department of Mathematics in the College of Arts and Sciences.

Chapel Hill
2023

Approved by:

Roberto Camassa

Rich McLaughlin

Alberto Scotti

Jeremy Marzuola

Katie Newhall

ABSTRACT

Russell Arnold: Hamiltonian Shocks and Other Singular Fronts in
Hyperbolic Systems of Conservation Laws
(Under the direction of Roberto Camassa)

The nature of wave interaction in a continuum dynamical model may undergo a qualitative change in certain asymptotic regimes, most notably when linearity or complete integrability is introduced. This occurs in particular when the mKdV equation is used to model the unidirectional dispersive dynamics of two layer shallow water fluid flow near a critical interfacial height. Motivated by the symmetric properties of conjugate states which have been observed for the MCC equations in the Boussinesq limit, this work elucidates a more subtle qualitative shift, residing purely in the dispersionless reduction of a 2×2 system, which determines whether a Hamiltonian undercompressive shock, representing a profile connecting two conjugate states, may interact with a continuous background wave without producing a loss of regularity, which would take the form of a classical dispersive shock. The resulting criterion is also related to an infinitude of conservation laws, drawing a further parallel to the integrable case.

Then, motivated by the study of shallow water fluid flow, criteria are derived for the splitting of corner points in the initial conditions of a solution to a one dimensional quasilinear hyperbolic system of conservation laws. To this end, a distributional approach to moving singularities is elaborated. Then the class of systems admitting solutions with persisting infinite derivatives is shown to coincide with the class for which genuine nonlinearity does not hold uniformly and fails at such singular points in particular. In both cases the application to problems in fluid flow is demonstrated in the context of explicit solutions.

ACKNOWLEDGEMENTS

TABLE OF CONTENTS

LIST OF FIGURES

CHAPTER 1

Overview

This thesis presents new results in the theory of singular wave fronts for hyperbolic systems of conservation laws and applications to stratified fluid flow. In this context, studying the "morphology and evolution" [1] of nonlinear internal waves, including their interactions is an important step towards understanding flow properties in the ocean [2, 3] which affect marine wild life habitats [4], for example.

Traveling fronts of fixed form occur in the MCC model of strongly nonlinear dispersive two layer stratified fluid flow, corresponding to the large width limit of flat solitary waves [5, 6, 7]. In this context, as well as in the context of diffuse interfaces in liquid vapor mixtures, it has been pointed out that these fronts in dispersively perturbed systems can be viewed as undercompressive shocks [8, 9] (this connection has also been made in the theory of undercompressive shocks arising from perturbations where dispersion and diffusion enter at the same scale [10]). Chapter 2 of this thesis introduces a new general and systematic approach for understanding these shocks in the Hamiltonian setting. In particular, the realization that the kinetic condition for these *Hamiltonian shocks* simply amounts to a larger than usual set of Rankine-Hugoniot relations is used to place their study in a self contained hyperbolic theory. The set of solutions considered to be 'regular' is enlarged to include these shocks, expanding the scope of energy conserving wave dynamics that can be understood hyperbolically, without recourse to Whitham modulation [11, 12]. The elementary algebraic tools of classical hyperbolic theory are then leveraged to draw a connection between the existence of an infinitude of independent Hamiltonian shock-conserved quantities and regular wave interactions, i.e., interactions that do not lead to strong oscillations (classical dispersive shock formation). We emphasize that, strictly speaking, the results of chapter 2 only pertain to discontinuous solutions of hyperbolic systems and that to make the connection with the theory of dispersively perturbed systems rigorous would be far beyond the scope of this thesis.

The subject of chapter 3 is continuous but non-smooth solutions of hyperbolic systems of

1

conservation laws. Discontinuous derivatives provide geometric markers tracking the evolution of wavefronts between two distinct smooth profiles which meet continuously (but not smoothly). In [13], an asymptotic approach is provided to study the case where one profile represents a quiescent (flat) state and generalization to the non-quescient case is indicated. However, in the investigation self similar solutions to the Airy shallow water system connected to a constant background as a model for wetting of dry points [14, 15], explicit computations called attention to the splitting of corner points for which the approach provided in [13] is not applicable. The computation of corner position is accomplished in [16] using a distributional ansatz.

In chapter 3, the use of distributional ansatz to study corners is placed in a formal and general context. From this, criteria for the splitting of corners (discontinuous derivative points) are found, providing a qualified confirmation of a conjecture in [16]. Then, motivated again by phenomena observed in the splicing of explicit self similar solutions to shallow water fluid flow, this time in the case of two density stratified layers, the formal study of non-smooth continuous solutions concludes with a proof that persistence of a vertical gradient may occur if and only if the system fails to be genuinely nonlinear at some point.

In both chapters, the theoretical developments are complemented by revisitations of the physical systems which motivated the study, with new tools in hand. Motivated in turn by the possession of these theoretical tools, new explicit solutions are explored and new wave interaction scenarios formulated for numerical simulations.

The numerical simulations of dispersive systems were carried out by Lingyun Ding and the theoretical results of chapter 2 were developed in collaboration with Roberto Camassa, and those of chapter 3 with Roberto Camassa, Gregorio Falqui, Giovanni Ortenzi and Marco Pedroni.

Hamiltonian shocks

2.1 Introduction

In this chapter, motivated by systems in dispersive hydrodynamics admitting heteroclynic connections, known as conjugate state or kink solutions ([7, 17, 18, 19, 20, 21, 8, 22, 6], see also below), we study a class of undercompressive shocks (see e.g. [23, 24, 10, 25]) satisfying an excess of Rankine-Hugoniot conditions, including energy. Specifically, we consider a special class of shocks (see Appendix A for the definition of shocks) for the *hyperbolic quasilinear Hamiltonian system*

$$\boldsymbol{U}_t + (B\nabla H(\boldsymbol{U}))_x = 0, \tag{2.1}$$

where $\boldsymbol{U} = (u^1, u^2, ..., u^n)^T$, B is a constant, symmetric and non-singular matrix, H is convex and hyperbolicity requires that the eigenvalues of $B\nabla^2 H(\boldsymbol{U})$ are real and distinct:

$$\lambda_1 < \lambda_2 < ... < \lambda_n. \tag{2.2}$$

Because B is constant, such a Hamiltonian structure belongs to the class referred to as "canonical" or "in flat coordinates" in the Russian literature (see e.g. [26]). For $n = 1$ we will use the short hand $u^1 = u$, and for $n = 2$ we shall write $u^1 = u$ and $u^2 = v$.

The class of shocks which we study satisfy, in addition to the standard Rankine-Hugoniot conditions

$$-s[\boldsymbol{U}] + [B\nabla H(\boldsymbol{U})] = 0, \tag{2.3}$$

a further jump condition for the Hamiltonian density

$$-s[H] + [\frac{1}{2}\nabla H^T B\nabla H] = 0 \tag{2.4}$$

corresponding to the conservation law

$$H_t + (\frac{1}{2}\nabla H(\boldsymbol{U})^T B \nabla H(\boldsymbol{U}))_x = 0 \tag{2.5}$$

which is implied by (2.1) for strong solutions. Here square brackets denote jumps across a discontinuity

$$[\boldsymbol{U}] = \boldsymbol{U}_r - \boldsymbol{U}_l, \tag{2.6}$$

where $\boldsymbol{U}_l$ and $\boldsymbol{U}_r$ are the left and right limits of $\boldsymbol{U}$ at a jump discontinuity and s is the shock speed.

We recall [10] that undercompressive shocks may occur in a hyperbolic system when certain singularities occur that interrupt the Lax shock construction [27], in particular, when the condition

$$\nabla \lambda_k(\boldsymbol{U}) \cdot \boldsymbol{r}_k \neq 0, \tag{2.7}$$

known as genuine nonlinearity, fails non-uniformly, where r_k is the right eigenvector corresponding to λ_k. We shall refer to this manifold, the locus of

$$\nabla \lambda_k(\boldsymbol{U}) \cdot \boldsymbol{r}_k = 0, \tag{2.8}$$

as the NGNL manifold. Undercompressive shocks are exceptional in that they are impinged upon by exactly n characteristics while Lax shocks are impinged upon by $n+1$ characteristics [27, 28] as illustrated in figure 2.1 for $n=2$ (see appendix A for a review of basic definitions and constructions in hyperbolic systems of conservation laws). Thus the $2n$ variables $\boldsymbol{U}_l = (u_l^1, u_l^2, ..., u_l^n)^T$ and $\boldsymbol{U}_r = (u_r^1, u_r^2, ..., u_r^n)^T$ may be subjected to n further constraints for the undercompressive case in contrast to Lax shocks for which only $n-1$ constraints remain to be dictated by the Rankine-Hugoniot conditions (2.3)(note: one constraint is eliminated by solving for s). Thus for undercompressive shocks in the Hamiltonian system (2.1) an additional shock conservation law, i.e., Rankine-Hugoniot condition, may be imposed. We recall that in the non-Hamiltonian case, a "kinetic condition" which does not represent a Rankine-Hugoniot condition can be formulated to fully constrain an undercompressive shock (see e.g. [24, 10]).

As alluded to above, the study of Hamiltonian shocks is motivated by certain wave behaviors in

4
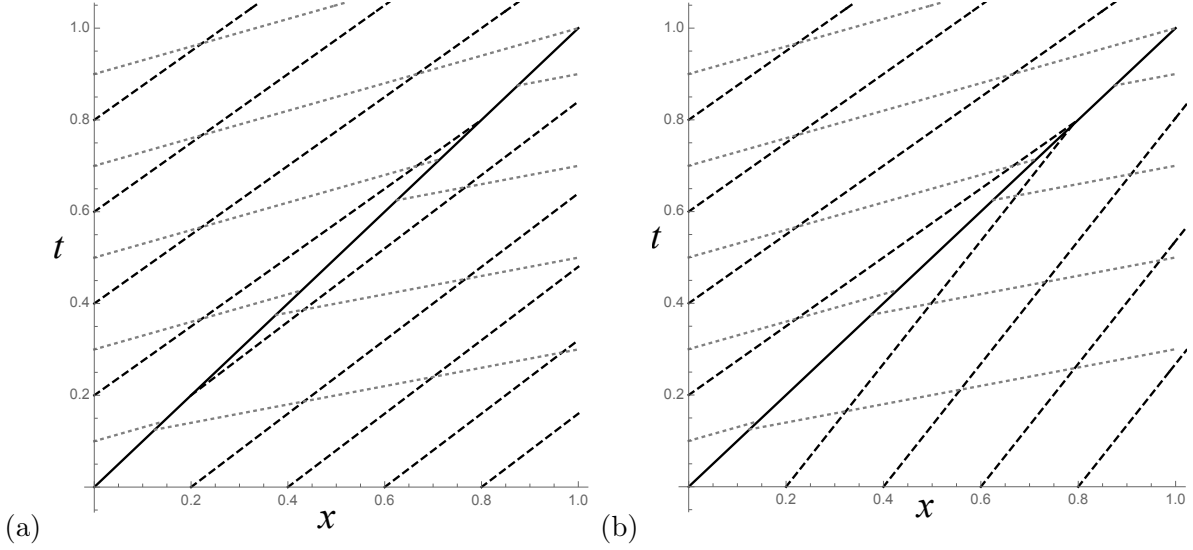
Figure 2.1: Characteristic diagrams are shown for (a) an undercompressive shock and (b) a lax shock when $n = 2$. In the former case a total of n characteristic families impinge upon the shock while for the latter case $n + 1 = 3$ impingements occur. The dashed lines represent characteristics of the 1-family while the dotted lines represent those of the 2-family.

a dispersive system which may be expressed as a Hamiltonian perturbation of a hyperbolic system.

Following [29], we define a *Hamiltonian perturbation* of the hyperbolic system (2.1) to be the system

$$\boldsymbol{U}_t^\epsilon + B\delta H^\epsilon[\boldsymbol{U}^\epsilon]_x = 0, \qquad \epsilon \geq 0, \tag{2.9}$$

where δ denotes the variational gradient,

$$H^\epsilon[\boldsymbol{U}] = \mathcal{H}(\boldsymbol{U}, \epsilon\boldsymbol{U}_x, \epsilon^2\boldsymbol{U}_{xx}, \epsilon^3\boldsymbol{U}_{xxx}, ...) \tag{2.10}$$

and

$$\mathcal{H}(\boldsymbol{U}, 0, 0, 0, ...) = H(U). \tag{2.11}$$

The perturbed system (2.9) also satisfies conservation of energy:

$$H^\epsilon[\boldsymbol{U}^\epsilon]_t + F^\epsilon[\boldsymbol{U}^\epsilon]_x = 0 \tag{2.12}$$

where

$$F^\epsilon[\boldsymbol{U}] = \mathcal{F}(\boldsymbol{U}, \epsilon\boldsymbol{U}_x, \epsilon^2\boldsymbol{U}_{xx}, \epsilon^3\boldsymbol{U}_{xxx}, ...) \tag{2.13}$$

and

$$\mathcal{F}(\boldsymbol{U},0) = \frac{1}{2}\nabla H(\boldsymbol{U})^T B \nabla H(\boldsymbol{U}). \tag{2.14}$$

The system (2.9) is homogeneous in ϵ in the sense that $\boldsymbol{U}^\epsilon$ satisfies (2.9) if and only if

$$\boldsymbol{U}^\epsilon(x,t) = \boldsymbol{U}^1(x/\epsilon, t/\epsilon) \tag{2.15}$$

for some $\boldsymbol{U}^1$ which solves (2.9) with $\epsilon = 1$, when $\epsilon > 0$.

We recall that a *kink* is a traveling wave solution of (2.9):

$$\boldsymbol{U}^\epsilon(x,t) = \boldsymbol{V}^\epsilon(x - st) = \boldsymbol{V}^1\left(\frac{x - st}{\epsilon}\right), \tag{2.16}$$

for which

$$\lim_{\xi \to -\infty} \boldsymbol{V}^1(\xi) = \boldsymbol{U}_l \tag{2.17}$$

and

$$\lim_{\xi \to \infty} \boldsymbol{V}^1(\xi) = \boldsymbol{U}_r. \tag{2.18}$$

Integrating (2.9) and (2.12) shows that the left and right states $\boldsymbol{U}_l$, $\boldsymbol{U}_r$ and the propagation speed s satisfy the Hamiltonian shock conditions (2.3) and (2.4):

$$0 = \int_{-\infty}^{\infty} \frac{\partial}{\partial t}\boldsymbol{V}^1(x - st) + \frac{\partial}{\partial x}B\delta H^1[\boldsymbol{V}^1(x - st)]dx \tag{2.19}$$

$$= \int_{-\infty}^{\infty} \frac{d}{d\xi}\left(-s\boldsymbol{V}^1(\xi) + B\delta H^1[\boldsymbol{V}^1(\xi)]\right) d\xi \tag{2.20}$$

$$= -s[\boldsymbol{U}] + [B\nabla H(\boldsymbol{U})] \tag{2.21}$$

and similarly

$$0 = \int_{-\infty}^{\infty} \frac{\partial}{\partial t}H^1[\boldsymbol{V}^1(x - st)] + \frac{\partial}{\partial x}F^1[\boldsymbol{V}^1(x - st)]dx \tag{2.22}$$

$$= \int_{-\infty}^{\infty} \frac{d}{d\xi}\left(-sH^1[\boldsymbol{V}^1(\xi)] + F^1[\boldsymbol{V}^1(\xi)]\right) d\xi \tag{2.23}$$

$$= -s[H] + [\frac{1}{2}\nabla H^T B \nabla H]. \tag{2.24}$$

6

Thus a Hamiltonian shocks is reached in the $\epsilon \to 0$ limit.

In keeping with a common paradigm in the theory of shocks and perturbed systems (e.g. [30, 31, 25, 10, 24]) we may (non-rigorously) view solutions containing Hamiltonian shocks as arising from a matching problem where traveling wave dynamics dominate in a strip of thickness proportional to ϵ which must be fitted into a solution outside of the strip, approximating to a continuous solution of (2.1) as $\epsilon \to 0$. In the dispersive case however, periodic traveling waves are typical and lead to a strip with width independent of ϵ, and growing in time, known as a classical dispersive shock wherein traveling wave dynamics dominate (see e.g. [12, 11, 32, 33, 34], or, for richer traveling wave dynamics with higher order non-convex dispersion see [35]). Thus for the perturbed system (2.9), kinks are exceptional in that they approximate to a jump in the dispersionless limit, in particular a Hamiltonian shock by (2.22) and (2.19).

The present chapter seeks to address two natural question which arise in connection with Hamiltonian shocks: *i.* Can conditions be delineated under which some class of initial conditions, continuous except at a Hamiltonian shock, will evolve in such a way that this property is maintained? alternatively: can conditions be found ensuring that a Hamiltonian shock will interact with a continuous wave in such a way that gradient catastrophe does not occur? (section 2.2) and *ii.* can an infinitude of shock conservation constraints be enforced? (section 2.3).

We restrict to the cases $n = 1$ and $n = 2$ (though we shall proceed with n left unconstrained where possible in order to indicate how similar results can be obtained in larger systems as well), and find that a necessary condition for *i.* is that the *Hamiltonian shock map*

$$\boldsymbol{U}_r = \tilde{\boldsymbol{U}}(\boldsymbol{U}_l), \tag{2.25}$$

defined implicitly by the constraints (2.3) and (2.4), maps simple waves to simple waves. We shall refer to systems (2.1) having this property as *simple wave preserving*. We also find a sufficient but not necessary condition, namely the existence of a map sending Hamiltonian shocks to continuous solutions of an auxilliary system. This provides a generalization of the map from a model of two layer shallow water flow in the Boussinesq limit to the Airy system (see e.g. [36, 15] or below) which was applied in connection to kinks in [17]. In this case characteristics pass through the Hamiltonian shock unaffected and we refer to the system (2.1) as *Hamiltonian shock symmetric.*

7

We shall see that the answers to question *ii.* closely parallel those of *i.*, providing a link between conservation laws and coherent wave interaction, reminiscent of the well known connection between these properties for integrable systems. Violation of simple wave preservation places additional differential constraints (linear PDEs) on conserved quantities beyond the $n(n-1)/2$ that must be satisfied by virtue of equation (2.1). For $n > 2$ the system of equations required for a conservation law is already overdetermined (see e.g. [28]) and for $n = 2$ we show explicitly that only a finite number of conserved quantities may be Hamiltonian shock conserved when simple wave preservation fails. Furthermore, for the Hamiltonian shock symmetric case, any quantity conserved for strong solutions of the auxiliary system can be pulled back to produce a Hamiltonian shock conserved quantity. This produces an infinitude of Hamiltonian shock conservation laws in the two layer Boussinesq case, for example.

We will see that an infinitude of Hamiltonian shock conserved quantities is a necessary condition for integrability, as formulated by Dubrovin [29], for a perturbed system (2.9) admitting kinks. Thus simple wave preservation and Hamiltonian shock symmetry can be viewed as intermediate conditions between the integrable case and the generic non-integrable case, determined purely from the hyperbolic reduction (note: we make no claim that this extends to arbitrary notions of integrability).

The foregoing considerations indicate that gradient catastrophe in the interaction problem signals the appearance of classical dispersive shocks (we emphasize again that, as with Whitham modulation theory in the integrable case, the connection between the hyperbolic system and the perturbed system is not rigorous). This is shown below in numerical simulations of systems from dispersive hydrodynamics that do not satisfy the simple wave preserving property, namely a two layer shallow water model with unequal densities, and a non-linear wave equation, in the class referred to as Korteweg models in [22], which is a dispersive perturbation of an equation for a deformable medium in Lagrangian coordinates. For the simple wave preserving case on the other hand, numerical simulations of the interaction of a kink with a continuous wave for the Boussinesq (equal density) limit of the two later model shows strong agreement with the corresponding analytically computed Hamiltonian shock solution. This was also observed for the scalar case (which is trivially simple wave preserving) in the study [20] which catalogued a comprehensive array of different types of nonlinear wave interactions for the mKdV equation.

2.2 Wave interaction

In this section we give the precise statement of the Hamiltonian shock interaction problem with which we shall be concerned and demonstrate, for the cases $n = 2$ and $n = 1$, respectively, its relation to simple wave preservation and Hamiltonian shock symmetry. Essentially, a Hamiltonian shock enters from a quiescent state into a wave background that, evolving of its own accord would not develop gradient catastrophe. We show that if simple waves are not preserved by the Hamiltonian shock map then there will be initial conditions of this type for a solution at all times cannot be defined without introducing Lax shocks (precise statement given in 2.2.2).

2.2.1 Set up
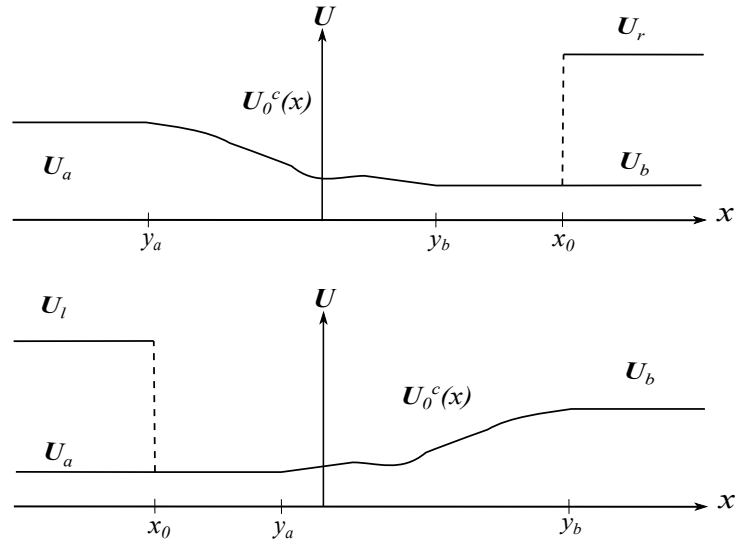
Figure 2.2: schematic of Initial conditions $\boldsymbol{U}_0^c(x)$ and $\boldsymbol{U}_0(x)$ in the slow undercompressive case and fast undercompressive case, respectively.

We take $\boldsymbol{U}_0^c(x)$ to be an initial condition giving rise to a strong solution $\boldsymbol{U}^c(x,t)$ at all time under the evolution of (2.1) with

$$\boldsymbol{U}_0^c(x) = \boldsymbol{U}_a, \qquad x < y_l, \tag{2.26}$$

$$\boldsymbol{U}_0^c(x) = \boldsymbol{U}_b, \qquad y_r < x \tag{2.27}$$

where $y_l < y_r$. The simplest non-trivial example is a centered simple wave (see appendix A). Then

we construct initial conditions

$$\boldsymbol{U}(x,0) = \boldsymbol{U}_0(x) \tag{2.28}$$

which will give a single Hamiltonian shock front interacting with the gradual wave produced by $\boldsymbol{U}^c(x,t)$.

The front may enter either from the right or from the left depending on whether the speed s is slower or faster than the speed of propagation of the left boundary of the continuous wave or slower than that of the right boundary (if neither holds then the shock does not interact with the continuous wave). In the former case, we define

$$\boldsymbol{U}_0(x) = \begin{cases} \boldsymbol{U}_0^c(x), & x < x_0 \\ \boldsymbol{U}_r, & x_0 \leq x \end{cases} \tag{2.29}$$

with $x_0 > y_r$, and $\boldsymbol{U}_b = \boldsymbol{U}_l$ and $\boldsymbol{U}_r$ satisfying the Rankine-Hugoniot conditions (2.3) and (2.4). This case is known as a slow undercompressive shock (see e.g. [10] or appendix C) because

$$s < \lambda_k(\boldsymbol{U}_l), \ \lambda_k(\boldsymbol{U}_r) \tag{2.30}$$

where λ_k is the characteristic speed of the family which propagates the boundary of the non-constant region for $\boldsymbol{U}^c$ to the right. Similarly for the latter case:

$$\boldsymbol{U}_0(x) = \begin{cases} \boldsymbol{U}_l, & x \leq x_0 \\ \boldsymbol{U}_0^c(x), & x_0 < x \end{cases} \tag{2.31}$$

with $x_0 < y_l$, and $\boldsymbol{U}_a = \boldsymbol{U}_r$ and $\boldsymbol{U}_l$, again, satisfying (2.3) and (2.4). This shock is known as fast undercompressive since

$$s > \lambda_k(\boldsymbol{U}_l), \ \lambda_k(\boldsymbol{U}_r). \tag{2.32}$$

2.2.2 Interaction

We refer solution of (2.1) with initial data (2.31)/(2.29) continuous, except at a moving point

$$x = \mathfrak{s}(t) \tag{2.33}$$

10

with $\mathfrak{s}(0) = x_0$ at which a Hamiltonian shock with speed

$$\mathfrak{s}'(t) = s \tag{2.34}$$

is present, as a *continuity preserving Hamiltonian shock interaction*. We seek necessary conditions on the system (2.1) for all such initial value problems to give rise to continuity preserving Hamiltonian shock interactions.

At this point we restrict to the case $n = 2$ so that we may make use of Riemann invariants, though we conjecture that the presence of Riemann invariants is not necessary for the conclusions of this section to hold. We shall now need to distinguish between three different cases:

i. $\lambda_1 < \lambda_2 < s$

ii. $\lambda_1 < s < \lambda_2$

iii. $s < \lambda_1 < \lambda_2$.

We refer to case *i.* as a *strictly fast*, case *ii.* as *fast-slow*, and case *iii.* as *strictly slow*. We shall need the following lemma

Lemma. *Take points (u_l, v_l) and (u_r, v_r) related by (2.3) and (2.4) and assume that both points contain neighborhoods for which the change to Riemann invariants: $(u, v) \mapsto (\phi^1(u, v), \phi^2(u, v))$ is a diffeomorphism. Furthermore, assume H is convex. Then $(\phi_l^1, \phi_l^2) = (\phi^1(u_l, v_l), \phi^2(u_l, v_l))$ and $(\phi_r^1, \phi_r^2) = (\phi^1(u_r, v_r), \phi^2(u_r, v_r))$ are related by diffeomorphism*

$$(\phi_r^1, \phi_r^2) = (\tilde{\phi}^1(\phi_l^1, \phi_l^2), \tilde{\phi}^2(\phi_l^1, \phi_l^2)). \tag{2.35}$$

Proof. Let

$$\mathbf{\Omega}(\mathbf{U}_l, \mathbf{U}_r, s) = -s \begin{pmatrix} [\mathbf{U}] \\ [H] \end{pmatrix} + \begin{pmatrix} [B\nabla H] \\ [\frac{1}{2}\nabla H^T B \nabla H]. \end{pmatrix} \tag{2.36}$$

Then the simultaneous satisfaction of (2.3) and (2.4) can be expressed by

$$\mathbf{\Omega}(\mathbf{U}_l, \mathbf{U}_r, s) = 0. \tag{2.37}$$

11

We compute

$$\frac{\partial \boldsymbol{\Omega}}{\partial(u_l, v_l)} = \begin{pmatrix} I \\ \nabla H(\boldsymbol{U}_l) \end{pmatrix} (sI - B\nabla^2 H(\boldsymbol{U}_l)) \tag{2.38}$$

where I is the 2×2 identity matrix, and

$$\frac{\partial \boldsymbol{\Omega}}{\partial(u_l, v_l)} = \begin{pmatrix} I \\ \nabla H(\boldsymbol{U}_r) \end{pmatrix} (sI - B\nabla^2 H(\boldsymbol{U}_r)), \tag{2.39}$$

and

$$\frac{\partial \boldsymbol{\Omega}}{\partial s} = - \begin{pmatrix} [\boldsymbol{U}] \\ [H] \end{pmatrix}. \tag{2.40}$$

Thus if

$$\tilde{\boldsymbol{\Omega}}(\phi_l^1, \phi_l^2, \phi_r^1, \phi_r^2, s) = \boldsymbol{\Omega}(\boldsymbol{U}(\phi_l^1, \phi_l^2), \boldsymbol{U}(\phi_r^1, \phi_r^2), s) \tag{2.41}$$

then

$$\frac{\partial \tilde{\boldsymbol{\Omega}}}{\partial(u_l, v_l)} = \begin{pmatrix} I \\ \nabla H(\boldsymbol{U}_l) \end{pmatrix} (sI - B\nabla^2 H(\boldsymbol{U}_l)) \frac{\partial \boldsymbol{U}}{\partial(\phi_l^1, \phi_l^2)}, \tag{2.42}$$

$$\frac{\partial \tilde{\boldsymbol{\Omega}}}{\partial(u_l, v_l)} = \begin{pmatrix} I \\ \nabla H(\boldsymbol{U}_r) \end{pmatrix} (sI - B\nabla^2 H(\boldsymbol{U}_r)) \frac{\partial \boldsymbol{U}}{\partial(\phi_r^1, \phi_r^2)}, \tag{2.43}$$

and

$$\frac{\partial \tilde{\boldsymbol{\Omega}}}{\partial s} = - \begin{pmatrix} [\boldsymbol{U}] \\ [H] \end{pmatrix}. \tag{2.44}$$

The lemma will follow from the implicit function theorem if we may show that

$$\frac{\partial \tilde{\boldsymbol{\Omega}}}{\partial u_r}, \frac{\partial \tilde{\boldsymbol{\Omega}}}{\partial v_r} \quad \text{and} \quad \frac{\partial \tilde{\boldsymbol{\Omega}}}{\partial s} \tag{2.45}$$

are linearly independent. Let $\boldsymbol{V}_1$ and $\boldsymbol{V}_2$ be the columns

$$(\boldsymbol{V}_1, \boldsymbol{V}_2) = (sI - B\nabla^2 H(\boldsymbol{U}_r)) \frac{\partial \boldsymbol{U}}{\partial(\phi_r^1, \phi_r^2)}. \tag{2.46}$$

12

Then a dependence between the vectors in (2.45) takes the form

$$[\boldsymbol{U}] = \alpha \boldsymbol{V}_1 + \beta \boldsymbol{V}_2, \tag{2.47}$$

$$[H] = \nabla H(\boldsymbol{U}_r)^T (\alpha \boldsymbol{V}_1 + \beta \boldsymbol{V}_2). \tag{2.48}$$

These may be combined to obtain

$$H(\boldsymbol{U}_r) + \nabla H(\boldsymbol{U}_r)^T (\boldsymbol{U}_l - \boldsymbol{U}_r) \tag{2.49}$$

which contradicts convexity. Thus the dependence (2.45) must not hold and the lemma follows. □

The main result of this section is split into two cases. We start with the strictly fast/strictly slow case.

Theorem. *Assume that a system (2.1) of two equations for which the initial value problem for (2.1) with initial data (2.31)/(2.29) always gives rise to a continuity preserving Hamiltonian shock interaction. Assume that this system admits strictly fast or strictly slow Hamiltonian shocks. Also make two non-degeneracy assumptions at a point (u_a, v_a), $(u_q, v_q) = (\tilde{u}(u_a, v_a), \tilde{v}(u_a, v_a))$: (i) that the system (2.1) is genuinely non-linear within sufficiently small neighborhoods of (u_a, v_a) and (u_q, v_q), and (ii) that the shock connecting (u_a, v_a) and (u_q, v_q) is not a contact discontinuity, i.e., the speed s is not an eigenvalue of $B\nabla^2 H(u_a, v_a)$ or $B\nabla^2 H(u_q, v_q)$.*

Then the Hamiltonian shock map $\tilde{\boldsymbol{U}}$ is simple wave preserving, i.e., level sets of the Riemann invariants (see Appendix A) ϕ^j, $j = 1, 2$, are mapped to the same.

Proof. We begin by changing coordinates to the Riemann invariant form

$$\boldsymbol{\Phi}(\boldsymbol{U}) = \begin{pmatrix} \phi^1(\boldsymbol{U}) \\ \phi^2(\boldsymbol{U}) \end{pmatrix} \tag{2.50}$$

in which we express the Hamiltonian shock map by

$$\tilde{\boldsymbol{\Phi}}(\boldsymbol{\Phi}(\boldsymbol{U})) = \boldsymbol{\Phi}(\tilde{\boldsymbol{U}}(\boldsymbol{U})). \tag{2.51}$$

13

By genuine nonlinearity, $\boldsymbol{\Phi}$ can be defined in such a way that (see e.g. [28])

$$\frac{\partial \lambda_j}{\partial \phi^j} > 0, \tag{2.52}$$

$j = 1, 2$. Then for continuity of the solution to hold at all times, it is necessary [37] and sufficient [38] that ϕ_1 and ϕ_2 are non-decreasing. Thus the initial conditions leading to continuous solutions at all times,

$$\boldsymbol{\Phi}_0^c = \boldsymbol{\Phi}(\boldsymbol{U}_0^c) \tag{2.53}$$

satisfy this property. For the solution to be continuous except at the Hamiltonian shock curve $x = \mathfrak{s}(t)$, this condition must be satisfied away from this curve. We proceed to show that if simple wave preservation does not hold then there will exist initial conditions having non-decreasing Riemann invariants which lead, after interaction, to a solution which has decreasing Riemann invariants. Thus such a system will not be continuity preserving.

Plugging (2.26) and (2.27) into Φ we may write

$$\boldsymbol{\Phi}_0^c(x) = \begin{pmatrix} \phi_a^1 \\ \phi_a^2 \end{pmatrix}, \qquad x < y_a, \tag{2.54}$$

and

$$\boldsymbol{\Phi}_0^c(x) = \begin{pmatrix} \phi_b^1 \\ \phi_b^2 \end{pmatrix}, \qquad x > y_b. \tag{2.55}$$

For 1-simple wave solutions $\phi_b^2 = \phi_a^2$ and for 2-simple wave solutions $\phi_b^1 = \phi_a^1$. In any case, the requirement for continuity is that

$$\phi_a^1 < \phi_b^1 \tag{2.56}$$

and

$$\phi_a^2 < \phi_b^2. \tag{2.57}$$

A fundamental property of the Riemann invariants ϕ^j is that they are constant on the corresponding characteristics

$$\phi^j(\chi_j(t; \xi), t) = \phi^j(\xi, 0) \tag{2.58}$$

14

where

$$\frac{d\chi_j}{dt} = \lambda_j, \qquad \chi_j(0;\xi) = \xi. \tag{2.59}$$

Thus the values of $\mathbf{\Phi}$ on the left and right sides of the jump at $x = \mathfrak{s}(t)$ may be determined by considering which characteristics impinge upon the shock. In particular, the distance between the shock and a characteristic starting at ξ is

$$|\chi_j(t;\xi) - \mathfrak{s}(t)| = |\xi - x_0 + \int_0^t (\lambda_j - s)dt| \tag{2.60}$$

(we have omitted the dependence of s and λ_j).

We shall now focus on the strictly fast case since the strictly slow case is proven by symmetric but otherwise identical reasoning. We take the inequality $\lambda_1 < \lambda_2 < s$ characterizing this case to be uniform in the sense that

$$s - \lambda_2, \lambda_2 - \lambda_1 > m. \tag{2.61}$$

This can be achieved by taking $\mathbf{\Phi}_b$ sufficiently close to $\mathbf{\Phi}_a$ since it follows from Lemma 2.2.2 that the codomain of the solution, consisting of neighborhoods of $\mathbf{\Phi}_a$ and $\mathbf{\Phi}_q$, depends continuously on the difference between $\mathbf{\Phi}_b$ and $\mathbf{\Phi}_a$. In particular, the solution must lie within the union of the rectangles

$$(\phi_a^1, \phi_b^1) \times (\phi_a^2, \phi_b^2) \cup (\tilde{\phi}_a^1, \tilde{\phi}_b^1) \times (\tilde{\phi}_a^2, \tilde{\phi}_b^2) \tag{2.62}$$

where $\tilde{\phi}_a^1 = \tilde{\phi}(\phi_a^1, \phi_a^2)$, etc.

We set

$$\mathbf{\Phi}_l = \tilde{\mathbf{\Phi}}(\mathbf{\Phi}_a) \tag{2.63}$$

(cf. figure 2.2). Then for $\xi > x_0$,

$$\chi_j(t;\xi) - \mathfrak{s}(t) = \xi - x_0 + \int_0^t (\lambda_j - s)dt \tag{2.64}$$

$$\leq \xi - x_0 - mt \tag{2.65}$$

which vanishes for some t. According to the constancy of Riemann invariants along characteristics (equation (2.58)), this implies that for t sufficiently large, the value of $\mathbf{\Phi}$ on the right side of the

15

shock will be given by

$$\mathbf{\Phi}(\mathfrak{s}(t)^+, t) = \mathbf{\Phi}_b \tag{2.66}$$

and on the left side by

$$\mathbf{\Phi}(\mathfrak{s}(t)^-, t) = \tilde{\mathbf{\Phi}}(\mathbf{\Phi}_b) \tag{2.67}$$

Now in order for the Riemann invariants to be non-decreasing on the left side of the shock (which is required for continuity as noted in the beginning of the proof), it must be the case that

$$\phi_l^1 = \tilde{\phi}^1(\phi_a^1, \phi_a^2) < \tilde{\phi}^1(\phi_b^1, \phi_b^2) \tag{2.68}$$

and

$$\phi_l^2 = \tilde{\phi}^2(\phi_a^1, \phi_a^2) < \tilde{\phi}^2(\phi_b^1, \phi_b^2). \tag{2.69}$$

Since $\mathbf{\Phi}_b$ may be taken arbitrarily close to $\mathbf{\Phi}_a$ and because equations (2.56) and (2.57) must hold, the elements of the Jacobian

$$\frac{\partial \tilde{\phi}^i}{\partial \phi^j} \geq 0 \tag{2.70}$$

for $i, j = 1, 2$. However, because the Hamiltonian shocks are reversible (unlike classical shocks) the roles of $\mathbf{\Phi}_a$ and $\mathbf{\Phi}_l$ may be switched. Then identical reasoning leads to the conclusion that the components of the inverse Jacobian satisfy

$$\frac{\partial \phi^j}{\partial \tilde{\phi}^i} \geq 0. \tag{2.71}$$

It is only possible to simultaneously enforce these order relations for the Jacobian (equation (2.70)) and its inverse (equation (2.71)), if it is diagonal or off diagonal, which in either case implies that level sets of Riemann invariants are mapped to level sets of Riemann invariants and thus simple waves are preserved. $\qquad\square$

For the fast-slow case, the proof follows from similar reasoning except that an additional solvability assumption is needed, namely that given ϕ_l^1 and ϕ_r^2, ϕ_r^1 and ϕ_l^2 satisfying (2.3) and (2.4) can be solved for continuously. For the strictly fast and strictly slow cases, solvability is guaranteed by Lemma (2.2.2). In the fast-slow case however, the implicit function theorem argument does not lead

to a contradiction to convexity. Thus we include the solvability assumption in the general case where strictly slow or strictly fast Hamiltonian shocks may not exist.

Theorem. *Assume that a system (2.1) of two equations for which the initial value problem for (2.1) with initial data (2.31)/(2.29) always gives rise to a continuity preserving Hamiltonian shock interaction. Assume further that if ϕ_l^1 and ϕ_r^2 are fixed, (2.3) and (2.4), may be solved smoothly for ϕ_r^1 and ϕ_l^2 or vice versa, i.e., there exists a diffeomorphism*

$$(\phi_l^1, \phi_r^2) \mapsto (\phi_r^1, \phi_l^2), \tag{2.72}$$

which we denote by

$$(\phi_r^1, \phi_l^2) = (\hat{\phi}^1(\phi_l^1, \phi_r^2), \hat{\phi}^2(\phi_l^1, \phi_r^2)). \tag{2.73}$$

Also make two non-degeneracy assumptions at a point (u_a, v_a), $(u_q, v_q) = (\tilde{u}(u_a, v_a), \tilde{v}(u_a, v_a))$: (i) that the system (2.1) is genuinely non-linear within sufficiently small neighborhoods of (u_a, v_a) and (u_q, v_q), and (ii) that the shock connecting (u_a, v_a) and (u_q, v_q) is not a contact discontinuity, i.e., the speed s is not an eigenvalue of $B\nabla^2 H(u_a, v_a)$ or $B\nabla^2 H(u_q, v_q)$.

Then the Hamiltonian shock map $\tilde{U}$ is simple wave preserving, i.e., level sets of the Riemann invariants (see Appendix A) ϕ^j, $j = 1, 2$, are mapped to the same.

Proof. We only need to prove the theorem for the case where only fast-slow Hamiltonian shocks occur since otherwise it follows immediately from Theorem 2.2.2. This time, for concreteness, we consider interactions with simple waves, starting with the 1-simple wave case $\phi_b^2 = \phi_a^2$. Reasoning analogous to (2.64) applied to the order relation

$$\lambda_1 < s < \lambda_2 \tag{2.74}$$

for fast-slow Hamiltonian shocks shows that 2-characteristics impinge upon the shock curve $x = \mathfrak{s}(t)$ from the left and 1-characteristics from the right. In particular, a Hamiltonian shock enters on the right for a 1-simple wave, in which case we have

$$\phi^2(\mathfrak{s}(t)^-, t) = \phi_l^2 = \tilde{\phi}^2(\phi_a^1, \phi_a^2) \tag{2.75}$$

17

and

$$\phi^1(\mathfrak{s}(t)^+, t) = \phi_b^1. \tag{2.76}$$

Appealing again to the requirement for continuity, that Riemann invariants increase from left to right, we must have

$$\phi_l^1 \leq \hat{\phi}^1 \tag{2.77}$$

and

$$\hat{\phi}^2 \leq \phi_b^2 = \phi_a^2. \tag{2.78}$$

Returning to regarding the value of the solution on the left side of the shock in terms of the function $\boldsymbol{\Phi}$ applied to the solution on the right side, we have $\tilde{\phi}^2 = \phi_l^2$ on the left remaining fixed, $\tilde{\phi}^1$ on the left increasing along $x = \mathfrak{s}(t)$ through the course of the interaction (t increasing) and ϕ^1 increasing on the right while ϕ^2 decreases on the right. This may be expressed as

$$\frac{\partial \phi^1}{\partial \tilde{\phi}^1} \geq 0, \qquad \frac{\partial \phi^2}{\partial \tilde{\phi}^1} \leq 0. \tag{2.79}$$

Symmetric reasoning for the 2-simple wave case yields

$$\frac{\partial \phi^2}{\partial \tilde{\phi}^1} \leq 0, \qquad \frac{\partial \phi^2}{\partial \tilde{\phi}^2} \geq 0. \tag{2.80}$$

As before, the roles of $\boldsymbol{\Phi}_a$ and $\boldsymbol{\Phi}_l$ may be reversed ($\boldsymbol{\Phi}_a$ and $\boldsymbol{\Phi}_r$ in the 2-simple wave case), to conclude that

$$\frac{\partial \tilde{\phi}^1}{\partial \phi^1} \geq 0, \qquad \frac{\partial \tilde{\phi}^2}{\partial \phi^1} \leq 0, \tag{2.81}$$

$$\frac{\partial \tilde{\phi}^2}{\partial \phi^1} \leq 0, \qquad \frac{\partial \tilde{\phi}^2}{\partial \phi^2} \geq 0. \tag{2.82}$$

Again, these order relations for the Jacobian and its inverse may only hold if the Jacobian is diagonal or off-diagonal and thus simple wave preserving. $\qquad \square$

Thus far we have discussed necessary conditions for the maintenance of continuity under Hamiltonian shock interaction. In the following subsections we consider two cases where Hamiltonian shock interactions are *guaranteed* to be continuity preserving.

18
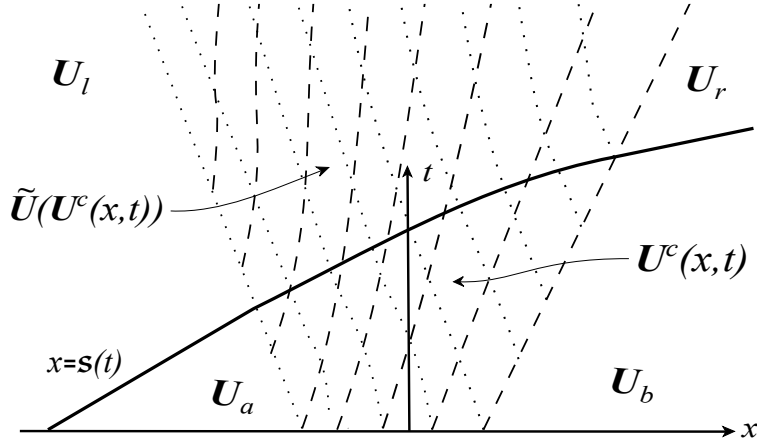
Figure 2.3: Schematic showning a Hamiltonian shock moving through without affecting the characteristic structure.

2.2.3 Hamiltonian shock symmetric case

In the Hamiltonian shock symmetric case, the system (2.1) is equivalent to a hyperbolic system

$$\boldsymbol{W}_t + A(\boldsymbol{W})\boldsymbol{W}_x = 0 \tag{2.83}$$

with

$$\boldsymbol{W}(\tilde{\boldsymbol{U}}(\boldsymbol{U})) = \boldsymbol{W}(\boldsymbol{U}). \tag{2.84}$$

The function $\boldsymbol{W}(\boldsymbol{U}^c(x,t))$ is a solution to this system, continuous at all time and a Hamiltonian shock solution may be obtained by splicing together two branches of its inverse across a Hamiltonian shock curve

$$\boldsymbol{U}(x,t) = \begin{cases} \boldsymbol{U}^c(x,t), & x \leq \mathfrak{s}(t) \\ \tilde{\boldsymbol{U}}(\boldsymbol{U}^c(x,t)), & \mathfrak{s}(t) < x. \end{cases} \tag{2.85}$$

In this case $\mathfrak{s}$ is found by solving the ODE

$$\mathfrak{s}'(t) = s(\boldsymbol{U}^c(\mathfrak{s}(t),t), \tilde{\boldsymbol{U}}(\boldsymbol{U}^c(\mathfrak{s}(t),t))), \qquad \mathfrak{s}(0) = x_0. \tag{2.86}$$

The characteristic diagram is shown in figure 2.3.

2.2.4 Scalar case

For a scalar law (2.1) with $n = 1$,

$$u_t + H'(u)_x = 0, \tag{2.87}$$

the initial value problem with boundary data

$$u(\mathfrak{s}(t), t) = \tilde{u}(u^c(\mathfrak{s}(t), t)), \tag{2.88}$$

given by the Hamiltonian shock map along the shock curve can be solved by the method of characteristics. We now show that gradient catastrophe will not be induced by Hamiltonian shock interaction. This demonstrates that Hamiltonian shock symmetry is not a necessary condition for this property, as it is easy to see that not all scalar laws are Hamiltonian shock symmetric.

First we recall that for the continuous state u^c solving (2.87) with initial condition

$$u^c(x, 0) = u_0^c(x) \tag{2.89}$$

is given by

$$u^c(x_0 + tH''(u_0^c(x_0)), t) = u_0^c(x_0), \tag{2.90}$$

and the continuity requirement holds if and only if none of the characteristic lines cross:

$$x_1 + tH''(u_0^c(x_1)) \neq x_2 + tH''(u_0^c(x_2)) \tag{2.91}$$

for $x_1 \neq x_2$ any $t > 0$. This in turn holds if and only if (see e.g. [13])

$$H'''(u_0^c(x_0))u_0^c(x_0)' > 0 \tag{2.92}$$

for all x_0. Similarly, the solution after interaction is given by

$$u(\mathfrak{s}(\tau) + tH''(\tilde{u}(u^c(\mathfrak{s}(\tau), t))), t) = \tilde{u}(u^c(\mathfrak{s}(\tau), \tau)) \tag{2.93}$$

20

where as before $\tilde{u}(u)$ is a right state to which the left state u can be connected by a Hamiltonian shock. For the fast case, the characteristics emanate from the left of the interaction curve $x = \mathfrak{s}(\tau)$ so in order to prevent crossing, the slope H'' must be increasing in τ (see figure 2.4):

$$0 < H'''(\tilde{u}(u^c))\tilde{u}'(u^c)(u_t^c + su_x^c) \tag{2.94}$$

$$= H'''(\tilde{u}(u^c))\tilde{u}'(u^c)(s - H''(u^c))u_x^c. \tag{2.95}$$

By continuity of u^c we must have

$$0 < H'''(u^c)(u_t^c + su_x^c) \tag{2.96}$$

and under the assumption that a single NGN point lies between $\tilde{u}(u^c)$ and u^c, $H'''(\tilde{u}(u^c))$ has the sign opposite to $H'''(u^c)$. Furthermore, by equation (2.154) below, we have $\tilde{u}'(u^c) < 0$ and by fast undercompressivity,

$$s - H''(\tilde{u}(u^c)) > 0 \tag{2.97}$$

so (2.96) holds. The slow case follows in the same way except that (2.96) is reversed because the characteristics emanate from the right of the interaction curve:

$$0 > H'''(\tilde{u}(u^c))\tilde{u}'(u^c)(u_t^c + su_x^c) \tag{2.98}$$

$$= H'''(\tilde{u}(u^c))\tilde{u}'(u^c)(s - H''(u^c))u_x^c. \tag{2.99}$$

which follows by applying slow undercompressivity, replacing (2.97) with

$$H''(u^c) - s > 0. \tag{2.100}$$

In appendix D, we demonstrate the same procedure for a classical undercompressive shock.

2.3 Additional conserved quantities

In this section we consider conservation laws

$$G(\boldsymbol{U})_t + M(\boldsymbol{U})_x = 0 \tag{2.101}$$
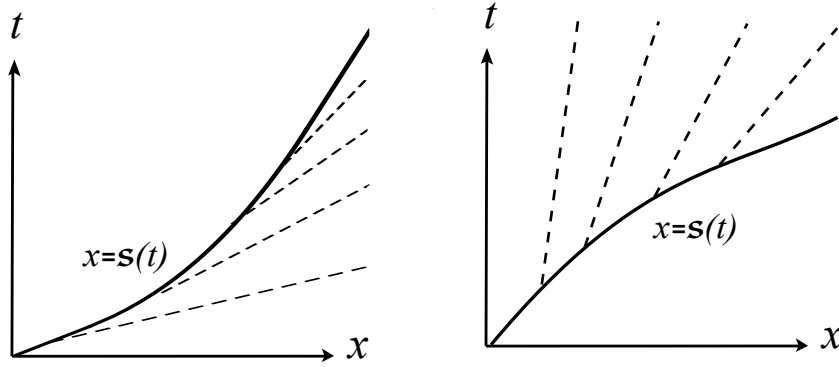
Figure 2.4: Schematics for a Hamiltonian shock interaction in the scalar case. The left panel shows a slow undercompressive shock, along which the slope of the characteristics must decrease and the right a fast undercompressive shock, along which the slope of the characteristics must increase.

which hold for the evolution of (2.1) and which, furthermore, satisfy Rankine-Hugoniot jump conditions:

$$-s[G] + [M] = 0 \tag{2.102}$$

across a Hamiltonian shock. These conservation laws may arise in the dispersionless limit from local conserved quantities G^ϵ of equation (2.9):

$$G^\epsilon[\boldsymbol{U}^\epsilon, \epsilon]_t + M^\epsilon[\boldsymbol{U}^\epsilon, \epsilon]_x = 0, \tag{2.103}$$

in the same fashion as was discussed for conservation of energy in the introduction. For the dispersively perturbed system (2.9) to be integrable in the sense of Dubrovin (see e.g. [39] or [29]) it is necessary (though not sufficient) that an infinite number of independent conservation laws of the form (2.101) for the Hamiltonian hyperbolic system (2.1) exist arising as dispersionless reductions of conservation laws of the form (2.103) for the evolution of the perturbed system (2.9).

In this section we show that $\tilde{\boldsymbol{U}}$ must be simple wave preserving in order for an infinitude of Hamiltonian shock conserved quantities to exist in the case of n=2. The argument we will use applies to $n > 2$ as well by producing additional PDEs that G must satisfy in addition to (2.101), however, we do not provide explicit proof in the latter case that the resulting overdetermined system only has trivial solutions. For the case $n = 1$ on the other hand, we show that an infinitude of independent conservation laws will always exist by explicit construction.

2.3.1 Jump conditions from Hamiltonian symmetries

Impulse conservation and flow force balance We begin by recalling one additional conserva-tion law beyond $u^1, u^2, ..., u^n$ and $H^\epsilon[\boldsymbol{U}]$ which can always be found, namely the impulse defined by

$$\mathfrak{I} = \frac{1}{2}\boldsymbol{U}^T B^{-1}\boldsymbol{U}. \tag{2.104}$$

For the disperionless reduction (2.1), this conservation law takes the form

$$(\frac{1}{2}\boldsymbol{U}^T B^{-1}\boldsymbol{U})_t + (\boldsymbol{U}^T\nabla H - H)_x = 0 \tag{2.105}$$

with corresponding jump conditions

$$-s[\frac{1}{2}\boldsymbol{U}^T B^{-1}\boldsymbol{U}] + [\boldsymbol{U}^T\nabla H - H] = 0. \tag{2.106}$$

We can see from direct computation that (2.106) implies conservation of energy (2.4) since (2.3) implies that

$$(-s\boldsymbol{U}_r + B\nabla H_r)^T B^{-1}(-s\boldsymbol{U}_r + B\nabla H_r) = (-s\boldsymbol{U}_l + B\nabla H_l)^T B^{-1}(-s\boldsymbol{U}_l + B\nabla H_l) \tag{2.107}$$

so

$$s^2[\boldsymbol{U}^T B^{-1}\boldsymbol{U}] - 2s[\nabla H^T\boldsymbol{U}] + [\nabla H^T B\nabla H] = 0 \tag{2.108}$$

which yields

$$-s[H] + [\frac{1}{2}\nabla H^T B\nabla H] = s(-s[\frac{1}{2}\boldsymbol{U}^T B^{-1}\boldsymbol{U}] + [\boldsymbol{U}^T\nabla H - H]). \tag{2.109}$$

Remark. *The quantity*

$$-s[\frac{1}{2}\boldsymbol{U}^T B^{-1}\boldsymbol{U}] + [\boldsymbol{U}^T\nabla H - H] \tag{2.110}$$

arising in the above computation is referred to in [40] as the "flow force", a title justified physically by equation (2.109) in which the latter can be interpreted as introducing external work done on the system.

Hamiltonian shock symmetry conditions As was illustrated in the impulse case, for G to be conserved across a Hamiltonian shock, its jump conditions (2.102) must depend on the extended Rankine-Hugoniot conditions (2.3) and (2.4). So, leaving s free now for convenience, if the map $\boldsymbol{\Phi} : \mathbb{R}^{2n+1} \to \mathbb{R}^{n+2}$ is defined by

$$\boldsymbol{\Phi}(\boldsymbol{U}_l, \boldsymbol{U}_r, s) = -s \begin{pmatrix} [\boldsymbol{U}] \\ [H] \\ [G] \end{pmatrix} + \begin{pmatrix} [B\nabla H] \\ [\frac{1}{2}\nabla H^T B \nabla H] \\ [M] \end{pmatrix} \tag{2.111}$$

in block matrix form, then its differential, also in block matrix form:

$$\begin{pmatrix} \boldsymbol{\Phi}_{U_l} & \boldsymbol{\Phi}_{U_r} & \boldsymbol{\Phi}_s \end{pmatrix}, \tag{2.112}$$

must have rank $n+1$ by the implicit function theorem. The vector valued partial derivatives are given by:

$$\boldsymbol{\Phi}_{U_r} = -s \begin{pmatrix} I \\ \nabla H_r^T \\ \nabla G_r^T \end{pmatrix} + \begin{pmatrix} B\nabla^2 H_r \\ \nabla H_r^T B \nabla^2 H_r \\ \nabla G_r^T B \nabla^2 H_r \end{pmatrix} = \begin{pmatrix} I \\ \nabla H_r^T \\ \nabla G_r^T \end{pmatrix} (B\nabla^2 H_r - sI), \tag{2.113}$$

$$\boldsymbol{\Phi}_{U_l} = s \begin{pmatrix} I \\ \nabla H_l^T \\ \nabla G_l^T \end{pmatrix} - \begin{pmatrix} B\nabla^2 H_l \\ \nabla H_r^T B \nabla^2 H_l \\ \nabla G_r^T B \nabla^2 H_l \end{pmatrix} = - \begin{pmatrix} I \\ \nabla H_l^T \\ \nabla G_l^T \end{pmatrix} (B\nabla^2 H_l - sI), \tag{2.114}$$

and

$$\boldsymbol{\Phi}_s = - \begin{pmatrix} [U] \\ [H] \\ [G] \end{pmatrix} \tag{2.115}$$

where I is the $n \times n$ identity matrix. As long as s is not an eigenvalue of each side, i.e. the shock is not a contact discontinuity, the latter matrix is column equivalent to the block matrix

$$\begin{pmatrix} I & I & [\boldsymbol{U}] \\ \nabla H_l^T & \nabla H_r^T & [H] \\ \nabla G_l^T & \nabla G_r^T & [G] \end{pmatrix}. \tag{2.116}$$

24

Multiplying on the right by the non-singular matrix,

$$
\begin{pmatrix}
I & -I & -\boldsymbol{U}_l \\
0 & I & \boldsymbol{U}_r \\
0 & 0 & -1
\end{pmatrix},
\tag{2.117}
$$

the matrix (2.112) is, furthermore, column equivalent to

$$
\begin{pmatrix}
I & 0 & 0 \\
\nabla H_l^T & [\nabla H^T] & [\nabla H^T \boldsymbol{U} - H] \\
\nabla G_l^T & [\nabla G^T] & [\nabla G^T \boldsymbol{U} - G]
\end{pmatrix}
\tag{2.118}
$$

where zero matrices are given appropriate dimensions of $n \times n$, $1 \times n$, $n \times 1$ or 1×1 depending on the context. The dimensional restriction dictated by the implicit function theorem implies that the $2 \times (n+1)$ matrix in the bottom has rank 1. This immediately produces a set of jump conditions for G which do not require the explicit form of M to be known:

$$
-\sigma[\boldsymbol{U}] + [B \cdot \nabla G] = 0,
\tag{2.119}
$$

and

$$
-\sigma[\frac{1}{2}\boldsymbol{U}^T B^{-1} \boldsymbol{U}] + [\boldsymbol{U}^T \nabla G - G] = 0,
\tag{2.120}
$$

and by a manipulation mirroring the flow force balance (2.109):

$$
-\sigma[G] + [\frac{1}{2}\nabla G^T B \nabla G] = 0.
\tag{2.121}
$$

From the foregoing, an analogy may be seen with the theory of Hamiltonian symmetries. Any quantity G conserved for strong solutions of (2.1) satisfies

$$
B\nabla^2 H B \nabla^2 G - B\nabla^2 G B \nabla^2 H = 0
\tag{2.122}
$$

25

and correspondingly, the evolution of

$$\boldsymbol{U}_\tau + B\nabla G(\boldsymbol{U})_x = 0, \tag{2.123}$$

under τ commutes with that of (2.1) under t (see e.g. [41] or [40]). The latter system has further conservation laws for G and S:

$$G_\tau + (\nabla G^T B \nabla G)_x = 0, \tag{2.124}$$

and

$$(\frac{1}{2}\boldsymbol{U}^T B^{-1}\boldsymbol{U})_\tau + (\boldsymbol{U}^T \nabla G - G)_x = 0 \tag{2.125}$$

for which (2.119), (2.121) and (2.120) are the state, energy and impulse Rankine-Hugoniot conditions for Hamiltonian shocks corresponding to (2.3), (2.4) and (2.106). Thus the well known comutatitvity of flows for Hamiltonian systems extends also to Hamiltonian shocks.

2.3.2 Overdetermined system

We now find an overdetermined system on conserved quantities G that are Hamiltonian shock conserved, i.e. satisfy the Rankine-Hugoniot condition (2.102) or, equivalently, the jump conditions of the form (2.119), (2.120), (2.121) arising from the Hamiltonian flow generated by G. We set

$$\boldsymbol{U}_l = \boldsymbol{U}, \text{ and } \boldsymbol{U}_r = \tilde{\boldsymbol{U}}(\boldsymbol{U}). \tag{2.126}$$

Then differentiating the jump conditions (2.119) and (2.120) with respect to $\boldsymbol{U}$ yields

$$-[\boldsymbol{U}]\nabla\sigma^T + (B\nabla^2 G_r - \sigma I)J - (B\nabla^2 G_l - \sigma I) = 0 \tag{2.127}$$

and

$$-[\frac{1}{2}\boldsymbol{U}^T B^{-1}\boldsymbol{U}]\nabla\sigma^T + \boldsymbol{U}_r^T B^{-1}(B\nabla^2 G_r - \sigma I)J - \boldsymbol{U}_l^T B^{-1}(B\nabla^2 G_l - \sigma I) = 0 \tag{2.128}$$

where J is the matrix of partial derivatives of $\tilde{\boldsymbol{U}}$.

We may assume that $[\frac{1}{2}\boldsymbol{U}^T B^{-1}\boldsymbol{U}]$ does not vanish, since if it does we may transform the system

(2.1) by $\boldsymbol{U} \to \boldsymbol{U} + \boldsymbol{C}$ where $\boldsymbol{C}$ is a constant shift. Then we may solve (2.128) for $\nabla \sigma^T$:

$$\nabla \sigma^T = \frac{1}{[\frac{1}{2}\boldsymbol{U}^T B^{-1} \boldsymbol{U}]} \left(\boldsymbol{U}_r^T B^{-1} (B\nabla^2 G_r - \sigma I) J - \boldsymbol{U}_l^T B^{-1} (B\nabla^2 G_l - \sigma I) \right). \tag{2.129}$$

Plugging this into (2.127) gives

$$Y_r(B\nabla^2 G_r - \sigma I)J = Y_l(B\nabla^2 G_l - \sigma I) \tag{2.130}$$

where

$$Y_r = [\frac{1}{2}\boldsymbol{U}^T B^{-1} \boldsymbol{U}]I - [\boldsymbol{U}]\boldsymbol{U}_r^T B^{-1} \tag{2.131}$$

and

$$Y_l = [\frac{1}{2}\boldsymbol{U}^T B^{-1} \boldsymbol{U}]I - [\boldsymbol{U}]\boldsymbol{U}_l^T B^{-1}. \tag{2.132}$$

We rearrange to obtain

$$B\nabla^2 G_r - \sigma I = W(B\nabla^2 G_l - \sigma I)J^{-1} \tag{2.133}$$

where $W = Y_r^{-1} Y_l$ and we have assumed that Y_r is invertible which is implied by convexity of H (see appendix C).

Let P_r be the matrix of right eigenvectors for $B\nabla^2 G_r$ which, by the commutation relation (2.122), is also that of $B\nabla^2 H_r$ and thus can be computed independently of G. We therefore diagonalize (2.133):

$$\Lambda_r - \sigma I = P_r^{-1} W (B\nabla^2 G_l - \sigma I)J^{-1} P_r \tag{2.134}$$

or equivalently

$$\Lambda_r + \sigma(P_r^{-1} W J^{-1} P_r - I) = P_r^{-1} W B\nabla^2 G_l J^{-1} P_r, \tag{2.135}$$

where Λ_r is the diagonalization of $B\nabla^2 G_r$. There are two cases to consider: either $P_r^{-1} W J^{-1} P_r$ has an off-diagonal entry which implies that σ may be expressed linearly in terms of the coefficients of $\nabla^2 G_l$ since the terms with an explicit right side dependence dwell on the diagonal, or else $D = P_r^{-1} W J^{-1} P_r$ is a diagonal matrix. In the former case (2.130) can be plugged into (2.129) to obtain a linear PDE that G must satisfy in addition to (2.122) causing the system to be overdetermined even in the 2×2 case. This can be expected to rule out Hamiltonian shock conservation laws beyond the span of the

naturally given: (2.1), (2.5) and (2.105), as will be shown explicitly below for the 2×2 case. In the case where σ cannot be thus solved,

$$D = P_r^{-1} W J^{-1} P_r \tag{2.136}$$

implies that

$$P_r^{-1} W = D P_r^{-1} J \tag{2.137}$$

which, when substituted into (2.135), gives

$$\Lambda_r + \sigma(D - I) = D(J^{-1} P_r)^{-1} B \nabla^2 G_l (J^{-1} P_r), \tag{2.138}$$

i.e., $B \nabla^2 G_l$ is diagonalized by $J^{-1} P_r$ which is therefore a matrix of right eigenvectors of $B \nabla^2 G_l$ and also $B \nabla^2 H_l$ by the commutation relation (2.122). This may be summarized by the statement that J^{-1} maps right eigenvectors on the right to right eigenvectors on the left and equivalently J maps right eigenvectors on the left to right eigenvectors on the right. By the elementary theory of ODEs, this holds if and only if $\tilde{U}$ maps simple waves to simple waves.

2.3.3 Systems of two conservation laws

We proceed to demonstrate how G can be constrained in the 2×2 case with

$$B = \begin{pmatrix} 0 & 1 \\ 1 & 0 \end{pmatrix}. \tag{2.139}$$

When $P_r^{-1} W J^{-1} P_r$ is not diagonal, (2.134) can be solved for $G_{uv}^l - \sigma$ in terms of G_{uu} and G_{vv}. However, for this Hamiltonian structure the commutativity relation (2.122) becomes

$$H_{uu} G_{vv} + H_{vv} G_{uu} = 0. \tag{2.140}$$

So G_{vv} may be eliminated to obtain a relation of the form

$$\sigma = G_{uv} + C G_{uu}. \tag{2.141}$$

28

Then multiplying (2.127) on the left by $\frac{[\boldsymbol{U}]^T}{[\boldsymbol{U}]^T[\boldsymbol{U}]}$ and applying (2.130) and the relation

$$Y_r - Y_l = -[\boldsymbol{U}][\boldsymbol{U}]^T B^{-1}, \tag{2.142}$$

we obtain

$$\nabla\sigma^T = \frac{[\boldsymbol{U}]^T}{||[\boldsymbol{U}]||^2}(Y_r^{-1}Y_l - I)(B\nabla^2 G_l - \sigma I) \tag{2.143}$$

$$= \frac{1}{[u][v]([u]^2 + [v]^2)}\begin{pmatrix}[u] & [v]\end{pmatrix}\begin{pmatrix}[u][v] & [u]^2 \\ [v]^2 & [u][v]\end{pmatrix}\begin{pmatrix}-CG_{uu} & G_{vv} \\ G_{uu} & -CG_{uu}\end{pmatrix} \tag{2.144}$$

$$= G_{uu}\begin{pmatrix}\frac{1}{[u]} & \frac{1}{[v]}\end{pmatrix}\begin{pmatrix}-C & \frac{H_{vv}}{H_{uu}} \\ 1 & -C\end{pmatrix} \tag{2.145}$$

from (2.140) (note: $[v] = 0$ or $[u] = 0$ would imply a violation of the convexity of H as shown in appendix C). But (2.141) also implies that

$$\nabla\sigma^T = \begin{pmatrix}G_{uuv} + C_u G_{uu} + CG_{uuu} \\ G_{uvv} + C_v G_{uu} + CG_{uuv}\end{pmatrix}^T \tag{2.146}$$

$$= \left(\begin{pmatrix}C & 1 \\ \frac{H_{vv}}{H_{uu}} & C\end{pmatrix}\begin{pmatrix}G_{uuu} \\ G_{uuv}\end{pmatrix} + \begin{pmatrix}C_u G_{uu} \\ (\frac{H_{vv}}{H_{uu}})_u G_{uu} + C_v G_{uu}\end{pmatrix}\right)^T. \tag{2.147}$$

Equation (2.141) is invariant under the choice of conservation law G. Taking $G = H$ then gives

$$C = \frac{s - H_{uv}}{H_{uu}} \tag{2.148}$$

which implies that

$$\begin{pmatrix}C & 1 \\ \frac{H_{vv}}{H_{uu}} & C\end{pmatrix} = \frac{1}{H_{uu}}\begin{pmatrix}s - H_{uv} & H_{uu} \\ H_{vv} & s - H_{uv}\end{pmatrix} \tag{2.149}$$

which has determinant $(s - H_{uv})^2 - H_{uu}H_{vv}$, vanishing exactly when s is a characteristic speed. Thus if we again assume that the shock is not a contact discontinuity, we invert this matrix to arrive

29

at

$$\nabla (\log G_{uu})^T = \frac{1}{G_{uu}} (\nabla G_{uu})^T \tag{2.150}$$

$$= \left(\begin{pmatrix} \frac{1}{[u]} & \frac{1}{[v]} \end{pmatrix} \begin{pmatrix} -C & \frac{H_{vv}}{H_{uu}} \\ 1 & -C \end{pmatrix} - \begin{pmatrix} C_u & (\frac{H_{vv}}{H_{uu}})_u + C_v \end{pmatrix} \right) \begin{pmatrix} -C & \frac{H_{vv}}{H_{uu}} \\ 1 & -C \end{pmatrix}^{-1} \tag{2.151}$$

which determines G_{uu} up to a multiplicative factor. But from (2.140), we see that G is then also determined up to a multiplicative factor and linear combination with of u, v and uv. Thus we have proven the following Theorem

Theorem. *Consider a 2×2 Hamiltonian system (2.3) admitting Hamiltonian shocks, which are (generically) not contact discontinuities. If simple wave preservation fails then any conserved quantity G satisfying (2.101) and the corresponding Rankine-Hugoniot condition (2.102) across Hamiltonian shocks is given by*

$$G = g_1 u + g_2 v + g_3 uv + g_4 H \tag{2.152}$$

where g_i, $i = 1, ..., 4$ are constants.

2.3.4 Scalar case

For the scalar case a more direct approach is available which allows an infinite number of Hamiltonian shock conserved quantities G to be found in all cases. The Hamiltonian jump conditions (2.119) and (2.121) for the Hamiltonian symmetry generated by G, may be combined to obtain

$$[u][G'^2] - [G][G'] = 0 \tag{2.153}$$

and $W = -1$ so (2.133) becomes

$$\tilde{u}'(u_l) = J = -\frac{H_l'' - s}{H_r'' - s}. \tag{2.154}$$

If we assume for simplicity that the map $u_r = \tilde{u}(u_l)$ has just one fixed point (which will always hold locally) and we prescribe $G(u_r) = G_r(u_r)$, for an arbitrary smooth function G_r having the right side of this fixed point as its domain, we may find $G(u_l)$ on the other by solving the ODE

$$G_r(\tilde{u}(u_l)) - (\tilde{u}(u_l) - u_l)G_r'(\tilde{u}(u_l))/2 = G(u_l) - (u_l - \tilde{u}(u_l))G'(u_l)/2. \tag{2.155}$$

30

For an example we consider the simplest case: when H is even. Then H is conserved across $\tilde{u}(u_l) = -u_l$ since $[H] = 0$, so its Rankine-Hugoniot conditions hold automatically. Plugging this into (2.155):

$$G_r(-u_l) + u_l G_r'(-u_l) = G(u_l) - u_l G'(u_l) \tag{2.156}$$

which rearranges to

$$-u_l^2 \frac{d}{du_l}\left(\frac{G_r(-u_l)}{u_l}\right) = -u_l^2 \frac{d}{du_l}\left(\frac{G(u_l)}{u_l}\right) \tag{2.157}$$

that is solved by

$$G(u_l) = G_r(-u_l) + Bu_l \tag{2.158}$$

where B is an arbitrary constant. By enforcing continuous differentiability at $u_l = 0$ we get

$$G(u_l) = G_r(-u_l) = G(-u_l) \tag{2.159}$$

which shows that G is conserved across Hamiltonian shocks for even H when G is also even, assuming $\tilde{u}$ has only one fixed point.

2.4 Applications

In this section several examples admitting Hamiltonian shocks are considered and interactions of a kink with a rarefaction wave are numerically simulated. The presence or absence of classical dispersive shock generation in the interactions are in agreement with the theory. For the latter case the position of the kink and the evolution of the wave profile align with the analytic Hamiltonian shock computation.

2.4.1 Korteweg Models

The nonlinear wave equation

$$\begin{pmatrix} u \\ v \end{pmatrix}_t + \begin{pmatrix} -v \\ -\Sigma(u) \end{pmatrix}_x = 0 \tag{2.160}$$

arises in the description of a continuum system in Lagrangian coordinates. In this context, undercompressive shocks are often interpreted as phase boundaries (see e.g. [42], [43], [10], [24], [22] or [44]). These undercompressive shocks may be permitted due to failure of genuine nonlinearity

that occurs at inflection points of $\Sigma(u)$, but another possibility which arises is an elliptic strip $u_g < u < u_q$ dividing two hyperbolic half planes, which occurs when $\Sigma(u)$ is decreasing in u, on the elliptic interval.

Hamiltonian shocks arise in the $\epsilon \to 0$ limit of the dispersively perturbed systems admitting kinks which were studied in [22] with u representing the density and v the velocity for a liquid-vapor mixture with internal capillarity. In this case $\Sigma(u) = F'(u)$ with

$$H(u, v) = -\frac{v^2}{2} - F(u). \tag{2.161}$$

The nonlinear wave equation (2.160) then becomes

$$\begin{pmatrix} u \\ v \end{pmatrix}_t + \begin{pmatrix} -v \\ -F'(u) \end{pmatrix}_x = \begin{pmatrix} u \\ v \end{pmatrix}_t + \begin{pmatrix} 0 & 1 \\ 1 & 0 \end{pmatrix} \begin{pmatrix} H_u \\ H_v \end{pmatrix}_x = 0. \tag{2.162}$$

The Rankine-Hugoniot conditions, (2.3) and (2.4) for a Hamiltonian shock can be manipulated into the form

$$[v]^2 = [F'(u)][u] \tag{2.163}$$

and

$$(F'(u_r) + F'(u_l))[u] = 2[F(u)] \tag{2.164}$$

after eliminating s. So u_r depends entirely on u_l and

$$v_r = v_l \pm \sqrt{[F'(u)][u]}. \tag{2.165}$$

We now show that simple waves are not preserved by the Hamiltonian shock map when (2.162) is hyperbolic for all u, but first we derive the solvability condition for the fast-slow case in Theorem 2.2.2 is satisfied. Riemann invariants for (2.162) may be given by

$$\phi^k(u, v) = v + (-1)^k Q(u) \tag{2.166}$$

where $Q'(u) = \sqrt{F''(u)}$. Then from (2.165), the right side Riemann invariants are given by

$$\phi_r^k = v_l \pm \sqrt{[F'(u)][u]} + (-1)^k Q(u_r). \tag{2.167}$$

Thus, given knowledge of ϕ_l^1 and ϕ_r^2, v_l may be eliminated to obtain a relation between u_l and u_r from which u_l may be solved with the aid of (2.164):

$$\phi_r^2 - \phi_l^1 = \pm\sqrt{[F'(u)][u]} + Q(u_l) + Q(u_r). \tag{2.168}$$

Having found u_l, v_l and v_r may also be solved for determining the full problem.

Returning to the question of simple wave preservation, for $u > 0$, the eigenvectors are given by

$$\boldsymbol{r}_k = \begin{pmatrix} 1 \\ (-1)^k \sqrt{F''(u)} \end{pmatrix}, \tag{2.169}$$

and for $u < 0$ by

$$\boldsymbol{r}_k = \begin{pmatrix} 1 \\ (-1)^{k+1} \sqrt{F''(u)} \end{pmatrix} \tag{2.170}$$

and the Jacobian of the Hamiltonian shock map by

$$J = \begin{pmatrix} u_r'(u_l) & 0 \\ q & 1 \end{pmatrix} \tag{2.171}$$

where

$$q = \frac{d}{du_l}(\sqrt{[F'(u)][u]}) \tag{2.172}$$

$$= \frac{(F''(u_r)u_r'(u_l) - F''(u_l))[u] + [F'(u)](u_r'(u_l) - 1)]}{2\sqrt{[F'(u)][u]}}. \tag{2.173}$$

On the other hand, taking $u_l > 0$ without loss of generality,

$$J\boldsymbol{r}_k = \begin{pmatrix} u'_r(u_l) & 0 \\ q & 1 \end{pmatrix} \begin{pmatrix} 1 \\ (-1)^k \sqrt{F''(u)} \end{pmatrix} \tag{2.174}$$

$$= \begin{pmatrix} u'_r(u_l) \\ q + (-1)^k \sqrt{F''(u_l)} \end{pmatrix}. \tag{2.175}$$

So for simple wave preservation, it is required that

$$q + (-1)^k \sqrt{F''(u_l)} = \pm \sqrt{F''(u_r)} u'_r(u_l) \tag{2.176}$$

and

$$q - (-1)^k \sqrt{F''(u_l)} = \mp \sqrt{F''(u_r)} u'_r(u_l) \tag{2.177}$$

from which it immediately follows that $q = 0$. Equivalently, by (2.172),

$$(F''(u_r) u'_r(u_l) - F''(u_l))[u] + [F'(u)](u'_r(u_l) - 1)] = 0 \tag{2.178}$$

and differentiating (2.164) yields

$$(F''(u_r) u'_r(u_l) - F''(u_l))[u] - [F'(u)](u'_r(u_l) + 1) = 0 \tag{2.179}$$

which together imply that $[F'(u)]u'_r(u_l)$ vanishes identically. The quantity $u'_r(u_l)$ is non-vanishing and $F'(u_r) = F'(u_l)$ implies that the two are separated by an elliptic point u_*: $F''(u_*) < 0$. Thus simple waves are not preserved when hyperbolicity holds for all u, i.e., convex H. The lack of simple wave preservation for the case $H(u,v) = -\frac{1}{2}v^2 - u^4$ is shown in figure 2.5.

2.4.2   Internal waves for two layer sharply stratified fluids

Internal waves at the interface of two sharply stratified fluids of constant density $\rho_2 > \rho_1$ confined vertically between two plates can be modeled, in the long wave limit, by a quasilinear system, hyperbolic in an appropriate domain (see e.g. [36]). This system may be written in terms of the
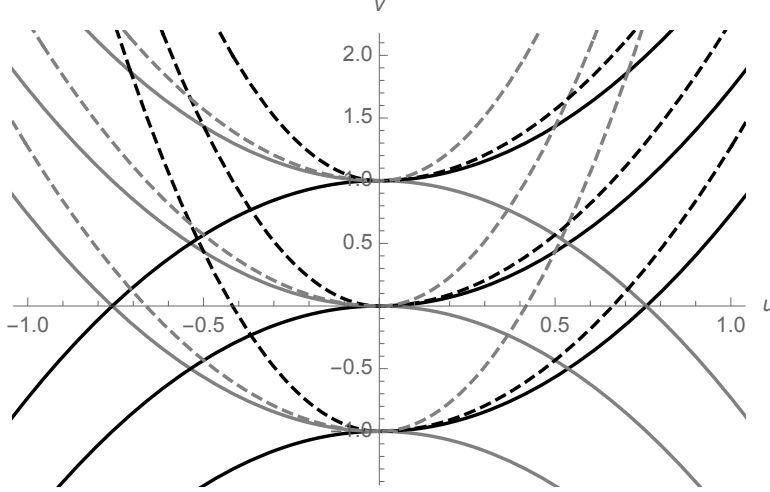
Figure 2.5: The simple wave curves (solid) for (2.162), with quartic Hamiltonian $H(u,v) = -\frac{1}{2}v^2 - u^4$, and their images under $\tilde{U}$ (dashed). The respective families are indicated by gray and black.

non-dimensional lower layer thickness u and momentum shear v:

$$\begin{pmatrix} u \\ v \end{pmatrix}_t + \begin{pmatrix} \frac{1-2u+ru^2}{(1-ru)^2}v & \frac{u(1-u)}{1-ru} \\ 1 - \frac{(1-r)v^2}{(1-ru)^3} & \frac{1-2u+ru^2}{(1-ru)^2}v \end{pmatrix} \begin{pmatrix} u \\ v \end{pmatrix}_x = 0. \tag{2.180}$$

This choice of variables admits the Hamiltonian structure (2.1) (see [45] and [15]):

$$0 = \begin{pmatrix} u \\ v \end{pmatrix}_t + \begin{pmatrix} \frac{u(1-u)}{1-ru}v \\ \frac{1}{2}\frac{1-2u+ru^2}{(1-ru)^2}v^2 + u \end{pmatrix}_x = \begin{pmatrix} u \\ v \end{pmatrix}_t + \begin{pmatrix} 0 & 1 \\ 1 & 0 \end{pmatrix} \begin{pmatrix} H_u \\ H_v \end{pmatrix}_x \tag{2.181}$$

Where

$$r = \frac{\rho_2 - \rho_1}{\rho_2} \tag{2.182}$$

and

$$H = \frac{1}{2}\left(\frac{u(1-u)v^2}{1-ru} + u^2\right). \tag{2.183}$$

Depending on the relative scales of effects not included in the model, e.g. viscosity or mixing, different pairs of Rankine-Hugoniot conditions will select weak solutions containing traveling fronts consistent with a given physical scenario (see [46]). In contrast, front solutions arising from the purely dispersive model of [7] must satisfy the jump condition (2.4) for conservation of energy in addition to the two conditions (2.3). In fact, it can be checked that this system may be written in

35

the perturbed Hamiltonian form (2.9) with

$$
H^\epsilon[u^\epsilon, v^\epsilon] = \frac{1}{2}\left(\frac{u^\epsilon(1-u^\epsilon)y^2}{1-ru^\epsilon} + u^{\epsilon 2}\right) +
$$
$$
\epsilon^2\frac{1}{6}\left((1-r+ru^\epsilon)(\frac{u^\epsilon(1-u^\epsilon)}{1-ru^\epsilon}y)^2_x - 2r\frac{u^\epsilon(1-u^\epsilon)}{1-ru^\epsilon}y(\frac{u^\epsilon(1-u^\epsilon)}{1-ru^\epsilon}y)_x u^\epsilon_x + \frac{u^\epsilon(1-^\epsilon u)}{1-r^\epsilon u}y^2u^{\epsilon 2}_x\right) \quad (2.184)
$$

and

$$
v^\epsilon = \mathcal{L}[u^\epsilon]y \quad (2.185)
$$
$$
= \left(1 + \frac{\epsilon^2}{3}\left(u^{\epsilon 2}_x + r\frac{u^\epsilon(1-u^\epsilon)}{1-ru^\epsilon}u^\epsilon_{xx} + r\partial\frac{u^\epsilon(1-u^\epsilon)}{1-ru^\epsilon}u^\epsilon_x - \partial^2(1-r+ru^\epsilon)\frac{u^\epsilon(1-u^\epsilon)}{1-ru^\epsilon}\right)\right)y. \quad (2.186)
$$

The Hamiltonian shock map has four branches:

$$
v_r = v_l \pm (1-(1+\sqrt{1-r})u_l) - \frac{\sqrt{1-r}}{1-ru_l}v_l \quad (2.187)
$$

$$
u_r = \frac{1}{1+\sqrt{1-r}}\left(1 \mp \frac{\sqrt{1-r}v_l}{1-ru_l}\right) \quad (2.188)
$$

for the first two branches, and for the other two branches

$$
v_r = v_l \pm (1-(1-\sqrt{1-r})u_l) + \frac{\sqrt{1-r}}{1-ru_l}v_l \quad (2.189)
$$

$$
u_r = \frac{1}{1-\sqrt{1-r}}\left(1 \pm \frac{\sqrt{1-r}v_l}{1-ru_l}\right). \quad (2.190)
$$

The fronts arising from the first two branches (2.189) and (2.190) have been studied previously [7] and connect two states across the NGN curves crossing in the center of the hyperbolic region (see figure 2.6). For these branches

$$
\{(u_l, v_l) : v_l = 0\} \leftrightarrow \{(u_r, v_r) : u_r = u_*\} \quad (2.191)
$$

where

$$
u_* = \frac{1}{1+\sqrt{1-r}} \quad (2.192)
$$

which is the well known critical depth ratio for which kinks survive when taking a weakly nonlinear

expansion (see section 2.4.3 below). The second pair of branches connect states which cross the NGN curves near the hyperbolic-elliptic boundary (see figure 2.6) and only produce substantial jumps in the presence of a large density difference.
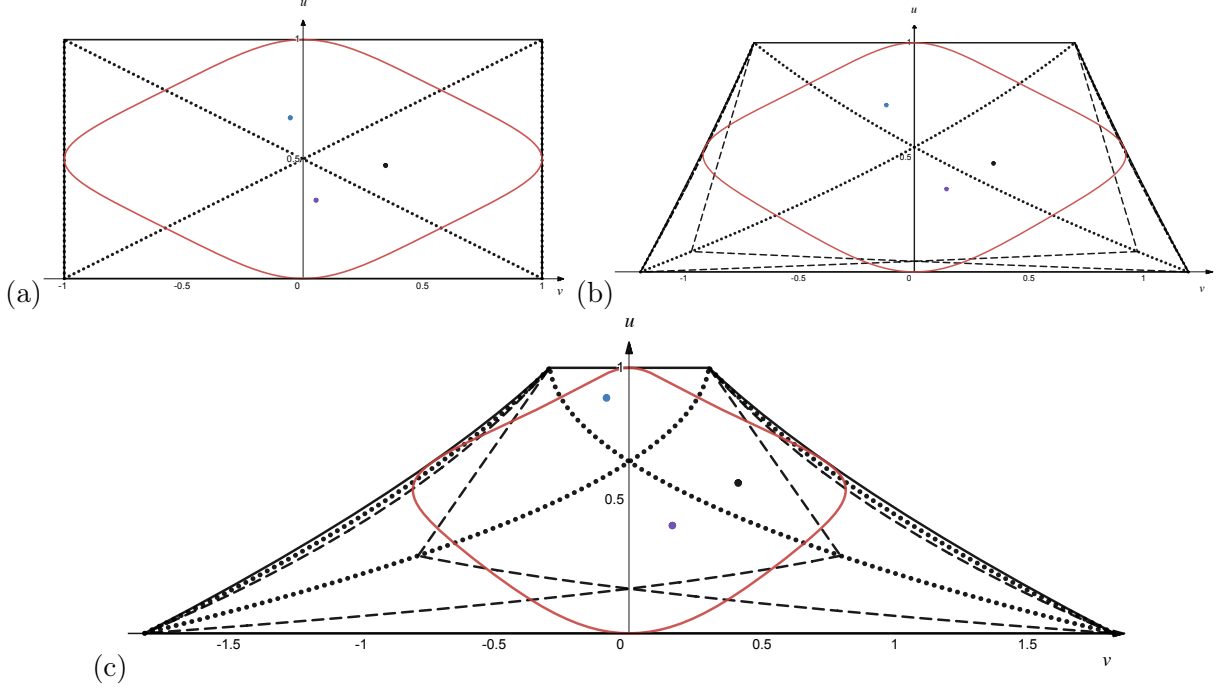
Figure 2.6: The hyperbolic region of (3.46) is shown for (a) $r = 0$, (b) $r = 0.3$, and (c) $r = 0.7$; its boundary is indicated by the bold curves. The NGN curves are dotted and the dashed curves are those which, when crossed by $\boldsymbol{U}_l$, result in one of the branches of $\tilde{\boldsymbol{U}}(\boldsymbol{U}_l)$ switching in or out of the hyperbolic region. For the curvilinear pentagon enclosed by black dashed curves and the top solid boundary, two branches are in the hyperbolic region. Each dashed line that is crossed in moving further out of this region corresponds to the departure of one more branch of $\tilde{\boldsymbol{U}}$ from the hyperbolic region. For the lower triangle (again, enclosed by curves in black), $\tilde{\boldsymbol{U}}$ has no branches going into the hyperbolic region. For $r = 0$, this pentagon degenerates to the entire (rectangular) hyperbolic region and two of the four smooth curves comprising the NGN locus merge into the boundary. The red curve encloses the region where H is convex. The black dot is a typical value of (u_l, v_l) and the blue and purple dots are its images (u_r, v_r) under the Hamiltonian shock maps given by the two branches of (2.189), (2.190).

Hamiltonian shock interaction The Jacobian J of the Hamiltonian shock map is given by

$$\begin{pmatrix} J_{11} & J_{12} \\ J_{21} & J_{22} \end{pmatrix} = \begin{pmatrix} -\frac{(1-\sqrt{1-r})\sqrt{1-rv}}{(1-ru)^2} & -\frac{\sqrt{1-r}}{(1+\sqrt{1-r})(1-ru)} \\ -(1+\sqrt{1-r}) - \frac{r\sqrt{1-r}}{(1-ru)^2}v & 1 - \frac{\sqrt{1-r}}{1-ru_l} \end{pmatrix}. \tag{2.193}$$

Simple wave preservation holds if and only if the right eigenvectors

$$\boldsymbol{r}_k(u_l, v_l) = \begin{pmatrix} \sqrt{\frac{u_l(1-u_l)}{1-ru_l}} \\ (-1)^k\sqrt{1 - \frac{(1-r)v_l^2}{(1-ru_l)^3}} \end{pmatrix}, \tag{2.194}$$

for $j = 1, 2$, on the left are mapped by J to the right eigenvectors on the right, i.e., become parallel to

$$\boldsymbol{r}_k(u_r, v_r) = \begin{pmatrix} \sqrt{\frac{u_r(1-u_r)}{1-ru_r}} \\ (-1)^k\sqrt{1 - \frac{(1-r)v_r^2}{(1-ru_r)^3}} \end{pmatrix}. \tag{2.195}$$

A lengthy calculation (using a symbolic manipulator) shows that this does not hold for $r \neq 0$. For $r = 0$

$$u_r = \frac{1}{2}(1 \pm v_l), \tag{2.196}$$

$$v_r = \mp(1 - 2u_l) \tag{2.197}$$

so the Jacobian becomes

$$\begin{pmatrix} J_{11} & J_{12} \\ J_{21} & J_{22} \end{pmatrix} = \begin{pmatrix} 0 & \pm\frac{1}{2} \\ \pm 2 & 0 \end{pmatrix}, \tag{2.198}$$

and the right eigenvectors on the left and right sides of the jump are

$$\boldsymbol{r}_{kl} = \begin{pmatrix} \sqrt{u_l(1 - u_l)} \\ (-1)^k\sqrt{1 - v_l^2} \end{pmatrix} \tag{2.199}$$

and

$$\boldsymbol{r}_{kr} = \begin{pmatrix} \frac{1}{2}\sqrt{1 - v_l^2} \\ (-1)^k 2\sqrt{u_l(1 - u_l)} \end{pmatrix} \tag{2.200}$$

which with (2.196) and (2.197) yields

$$J\boldsymbol{r}_{kl} = \boldsymbol{r}_{kr} \tag{2.201}$$

so that in the $r = 0$ case simple waves are preserved. Theorem (2.2.2) applies because it is not hard to check that the Hamiltonian shocks occurring in this system are strictly fast or strictly slow (this check is most easily accomplished numerically).

Hamiltonian shock interaction problem for the Boussinesq limit For the $r = 0$ case we can compute the Hamiltonian shock solution explicitly for a continuous solution (u^c, v^c) of the hyperbolic system (2.181) interacting with a shock starting at a point x_0 as in section 2.2. To accomplish this we make use of the map (see reference [36, 47])

$$\hat{u} = (1 - 2u)v, \qquad \hat{v} = (1 - v^2)(u - u^2) \tag{2.202}$$

transforming the system (2.181) into the Airy shallow water system

$$\hat{v}_t + (\hat{u}\hat{v})_x = 0, \tag{2.203}$$

$$\hat{u}_t + (\frac{1}{2}\hat{u}^2 + \hat{v})_x = 0. \tag{2.204}$$

The transformation (3.61) has four inverses (see [15]):

$$u_{ij} = \frac{1}{2}\left(1 + (\operatorname{sgn}\hat{u})^{i+1}(-1)^{(i+j+1)}\sqrt{Q - (-1)^i\sqrt{Q^2 - \hat{u}^2}}\right) \tag{2.205}$$

and

$$v_{ij} = -(\operatorname{sgn}\hat{u})^i(-1)^{(i+j+1)}\sqrt{Q + (-1)^i\sqrt{Q^2 - \hat{u}^2}} \tag{2.206}$$

where $j = 1, 2$ and

$$Q = \frac{\hat{u}^2 - 4\hat{v} + 1}{2} \tag{2.207}$$

(hereinafter we adorn the dependent variables with hats when they are obtained through the map (3.61)). Figure 3.2 shows the images of the four branches while figure 3.3 shows the image $\tilde{\Omega}$ of the hyperbolic region Ω of the two layer system (3.46) under the map (3.61) along with the singular curves

$$u = \frac{1}{2} \pm \frac{v}{2}. \tag{2.208}$$

Note that these are level curves of the Riemann invariants

$$R^j(\hat{u}, \hat{v}) = \hat{u} + 2(-1)^j\sqrt{\hat{v}} \tag{2.209}$$

39

since

$$Q^2 - \hat{u}^2 = \frac{1}{16}(1 - 2\hat{u}^2 + \hat{u}^4 - 4\hat{v} - 4\hat{v}\hat{u}^2 + 16\hat{v}^2) \tag{2.210}$$

$$= \frac{1}{16}((R^1)^2 - 1)((R^2)^2 + 1). \tag{2.211}$$

We assert that (u_{1j}, v_{1j}) is connected to (u_{2k}, v_{2k}) by a Hamiltonian shock, $j, k = 1, 2$. This follows from the identity

$$s := \frac{f_{2k} - f_{1j}}{u_{2k} - u_{1j}} = \frac{g_{2k} - g_{1j}}{v_{2k} - v_{1j}} = \frac{1}{2}(\hat{u} + (-1)^{j+k}) \tag{2.212}$$

where f and g are the fluxes for (2.181):

$$f_{jk} = \frac{1}{2}(u_{jk}(1 - u_{jk}))v_{jk}, \qquad g_{jk} = \frac{1}{2}(1 - 2u_{jk})v_{jk} + u_{jk}. \tag{2.213}$$

That these are Hamiltonian follows since

$$H_{jk} = \frac{1}{2}(1 - v_{jk}^2)(u_{jk} - u_{jk}^2) + \frac{1}{2}u_{jk} \tag{2.214}$$

$$= \frac{1}{2}(u_{jk} - \hat{u}) \tag{2.215}$$

and the corresponding fluxes are given by

$$F_{jk} = H_u H_v|_{u=u_{jk}, v=v_{jk}} = \frac{1}{2}(f_{jk} - \hat{f}), \tag{2.216}$$

so

$$\frac{F_{2k} - F_{1j}}{H_{2k} - H_{1j}} = \frac{f_{2k} - f_{1j}}{u_{2k} - u_{1j}} = s. \tag{2.217}$$

For concrete illustration, we consider the slow undercompressive case with (u^c, v^c) in the $1, 1$ quadrant (see figure 3.2) and (u_r, v_r) is in the $2, 1$ quadrant; the other cases are solved simliarly. The solution is given by

$$u(x, t) = \begin{cases} u_c(x, t), & x \le \mathfrak{s}(t) \\ u_{21}(\hat{u}(u_c(x, t), v_c(x, t)), \hat{v}(u_c(x, t), v_c(x, t))), & x > \mathfrak{s}(t), \end{cases} \tag{2.218}$$

40
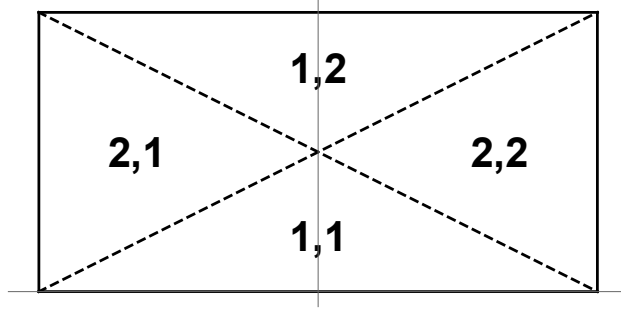
Figure 2.7: The i, j quadrant is the image of the curved triangle in figure 3.3 under $(\hat{u}_{ij}, \hat{v}_{ij})$ with v and u plotted on the horizontal and vertical axes respectively. The dotted lines are the singular curves of the map $(u, v) \to (\hat{u}, \hat{v})$.
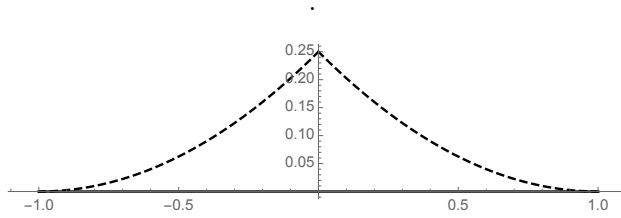
Figure 2.8: The image $\tilde{\Omega}$ of the hyperbolic region Ω under the map $(u, v) \to (\hat{u}, \hat{v})$, with $\hat{u}$ and $\hat{v}$ plotted on the horizontal and vertical axes respectively. The dotted curves are the image of the singular curves.

and

$$v(x, t) = \begin{cases} v_c(x, t), & x \leq \mathfrak{s}(t) \\ v_{21}(\hat{u}(u_c(x,t), v_c(x,t)), \hat{v}(u_c(x,t), v_c(x,t))), & x > \mathfrak{s}(t) \end{cases} \tag{2.219}$$

and $\mathfrak{s}(t)$ solves the initial value problem

$$\mathfrak{s}'(t) = \frac{1}{2}(\hat{u}(u_c(\mathfrak{s}(t), t), v_c(\mathfrak{s}(t), t)), \hat{v}(u_c(\mathfrak{s}(t), t), v_c(\mathfrak{s}(t), t)) + 1), \tag{2.220}$$

$$a(0) = x_0. \tag{2.221}$$

For an explicit example, let (u_c, v_c) be a centered simple wave:

$$u_c(x, t) = \begin{cases} u_a, & x/t \leq \lambda_a = \hat{u}(u_a, v_a) + \sqrt{\hat{v}(u_a, v_a)} \\ u_{11}(\frac{\phi + 2x/t}{3}, (\frac{\phi - x/t}{3})^2), & \lambda_a < x/t < \lambda_l \\ u_l, & x/t \geq \lambda_l = \hat{u}(u_l, v_l) + \sqrt{\hat{v}(u_l, v_l)}, \end{cases} \tag{2.222}$$

41

$$
v_c(x, t) = \begin{cases} v_a, & x/t \leq \lambda_a = \hat{u}(u_a, v_a) + \sqrt{\hat{v}(u_a, v_a)} \\ v_{11}(\frac{\phi + 2x/t}{3}, (\frac{\phi - x/t}{3})^2), & \lambda_a < x/t < \lambda_l \\ v_l, & x/t \geq \lambda_l = \hat{u}(u_l, v_l) + \sqrt{\hat{v}(u_l, v_l)}, \end{cases} \tag{2.223}
$$

with ϕ a constant (a Riemann invariant) having

$$
u_{11}(\frac{\phi + 2\lambda_a}{3}, (\frac{\phi - \lambda_a}{3})^2) = u_a \tag{2.224}
$$

and

$$
u_{11}(\frac{\phi + 2\lambda_b}{3}, (\frac{\phi - \lambda_b}{3})^2) = u_b. \tag{2.225}
$$

Then the interaction is given according to (2.218) and (2.219) with

$$
\mathfrak{s}(t) = \begin{cases} x_0 + s_0 t, & t \leq t_i \\ \frac{R-3}{4}t + c_0 t^{1/3}, & t_i < t < t_e \\ x_e + s_e(t - t_e), & t \geq t_e \end{cases} \tag{2.226}
$$

where s_0 is the shock speed for the initial jump and

$$
t_i = \frac{x_0}{\lambda_r - s_0}, \qquad x_i = \lambda_r t_i, \qquad \lambda_r = \lambda_l, \tag{2.227}
$$

$$
c_0 = t_i^{-1/3}(x_i - t_i\frac{\phi - 3}{4}), \qquad t_e = \left(\frac{\lambda_l - \frac{R-3}{4}}{c_0}\right)^{-3/2}, \tag{2.228}
$$

and

$$
x_e = \lambda_l t_e. \tag{2.229}
$$

Figure 2.9 shows the passage of the hamiltonian shock through the centered simple wave for $u_l = 0.33$, $v_l = 0.2$, $u_a = 0.15$, $v_a \approx -0.225$, $u_r = 0.6$ and $v_r = -0.34$. Snapshots of this solution are also shown in figure 2.10 where comparison is made with a numerically computed solution for a Hamiltonian perturbation.
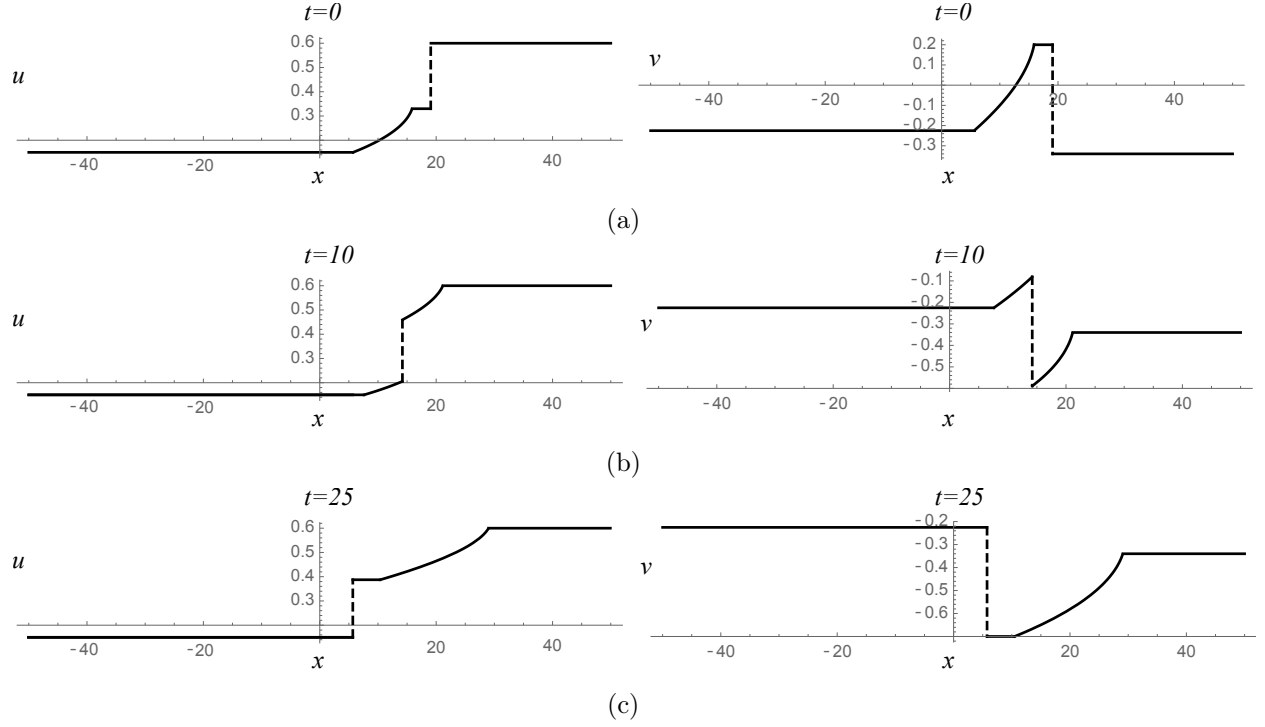
Figure 2.9: The interaction of a simple wave with a Hamiltonian shock with $u(x, t)$ shown on the left and $v(x, t)$ on the right.

2.4.3   Weakly nonlinear expansion

A weakly nonlinear expansion may be taken about a fixed layer thickness u_0 under the assumption of small velocity which corresponds to $v_0 = 0$ in the present variables.[1] Keeping four orders in the Hamiltonian (2.183), we get

$$H = \frac{1}{2}(z^2 + \alpha v^2 + \beta z v^2 - \gamma v^2 z^2), \tag{2.230}$$

Where

$$\alpha = u_0 \frac{1 - u_0}{1 - r u_0}, \tag{2.231}$$

$$\beta = \frac{1 - 2u_0 + r u_0^2}{(1 - r u_0)^2}, \tag{2.232}$$

---

[1]See [7] for careful assymptotic derivations.

and

$$\gamma = \frac{1-r}{(1-ru_0)^3}. \tag{2.233}$$

The system can then be written

$$0 = \begin{pmatrix} z \\ v \end{pmatrix}_t + \begin{pmatrix} \alpha v + \beta vz - \gamma vz^2 \\ z + \frac{\beta}{2}v^2 - \gamma v^2 z \end{pmatrix}_x = \begin{pmatrix} u \\ v \end{pmatrix}_t + \begin{pmatrix} 0 & 1 \\ 1 & 0 \end{pmatrix} \begin{pmatrix} H_z \\ H_v \end{pmatrix}_x. \tag{2.234}$$

In this case the dispersive term is linear (see [7]) and may be made to contain only spatial derivatives by exploiting asymptotic equivalencies. So the dispersive system may be written

$$H^\epsilon = \frac{1}{2}(z^2 + \alpha v^2 + \beta zv^2 - \gamma v^2 z^2 - \epsilon^2 z_x^2), \tag{2.235}$$

$$0 = \begin{pmatrix} z \\ v \end{pmatrix}_t + \begin{pmatrix} \alpha v + \beta vz - \gamma vz^2 \\ z + \frac{\beta}{2}v^2 - \gamma v^2 z + \epsilon z_{xx} \end{pmatrix}_x = \begin{pmatrix} z \\ v \end{pmatrix}_t + \begin{pmatrix} 0 & 1 \\ 1 & 0 \end{pmatrix} \begin{pmatrix} \delta_z H \\ \delta_v H \end{pmatrix}_x \tag{2.236}$$

and away from the critical value u_* (see (2.192)) which is the only physically relevant root of the equation $\beta = 0$, the fourth order term $\gamma v^2 z^2$ can be ignored because it of its higher asymptotic order. In this case (2.236) becomes the Boussinesq shallow water system with z replaced by

$$w = \beta z + \alpha. \tag{2.237}$$

Thus the system is described entirely in terms of one of the layers, which layer depending on the sign of β and the "bottom" as viewed from the corresponding single layer model. This is either the top or the bottom confining wall depending on which side of the critical value u_* the unperturbed interface height u_0 falls, with the other confining wall being lost to higher order asymptotics. On the other hand, when u_0 is sufficiently near the critical depth u_*, β will be small enough that the fourth order term becomes relevant and conjugate states will occur (see e.g. [48] or [7]).

We note that, by performing the change of variable $z = w + C$ with $C = \frac{-\beta \pm \sqrt{\beta^2 + 4\alpha\gamma}}{2\gamma}$, equation (2.230) becomes

$$H = \frac{1}{2}(w^2 + (2\beta \pm \sqrt{\beta^2 + 4\alpha\gamma})wv^2 - \gamma v^2 w^2) \tag{2.238}$$

and taking the plus branch guarantees that all coefficients are positive. But up to rescaling of constants, this is just the Hamiltonian (2.183) with $r = 0$. That is to say that in the weakly nonlinear limit, even at critical depth, the mathematical structure is independent of the densities and determines only a scaling of coefficients. Therefore, from the standpoint of Hamiltonian shocks, it suffices, in the weakly nonlinear case, to study the systems (2.181) since the case $r = 0$ of the latter subsumes the mathematical properties of the weakly nonlinear system for any densities.

2.4.4 Unidirectional model

A further simplification of (2.236) consists of considering the evolution of the system on a lower dimensional manifold (a curve in this case). For the hyperbolic system (2.234) this can be done exactly using simple waves, as seen above, and asymptotically in the dispersive case. The result is equivalent to the combined KdV-mKdV equation (see [7])

$$u_t + (\beta u^2/2 + u^3/3 - \epsilon^2 u_{xx})_x. \tag{2.239}$$

This is equivalent via the transformation

$$u(x,t) \to u(x - \frac{\beta^2}{4}t, t) + \frac{\beta}{2} \tag{2.240}$$

to the mKdV equation

$$u_t + (u^3/3 - u_{xx})_x = 0 \tag{2.241}$$

which can be written in Hamiltonian form:

$$u_t + \partial_x \delta H^\epsilon[u] = 0 \tag{2.242}$$

where

$$H^\epsilon = \frac{u^4}{12} + \epsilon^2 \frac{u_x^2}{2}. \tag{2.243}$$

The dispersionless reduction is

$$u_t + (u^3/3)_x = u_t + \partial_x H'(u) = 0 \tag{2.244}$$

where

$$H = \frac{u^4}{12}. \tag{2.245}$$

In this case, the computation of a non-dissipative shock moving through a rarefaction fan was carried out in [20].

2.4.5 Infinitude of conservation laws

According to the result of section 2.3, the nonlinear wave equation (2.162) and the two later system (2.181) with $r \neq 0$, for which the Hamiltonian shock map is not simple wave preserving, will not have local conserved quantities beyond u, v, uv and H. For the system (2.181) with $r = 0$ on the other hand, any conservation law

$$\hat{G}(\hat{u}, \hat{v})_t + \hat{M}(\hat{u}, \hat{v})_x = 0 \tag{2.246}$$

of the Airy system (2.203) gives rise, via the map (3.61), to a conservation law

$$G(u, v)_t + M(u, v)_x = 0 \tag{2.247}$$

where

$$G(u, v) = \hat{G}(\hat{u}(u, v), \hat{v}(u, v)) \tag{2.248}$$

and

$$M(u, v) = \hat{M}(\hat{u}(u, v), \hat{v}(u, v)). \tag{2.249}$$

The quantity G is Hamiltonian shock conserved since

$$-s[G] + [M] = -s[\hat{G}(\hat{u}, \hat{v})] + [\hat{M}(\hat{u}, \hat{v})] = 0. \tag{2.250}$$

Therefore an infinite number of conservation laws can be found.

Similarly for the unidirectional case, the map $\hat{u} = u^2$ sends (2.244) to

$$\hat{u}_t + \hat{u}\hat{u}_x = 0 \tag{2.251}$$

whose conservation laws may be pulled back in a like manner. We point out that in this case the

map $\tilde{u}$ extends to the well known Miura map

$$\hat{u}^\epsilon = u^\epsilon + \sqrt{6}\epsilon u_x^\epsilon \tag{2.252}$$

sending solutions of the perturbed (mKdV) equation (3.47) to the KdV equation

$$\hat{u}_t^\epsilon + \hat{u}^\epsilon \hat{u}_x^\epsilon - \epsilon \hat{u}_{xxx}^\epsilon = 0 \tag{2.253}$$

mapping kinks to solitary waves.

2.4.6   Numerics

Simulations of the interaction problem from section 2.2 were performed on dispersive perturbations of the nonlinear wave equation (2.162) and the two layer system (2.181). The results align with the theory, both in that classical dispersive shocks form when simple wave preservation fails and that when they do not form, the perturbed interaction is well approximated by the weak solution to the hyperbolic system given by Hamiltonian shock interaction.

Two layer stratified fluids   The dispersive two layer system from [7], which evolves under (2.9) with Hamiltonian H^ϵ given by (2.184), is ill-posed, a consequence of the Kelvin-Helmholtz instability. Thus further regularization is required in order to perform simulations. This is achieved in [17] by including terms corresponding to surface tension (see [49] for an alternative approach to stabliziation). The approach we have taken is to exclude several terms in the dispersive perturbation resulting in the following Hamiltonian:

$$H^\epsilon[u^\epsilon, v^\epsilon] = \frac{1}{2}\left(\frac{u^\epsilon(1-u^\epsilon)y^2}{1-ru^\epsilon} + u^{\epsilon 2}\right) + \epsilon^2 \frac{1}{2}\left(\frac{u^\epsilon(1-u^\epsilon)}{1-ru^\epsilon}y\right)_x^2 \tag{2.254}$$

and

$$v^\epsilon = \mathcal{L}[u^\epsilon]y \tag{2.255}$$

$$= \left(1 - \partial^2 \frac{u^\epsilon(1-u^\epsilon)}{1-ru^\epsilon}\right)y \tag{2.256}$$

$$= y + u_{xt}^\epsilon. \tag{2.257}$$

Then, dropping ϵ superscripts, the perturbed system (2.9) becomes

$$\begin{pmatrix} u \\ y + u_{xt} \end{pmatrix}_t + \begin{pmatrix} \frac{1-2u+ru^2}{(1-ru)^2}y & \frac{u(1-u)}{1-ru} \\ 1 - \frac{(1-r)y^2}{(1-ru)^3} & \frac{1-2u+ru^2}{(1-ru)^2}y \end{pmatrix} \begin{pmatrix} u \\ y \end{pmatrix}_x = 0. \tag{2.258}$$

Linearizing around a steady state via the typical ansatz

$$\begin{pmatrix} u(x,t) \\ y(x,t) \end{pmatrix} = \begin{pmatrix} u_0 \\ y_0 \end{pmatrix} + e^{i(kx-\omega t)} \begin{pmatrix} u_1 \\ y_1 \end{pmatrix} \tag{2.259}$$

yields the condition for well-posedness:

$$A \pm \sqrt{BC + (BC - A)(1 + Bk^2)} > 0 \tag{2.260}$$

for all real k where $A = H_{uy}$, $B = H_{yy}$ and $C = H_{uu}$ which holds exactly when H is convex (the region enclosed by the red curve in figure 2.6).

To find traveling wave solutions $u(x,t) = U(x - ct)$, $y(x,t) = V(x - ct)$, we integrate to obtain

$$\begin{pmatrix} -cU + \frac{U(1-U)V}{1-rU} \\ -cV + \frac{1}{2}\frac{1-2U+rU^2}{(1-rU)^2}V^2 + U + c^2 U'' \end{pmatrix} = \begin{pmatrix} A_1 \\ A_2 \end{pmatrix}. \tag{2.261}$$

From this we may deduce that

$$V = \frac{(A_1 + cU)(1 - rU)}{U(1 - U)}. \tag{2.262}$$

Substituting into the second equation and integrating once more we get

$$\frac{U'^2}{2} = \frac{U^4 - (1 + 2A_2 - rc^2)U^3 + (2A_2 - 2A_3 + c^2 - 2A_1cr)U^2 + (2A_3 + 2A_1c - A_1^2 r)U + A_1^2}{2c^2 U(1 - U)}. \tag{2.263}$$

Since U and $1 - U$ are both positive in the hyperbolic region, the right side is a positive multiple of an upward facing quartic on that region and thus has double roots yielding kink solutions when the numerator takes the form $(U - u_l)^2(U - u_r)^2$.

Figure 2.10 shows the interaction for the Boussinesq limit with the analytically computed Hamiltonian shock solution superimposed. Figure 2.11 shows the interaction of a kink with a simple
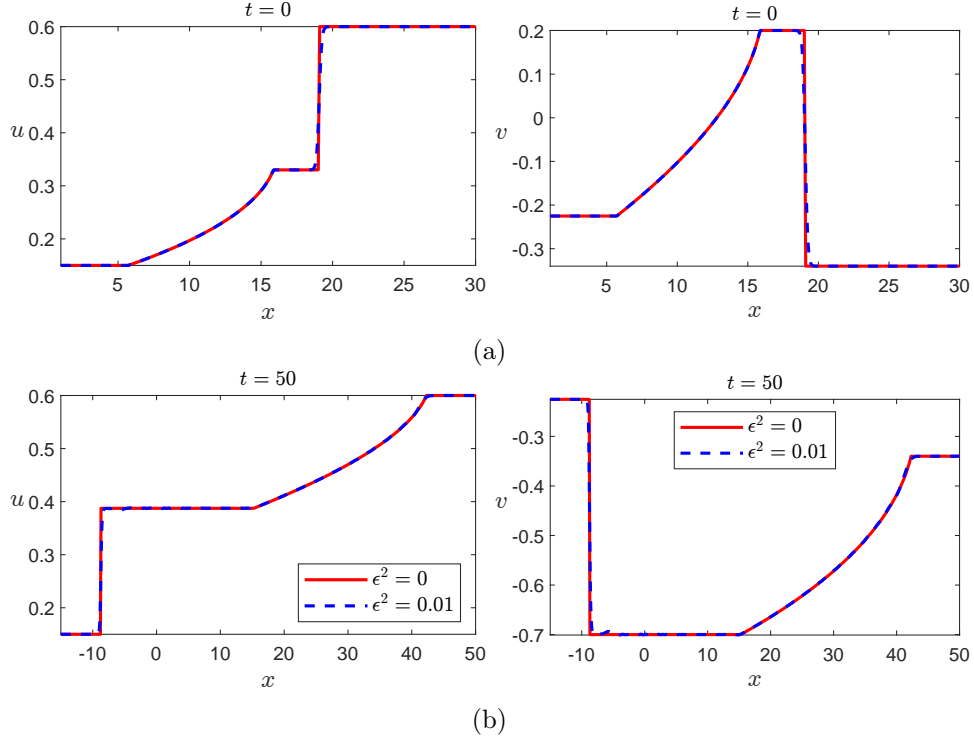
Figure 2.10: A Hamiltonian shock and a simple wave before and after interacting for the Boussinesq limit: (2.258) with $r = 0$.

wave for $r = 0$, 0.2 and 0.5. A dispersive shock forms when $r \neq 0$, in line with the failure of simple wave preservation in this case.

In interpreting the graphs of the $r = 0$ case, we note that, since the system (2.9) is dispersive, convergence to continuous hyperbolic solutions for small ϵ is well known to be subject to gentler ripples (see e.g. [50]) resulting from higher order effects, which have also been studied by asymptotic methods [51]. These ripples are qualitatively different than classical dispersive shocks; to begin with the left and right edges do not connect distinct states.

Korteweg model   In the case of a Korteweg model, we used a system with cubic flux

$$
\begin{pmatrix} u \\ v \end{pmatrix}_t + \begin{pmatrix} v \\ -4u^3 + \epsilon^2 u_{xx} \end{pmatrix}_x = \begin{pmatrix} u \\ v \end{pmatrix}_t + \begin{pmatrix} 0 & 1 \\ 1 & 0 \end{pmatrix} \begin{pmatrix} \delta_u H \\ \delta_v H \end{pmatrix}_x = 0 \tag{2.264}
$$

resulting from the Hamiltonian

$$
H = -\frac{v^2}{2} - u^4 - \epsilon^2 \frac{u_x^2}{2} \tag{2.265}
$$
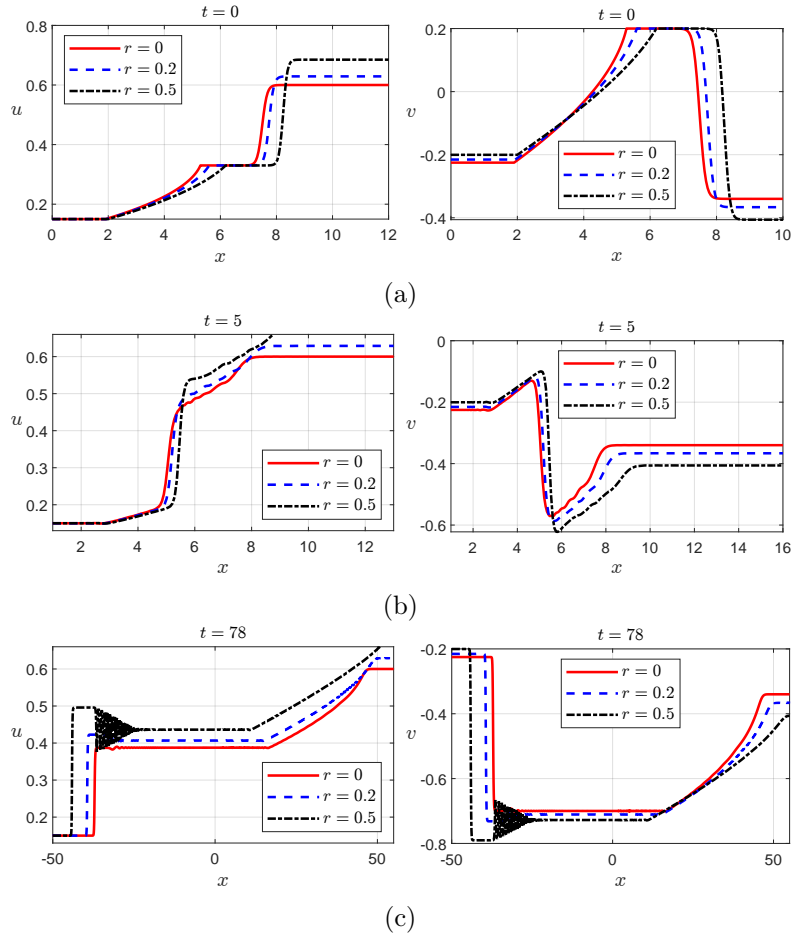
Figure 2.11: Snapshots of a Hamiltonian shock interaction for various values of r.
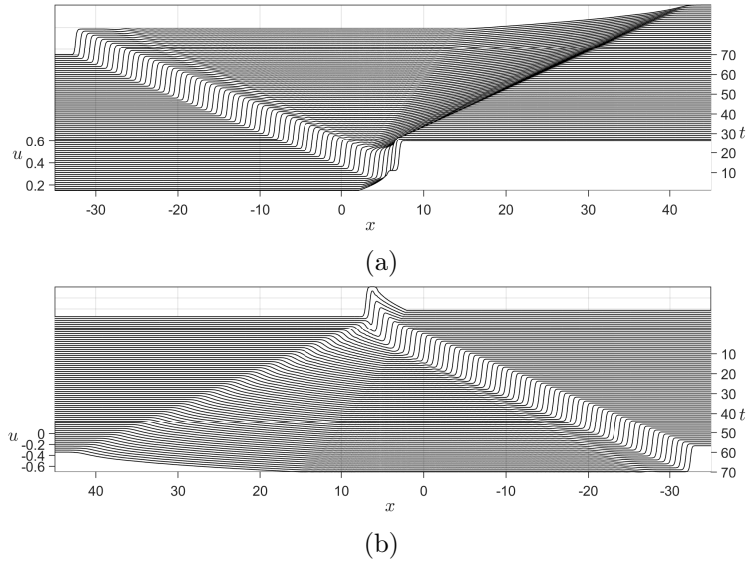
Figure 2.12: Evolution of the Hamiltonian shock interaction with $r = 0$, corresponding to the red curve in figure 2.11.
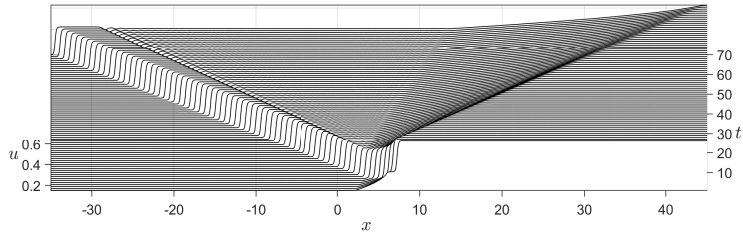
(a)
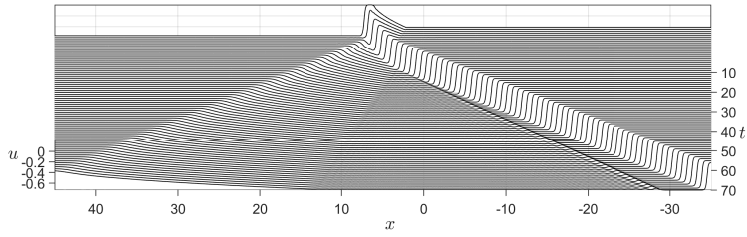
(b)

Figure 2.13: Evolution of the Hamiltonian shock interaction with $r = 0.2$, corresponding to the blue curve in figure 2.11.
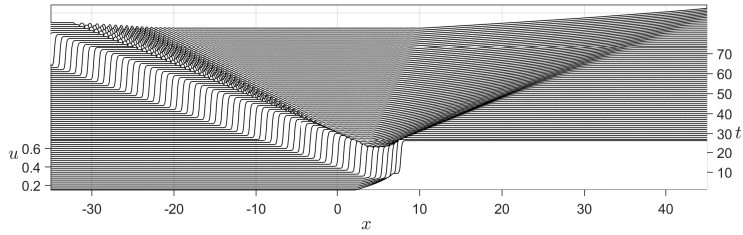
(a)
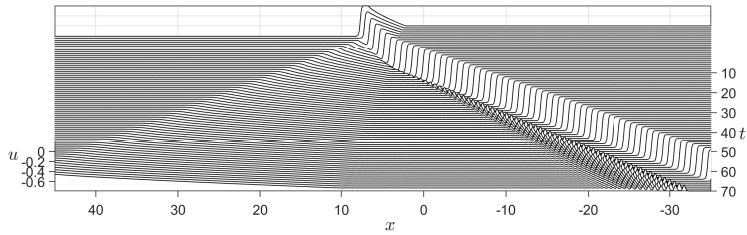
(b)

Figure 2.14: Evolution of the Hamiltonian shock interaction with $r = 0.5$, corresponding to the blue curve in figure 2.11.

whose unconditional well-posedness is easily checked.

To obtain traveling wave solutions $u(x,t) = U(x-ct)$, $v(x,t) = V(x-ct)$, we integrate

$$\begin{pmatrix} -cU - V \\ -cV - 4U^3 + \epsilon^2 U'' \end{pmatrix}' = 0. \tag{2.266}$$

From the first component equation we may solve $V = A_1 - cU$ where A_1 is a constant and putting this into the second we get

$$-cA_1 + c^2 U - 4U^3 + \epsilon^2 U'' = A_2. \tag{2.267}$$

Multiplying by U' and integrating yields

$$U'^2/2 = \frac{1}{\epsilon^2} \left(A_0 + (cA_1 + A_2)U - \frac{c^2}{2} U^2 + U^4 \right). \tag{2.268}$$

which is an upward facing quartic, producing heteroclynic orbits when double roots occur.

Figures 2.16 and 2.15 show the interaction of a kink with initial conditions, constant in u and piecewise linear in v which lead to global continuous solution in the absence of Hamiltonian shock interaction. A dispersive shock forms, in line with the failure of simple wave preservation for this system.
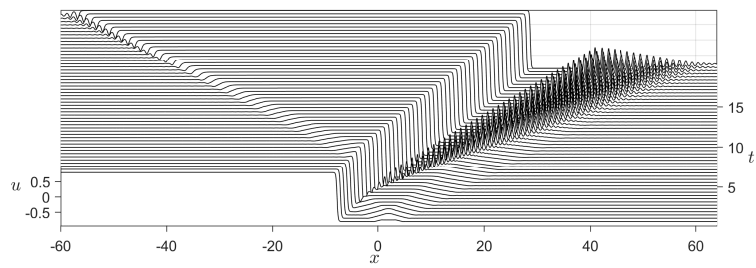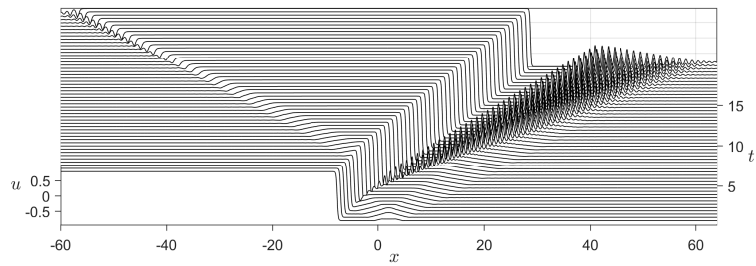
Figure 2.15: Evolution of the Hamiltonian shock interaction for (a) u and (b) v for the Korteweg model (2.264).
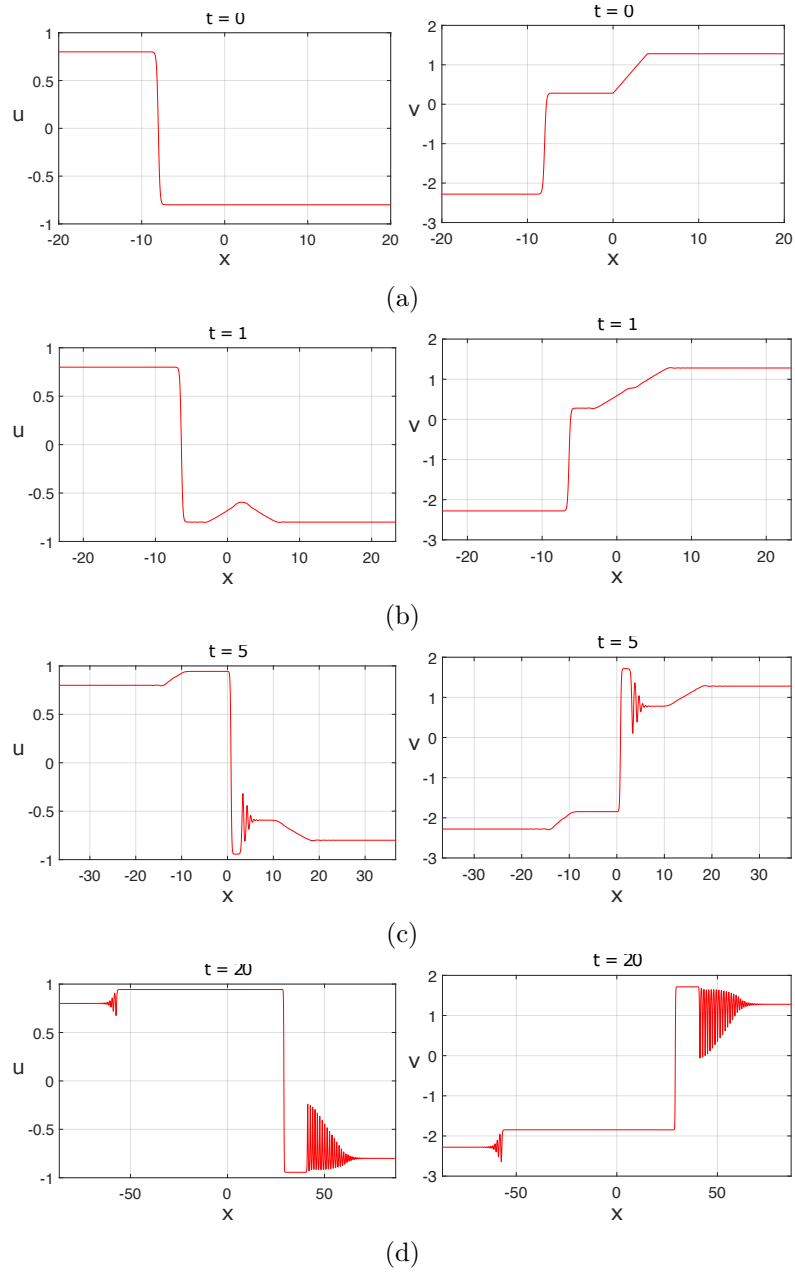
Figure 2.16: Snapshots of the Hamiltonian shock interaction for the Korteweg model portrayed in figure (2.15).

CHAPTER 3

Evolution of derivative singularities

3.1 Introduction

Models of water wave propagation, both surface and internal to a density stratified fluid, often lead to a "core" hyperbolic structure (see eg., [13, 36, 47] for a partial list), and in this context self-similar special exact solutions provide useful information on the evolution of more general initial data [15, 16]. However, in order to be physically relevant, these special solutions often generate discontinuous derivatives, whose evolution can then be tracked within the model thanks to general tools for hyperbolic systems. As is well known, a hyperbolic system of partial differential equations (see e.g. [13]) admits solutions with persisting discontinuous derivatives of some order along characteristics. An element of the aforementioned water wave models is the presence of corner-type singularities (i.e., first order derivative jumps) in the initial data, and fissioning of these points along multiple characteristics can be expected. In this work we study this phenomenon and related issues.

Specifically, this chapter considers *(i)* the splitting of corner points and *(ii)* solutions containing points where the spatial derivative is infinite but the solution evolves continuously without smoothing or the formation of a jump discontinuity for a quasilinear hyperbolic system of conservation laws. For the splitting of corners, an approach using distributional ansatzes is developed, further elaborating an idea from [16]. This generalizes the classical approach of [13] to the emergence of several corners from a single point. Then it is shown how the failure of genuine nonlinearity (see below for definition) is necessary and sufficient for the sustenance of an infinite spatial derivative along a characteristic without either of the most typical scenarios: instantaneous smoothing or shock formation. Finally, in the second half of the paper, these results are discussed in relation to explicit solutions of systems arising in shallow water flow.

3.2 Notation

Let $\boldsymbol{U}(x,t)$ be the mapping of (a subset of) the space-time half-plane $(x,t) \in \mathbb{R} \times \mathbb{R}^+$ to an n-dimensional vector in $\mathbb{R}^n$, i.e., $\boldsymbol{U} : \mathbb{R} \times \mathbb{R}^+ \to \mathbb{R}^n$, defined to be the solution of the quasilinear

system

$$\partial_t \boldsymbol{U} + \partial_x \big(\boldsymbol{F}(\boldsymbol{U}) \big) = 0, \tag{3.1}$$

or its weak form

$$\int_0^\infty \int_{-\infty}^\infty (\partial_t \phi) \boldsymbol{U} + (\partial_x \phi) \big(\boldsymbol{F}(\boldsymbol{U}) \big) dx dt + \int_{-\infty}^\infty \boldsymbol{U}(x,0) \phi(x,0) dx = 0, \tag{3.2}$$

for any ϕ supported on a compact subset of $(-\infty, \infty) \times [0, \infty)$ and differentiable on $(-\infty, \infty) \times (0, \infty)$, with initial condition

$$\boldsymbol{U}(x,0) = \boldsymbol{U}_0(x). \tag{3.3}$$

The Jacobian matrix $D\boldsymbol{F}$ with components $A_{ij} \equiv \partial F_i / \partial U_j$ where dropping bolds and adding subscripts indicates taking vector components, is assumed diagonalizable with real and distinct eigenvalues $\lambda_1(\boldsymbol{U}) < \lambda_2(\boldsymbol{U}) < ... < \lambda_n(\boldsymbol{U})$. We denote a corresponding set of right eigenvectors by $\boldsymbol{r}_1, \boldsymbol{r}_2, ..., \boldsymbol{r}_n$. For our purposes the function $\boldsymbol{F} : \mathbb{R}^n \to \mathbb{R}^n$ is assumed to be at least twice continuously differentiable.

A common assumption known as genuine nonlinearity, which was formulated in the seminal work [27] is (note, Einstein convention of summation over repeated indices is not used)

$$0 \neq D\lambda_k(\boldsymbol{U}) \boldsymbol{r}_k. \tag{3.4}$$

In the present work we shall consider the failure of this condition, i.e., the existence of points $\boldsymbol{U}$ where

$$0 = D\lambda_k(\boldsymbol{U}) \boldsymbol{r}_k, \tag{3.5}$$

in multiple settings (see also e.g. [52, 53, 24, 18, 54, 10] for further applications, in particular to the problem of shocks). We shall call the manifold of such points the NGNL manifold.

3.3   Splitting of corner points

In this section we consider how a gradient jump in an initial condition for a hyperbolic system (3.2) will split, traveling on a subset of the characteristics emanating from the point $(x, t) = (x_0, 0)$,

where $\boldsymbol{U}_0(x)$ is continuously differentiable except at $x = x_0$:

$$\lim_{x \to x_0^-} \boldsymbol{U}_0'(x) \neq \lim_{x \to x_0^+} \boldsymbol{U}_0'(x), \tag{3.6}$$

and derive criteria for the presence of such a corner on a given characteristic (given Lipschitz continuity of certain coefficients whose form is determined by the flux function $\boldsymbol{F}$). In this context a conjecture from reference [16] is resolved, namely that corners split exactly along the characteristics for which there are corners in the corresponding Riemann invariants, when these can be found.

Let $x = \chi_k(t; x_0)$ with $\chi_k(0; x_0) = x_0$ be one of the characteristics along which a derivative jump propagates. Then let

$$\lim_{x \to \chi_k(t;x_0)^-} \boldsymbol{U}_x(x,t) \equiv (\boldsymbol{U}_x^l)_k(t), \tag{3.7}$$

$$\lim_{x \to \chi_k(t;x_0)^+} \boldsymbol{U}_x(x,t) \equiv (\boldsymbol{U}_x^r)_k(t), \tag{3.8}$$

and we denote derivative jump by square brackets,

$$[\boldsymbol{U}_x]_k(t) \equiv (\boldsymbol{U}_x^r)_k(t) - (\boldsymbol{U}_x^l)_k(t). \tag{3.9}$$

Similarly

$$\lim_{x \to \chi_k(t;x_0)^-} \boldsymbol{F}(\boldsymbol{U})_x(x,t) \equiv (\boldsymbol{F}_x^l)_k(t), \tag{3.10}$$

$$\lim_{x \to \chi_k(t;x_0)^+} \boldsymbol{F}(\boldsymbol{U})_x(x,t) \equiv (\boldsymbol{F}_x^r)_k(t), \tag{3.11}$$

$$[\boldsymbol{F}_x]_k(t) \equiv (\boldsymbol{F}_x^r)_k(t) - (\boldsymbol{F}_x^l)_k(t). \tag{3.12}$$

We define $(\boldsymbol{U}_{xx}^l)_k$, $(\boldsymbol{U}_{xx}^r)_k$, $(\boldsymbol{F}_{xx}^l)_k$, $(\boldsymbol{F}_{xx}^r)_k$, $[\boldsymbol{U}_{xx}]_k$ and $[\boldsymbol{F}_{xx}]_k$ analogously. Then we may write

$$\boldsymbol{U}(x,t) = \tilde{\boldsymbol{U}}(x,t) + \sum_k [\boldsymbol{U}_x]_k(t) J_1(x - \chi_k(t;x_0)) + [\boldsymbol{U}_{xx}]_k(t) J_2(x - \chi_k(t;x_0)) \tag{3.13}$$

and

$$\boldsymbol{F}(x,t) = \tilde{\boldsymbol{F}}(x,t) + \sum_k [\boldsymbol{F}_x]_k(t) J_1(x - \chi_k(t;x_0)) + [\boldsymbol{F}_{xx}]_k(t) J_2(x - \chi_k(t;x_0)) \tag{3.14}$$

57

where $\tilde{\boldsymbol{U}}(x,t)$ is twice differentiable and

$$J_m(x) \equiv \frac{x^m}{m!} H(x) \tag{3.15}$$

where $H(x)$ is the Heaviside function. We use the further notation $J_m^k = J_m(x - \chi_k)$ and henceforth we will suppress various dependencies for ease of notation. From the weak system (3.2), we obtain the vanishing condition

$$0 = \sum_k (-\chi_k' [\boldsymbol{U}_x]_k + [\boldsymbol{F}_x]_k) J_0^k + (-\chi_k' [\boldsymbol{U}_{xx}]_k + [\boldsymbol{F}_{xx}]_k + [\boldsymbol{U}_x]_k') J_1^k + \psi(x,t) \tag{3.16}$$

where $\psi(x,t)$ is once continuously differentiable with respect to x. Both the coefficients of J_0^k and of J_1^k must vanish. The vanishing of the J_0^k coefficient may be written

$$0 = -\chi_k' [\boldsymbol{U}_x]_k + [D\boldsymbol{F}\boldsymbol{U}_x]_k$$
$$= (-\chi_k' I + D\boldsymbol{F})[\boldsymbol{U}_x]_k, \tag{3.17}$$

where I denotes the $n \times n$ identity matrix. Formula (3.17) is merely the characteristic equation and $[\boldsymbol{U}_x]_k$ is a corresponding eigenvector:

$$[\boldsymbol{U}_x]_k = \sigma_k \boldsymbol{r}_k. \tag{3.18}$$

The vanishing condition for the J_1^k coefficient is then

$$0 = (D\boldsymbol{F} - \lambda_k)[\boldsymbol{U}_{xx}]_k + [D^2\boldsymbol{F}(\boldsymbol{U}_x, \boldsymbol{U}_x)]_k + [\boldsymbol{U}_x]_k'$$
$$= \sigma_k' \boldsymbol{r}_k + \sigma_k (D\boldsymbol{r}_k(\lambda_k - D\boldsymbol{F})(\boldsymbol{U}_x^l)_k + 2D\boldsymbol{F}((\boldsymbol{U}_x^l)_k, \boldsymbol{r}_k)) + \sigma_k^2 D^2\boldsymbol{F}(\boldsymbol{r}_k, \boldsymbol{r}_k) + (D\boldsymbol{F} - \lambda_k)[\boldsymbol{U}_{xx}]_k. \tag{3.19}$$

Multiplying by the suitably normalized left eigenvector $\boldsymbol{l}_k$ yields (cf. [13])

$$0 = \sigma_k' + \sigma_k \boldsymbol{l}_k \cdot (D\boldsymbol{r}_k(\lambda_k I - D\boldsymbol{F})(\boldsymbol{U}_x^l)_k + 2D\boldsymbol{F}((\boldsymbol{U}_x^l)_k, \boldsymbol{r}_k)) + \sigma_k^2 \boldsymbol{l}_k \cdot D^2\boldsymbol{F}(\boldsymbol{r}_k, \boldsymbol{r}_k). \tag{3.20}$$

This is an ODE for σ_k which, if the coefficients are Lipschitz continuous will have a unique solution given an initial condition $\sigma_k(0) = \sigma_k^0$.

By considering the case $\sigma_k^0 = 0$, we see that a corner will propagate along precisely the characteristics for which

$$\boldsymbol{l}_k(\boldsymbol{U}_0(x_0)) \cdot [\boldsymbol{U}_0'] \neq 0. \tag{3.21}$$

For the case when Riemann invariants exist, denoted here by $R^j(\boldsymbol{U})$, we recall that they must satisfy the constraints [13]

$$DR^j = \beta_j \boldsymbol{l}_j. \tag{3.22}$$

So

$$\begin{aligned}
[R_x^j]_k &= DR^j \cdot [\boldsymbol{U}_x]_k \\
&= \beta_j \boldsymbol{l}_j \cdot (\sigma_k \boldsymbol{r}_k) \\
&= \delta_{jk} \beta_j \sigma_k.
\end{aligned} \tag{3.23}$$

This shows that a derivative discontinuity will propagate along the k'th characteristic when the Riemann invariant has a corner in its initial condition. A corner in the initial Riemann invariants is also necessary for corner propagation on the corresponding characteristic when $\beta_k(\boldsymbol{U}_0(x_0)) \neq 0$, i.e., $\boldsymbol{U}_0(x_0)$ is not a critical point for the given Riemann invariant. When the Riemann invariants have critical points, it is possible that they will be smooth even though the dependent variables are not. An example of this will be given in subsection 3.5.3 below.

Remark 1. *Our approach above differs from the approach of [13] in that by using distributions we are not confined to a single characteristic. However, our approach as such doesn't apply to the non-conservative case*

$$\boldsymbol{U}_t + A(\boldsymbol{U})\boldsymbol{U}_x = 0 \tag{3.24}$$

because solutions with derivative jumps are not strictly defined, in the distributional sense, but an expansion consistent with the conservative case may be obtained by taking a one sided Taylor expansion of the entire equation requiring the various order coefficients to vanish, as was done in [13].

Remark 2. *This form of expansion can be applied to shock formation at a point of parabolic degeneracy. This occurs in particular for vacuum points in the Airy shallow water system (see (3.45))*

at what is known as the "physical vacuum singularity" (see [16]).[1] In this case the vanishing of the J_0^k coefficient in (3.16), i.e., the characteristic equation, may not be satisfiable when the k family has a non-trival Jordan block at $\boldsymbol{U}_0(x_0)$. In particular, if $[\boldsymbol{U}_x]_k$ is a generalized eigenvector then

$$(D\boldsymbol{F} - \lambda_k I)[\boldsymbol{U}_x]_k \neq 0. \tag{3.25}$$

This can be remedied, however, by adding $[\boldsymbol{U}]_k J_0^k$ and $[\boldsymbol{F}]_k J_0^k$ terms to the respective expansions (3.13) and (3.14) (terms which we assume to vanish at initial time as we still wish to consider continuous initial conditions). Then the vanishing condition for the coefficient of J_0^k becomes

$$[\boldsymbol{U}]_k' = (D\boldsymbol{F} - \lambda_k I)[\boldsymbol{U}_x]_k, \tag{3.26}$$

producing a jump for any $t > 0$, even though the initial conditions do not suffer a gradient catastrophe.

Remark 3. *In the particular case of the Airy system, the formation of "shocks" in this way at the vacuum only appears when the velocity is regarded as being defined at the vacuum and is determined by Rankine-Hugoniot conditions for the conservation thereof. These conditions happen be to compatible with the physically correct Rankine-Hugoniot conditions for the conservation of momentum (see [16]), however the velocity cannot be computed from the a zero momentum and may be presumed on physical grounds not be defined at the vacuum.*

3.4   Persistent infinite derivatives in continuous solutions

In this section we show that a persistent vertical gradient in a continuous solution may only occur at points where genuine nonlinearity fails. Let $\chi(t)$ be a curve along which an infinite gradient persists in a continuous solution $\boldsymbol{U}$ in a hyperbolic system. Note, we do not assume from the outset that $\chi(t)$ is a characteristic since infinite derivatives could be associated with shocks which do not move along characteristics. The spatial derivative may be decomposed in terms of the right eigenvectors:

$$\boldsymbol{U}_x = \sum_k \alpha_k(x,t)\boldsymbol{r}_k(\boldsymbol{U}(x,t)). \tag{3.27}$$

---

[1]See [55] for a similar approach to the appearance of δ-shocks from functional initial conditions.

A vertical gradient is present exactly when

$$\lim_{x \to \chi(t)^-} \alpha_j(x, t) = \pm \infty \tag{3.28}$$

for at least one index j where we have assumed without loss of generality that the blowup occurs in the left limit $x \to \chi(t)^-$. Differentiating $\boldsymbol{U}$ along the curve $x = \chi(t)$ gives

$$\frac{d}{dt}\boldsymbol{U}(\chi(t), t) = \sum_k \alpha_k(\chi(t), t)\{\chi'(t) - \lambda_j(\boldsymbol{U}(\chi(t), t))\}\boldsymbol{r}_k(\boldsymbol{U}(\chi(t), t)) \tag{3.29}$$

and, assuming the solution has bounded variation along this curve, the derivative cannot blowup identically so $\chi'(t) = \lambda_j$ for some j, i.e., $\chi(t)$ is a characteristic (or an envelope of characteristics if we only require a continuous solution to exist on one side of the curve). Thus we write

$$\chi(t) = \chi_j(t; x_0) \tag{3.30}$$

where $x_0 = \chi(0)$ and

$$\lim_{x \to \chi_j(t;x_0)^-} \alpha_j(x, t) = \pm \infty. \tag{3.31}$$

We shall proceed to show by contradiction, that if genuine nonlinearity holds at a persistent infinite gradient then $(\lambda_j)_x$ is bounded along $x = \chi(t)$ contradicting the simultaneous assumptions that genuine nonlinearity holds and there is a persistent infinite gradient. The spatial gradient of λ_j is given by

$$(\lambda_j)_x = D\lambda_j \cdot \boldsymbol{U}_x \tag{3.32}$$

$$= \sum_k \alpha_k D\lambda_j \cdot \boldsymbol{r}_k \tag{3.33}$$

which is dominated by the α_j term going to $\pm \infty$ except when genuine nonlinearity fails on $x = \chi(t)$, in which case the whole expression may still be bounded. Without loss of generality we can assume that $\alpha_j \to \infty$ (otherwise we may replace $\boldsymbol{U}(x, t)$ with $\boldsymbol{U}(-x, -t)$ and work backwards in time) and, using the genuine nonlinearity assumption, choose $\boldsymbol{r}_j$ so that

$$D\lambda_j \boldsymbol{r}_j > 0. \tag{3.34}$$

In this case

$$\lim_{x \to \chi(t)} (\lambda_j)_x(x,t) = \infty \tag{3.35}$$

for all t (at least on some parameter interval). Then using (3.30), we have for $x_2 < x_1$ that

$$
\begin{aligned}
\infty &= \lim_{x_1,x_2 \to x_0} \frac{\lambda_j(\chi_j(t;x_1),t) - \lambda_j(\chi_j(t;x_2),t)}{\chi_j(t;x_1) - \chi_j(t;x_2)} \\
&\equiv \lim_{x_1,x_2 \to x_0} \frac{\lambda_j^1(t) - \lambda_j^2(t)}{\chi_j^1(t) - \chi_j^2(t)} \\
&= \lim_{x_1,x_2 \to x_0} \frac{\lambda_j^1(t) - \lambda_j^2(t)}{x_1 - x_2 + \int_0^t \lambda_j^1(\tau) - \lambda_j^2(\tau)d\tau} \\
&= \lim_{x_1,x_2 \to x_0} \frac{1}{\frac{x_1-x_2}{\chi_j^1(t)-\chi_j^2(t)}\frac{\chi_j^1(t)-\chi_j^2(t)}{\lambda_j^1(t)-\lambda_j^2(t)} + \int_0^t \frac{\lambda_j^1(\tau)-\lambda_j^2(\tau)}{\lambda_j^1(t)-\lambda_j^2(t)}d\tau} \\
&= \lim_{x_1,x_2 \to x_0} \frac{1}{\frac{x_1-x_2}{\chi_j^1(t)-\chi_j^2(t)}\frac{1}{(\lambda_j)_x(x_*(t),t)} + \int_0^t \frac{\lambda_j^1(\tau)-\lambda_j^2(\tau)}{\lambda_j^1(t)-\lambda_j^2(t)}d\tau}
\end{aligned}
\tag{3.36}
$$

for some $\chi_j^2(t) < x_*(t) < \chi_j^1(t)$ and we have used superscripts as a shorthand to denote quantities on the respective characteristics. We observe that each quantity in the denominator is positive and that the integrand approaches unity as $x_2 \to x_1$ and so also in the limit $x_1, x_2 \to x_0$. Therefore

$$\lim_{x_1,x_2 \to x_0} \frac{\lambda_j(\chi_j(t;x_1),t) - \lambda_j(\chi_j(t;x_2),t)}{\chi_j(t;x_1) - \chi_j(t;x_2)} \le \frac{1}{t} \tag{3.37}$$

which is finite for any $t > 0$, contradicting the assumption that the infinite gradient persists along $x = \chi(t)$. Therefore an infinite gradient may not persist in a continuous solution when genuine nonlinearity holds.

3.4.1 Scalar conservation laws

A simplified alternative version of the previous section's proof is available in the case of a scalar conservation law:

$$u_t + c(u)u_x = 0 \tag{3.38}$$

where $c(u) = F'(u)$ with initial conditions

$$u(x,0) = u_0(x). \tag{3.39}$$

Along characteristics

$$x = \chi(t; x_0) = x_0 + c(u_0(x_0))t \tag{3.40}$$

we have

$$u_x(x,t) = \frac{u_0'(x_0)}{1 + c'(u_0(x_0))u_0'(x_0)t} = \frac{u_0'(x_0)}{1 + c'(u(x,t))u_0'(x_0)t}. \tag{3.41}$$

If we consider a singularity where u_x is infinite along the characteristic $x = \chi(t; 0)$, say, then taking the limit $x \to \chi(t; 0)$ gives

$$u_x(x,t) \to \infty. \tag{3.42}$$

The corresponding limit for the initial condition implies that

$$u_0'(x_0) \to \infty \tag{3.43}$$

as $x_0 \to 0$, so that the blowup in the initial data is maintained:

$$u_x(x,t) = \frac{u_0'(x_0)}{1 + c'(u)u_0'(x_0)t} \to \infty. \tag{3.44}$$

However, the divergence of the numerator in the limit would be canceled by that in the denominator preventing a persistent infinite gradient in spatial derivative if it were not the case that $c'(u) = 0$, i.e., the failure of genuine nonlinearity in the scalar setting.

Remark 4. *We note that the scalar case above can be realized in the multidimensional setting by restricting to simple waves (see Appendix).*

3.5 Applications

For the remainder of the paper, we study cases of the singular points studied above in three quasilinear hyperbolic models. The first model we consider is the Airy shallow water system

$$\begin{pmatrix} v_t \\ u_t \end{pmatrix} + \begin{pmatrix} u & v \\ 1 & u \end{pmatrix} \begin{pmatrix} v_x \\ u_x \end{pmatrix} = 0. \tag{3.45}$$

63

The second model is a two layer shallow water model in the Boussinesq limit (see e.g. [15]):

$$\begin{pmatrix} u \\ v \end{pmatrix}_t + \begin{pmatrix} (1-2u)v & u(1-u) \\ 1-v^2 & (1-2u)v \end{pmatrix} \begin{pmatrix} u \\ v \end{pmatrix}_x = 0. \tag{3.46}$$

The third model we consider is the scalar law

$$u_t + u^2 u_x = 0 \tag{3.47}$$

which illustrates the key features of infinite gradients in simple wave solutions.

The examples are organized topically, starting with section 3.5.2 where a non-splitting corner in the Ariy system is constructed. In section 3.5.3 an example from the two layer system, equation (3.46), exhibits non-splitting of a corner as well as the necessity of no critical points in the Riemann invariants for the conclusions of section 3.3 to hold. Then sections 3.5.4 and 3.5.5 demonstrate persistent infinite derivatives in simple wave solutions. Finally, section 3.5.6 illustrates a persistent infinite gradient, not in a simple wave solution, making a dynamically evolving angle with the adjacent slope.

3.5.1 Methods of explicit solution

For explicit examples we shall make use of the linear core solutions of the Airy system (3.45) from reference [56]:

$$U(x,t) = \alpha(t)x + \beta(t) \tag{3.48}$$

and

$$V(x,t) = \omega(t)x + \zeta(t) \tag{3.49}$$

where

$$\alpha(t) = \frac{\alpha_0}{1+\alpha_0 t}, \qquad \beta(t) = \frac{\beta_0 - \frac{\omega_0}{\alpha_0}\log(1+\alpha_0 t)}{1+\alpha_0 t}, \tag{3.50}$$

$$\omega(t) = \frac{\omega_0}{(1+\alpha_0 t)^2}, \qquad \zeta(t) = \frac{\zeta_0}{1+\alpha_0 t} + \frac{\omega_0(\frac{\omega_0}{\alpha_0}-\beta_0)t}{(1+\alpha_0 t)^2} - \frac{\frac{\omega_0^2}{\alpha_0^2}\log(1+\alpha_0 t)}{(1+\alpha_0 t)^2}. \tag{3.51}$$

The formulae for the characteristics $\chi_j(t; x_0)$ may be found by solving the equations

$$u(\chi_j(t; x_0), t) + 2(-1)^j \sqrt{v(\chi_j(t; x_0), t)} = R^{j^0} = \alpha_0 x_0 + \beta_0 + 2(-1)^j \sqrt{\omega_0 x_0 + \zeta_0}, \qquad (3.52)$$

which yields

$$\chi_j(t; x_0) = (1 + \alpha_0 t)x_0 + t\left(\alpha_0 x_0 + \beta_0 + 2(-1)^j \sqrt{\omega_0 x_0 + \zeta_0}\right)$$
$$+ \frac{2}{\alpha_0^2}\left(\omega_0 + (-1)^j \alpha_0 \sqrt{\omega_0 x_0 + \zeta_0}\right)(1 - \sqrt{1 + \alpha_0 t}) + \frac{\omega_0}{\alpha_0^2} \log\left(1 + \alpha_0 t\right). \quad (3.53)$$

Such a solution may be spliced with a constant state via a simple wave (see [16]), i.e., the initial conditions are modified to be constant for $x > 0$ (or $x < 0$):

$$u_0(x) = \begin{cases} \beta_0 + \alpha_0 x, & x < 0 \\ \beta_0, & 0 \le x \end{cases} \qquad (3.54)$$

and

$$v_0(x) = \begin{cases} \zeta_0 + \omega_0 x, & x < 0 \\ \zeta_0, & 0 \le x. \end{cases} \qquad (3.55)$$

In this way, examples may be constructed satisfying physical boundary conditions at $\pm\infty$ by placing the core between two constant states within the hyperbolic region. Since we are only concerned with the evolution of singularities with a definite position, we will only require that solutions under consideration are in the hyperbolic region in the part of the space-time half plane where these singularities occur. Because the Riemann invariants R^j are constant on the corresponding characteristics, the region of the $x - t$ plane covered simultaneously by characteristics $x = \chi_j(t; x_0)$ for both $j = 1, 2$ with $x_0 \le 0$, will coincide with the linear core solution $(u, v) = (U, V)$ in (3.48) and (3.49). Similarly, for the region of the $x - t$ plane covered by characteristics of both families emanating from the constant region, the solution will be constant. The right boundary curve of the left (linear core) region will be the characteristic

$$b_1(t) = \chi_1(t; 0) \qquad (3.56)$$

of the first family. Similarly, the left boundary of the constant region will be a characteristic of the second family:

$$b_2(t) = \lambda_2(\beta_0, \zeta_0)t. \tag{3.57}$$

The solution can then be constructed in the middle region by enforcing the constancy of the Riemann invariants on characteristics:

$$R^1(x, t) = R^1(0, 0) \tag{3.58}$$

for $b_1(t) < x < b_2(t)$ and

$$R^2(b_1(t_0) + (t - t_0)\lambda_2(b_1(t_0), t_0), t) = R^2(b_1(t), t_0). \tag{3.59}$$

Then the identities

$$u = \frac{1}{2}(R^1 + R^2), \qquad v = \frac{1}{16}(R^1 - R^2)^2 \tag{3.60}$$

can be used to recover the solution in the simple wave region since R^1 is constant and $R^2(\chi_1(t_0; 0), t_0)$ is given explicitly in terms of the linear core solution. We note that u and v are also constant on the characteristics $x = b_1(t_0) + (t - t_0)\lambda_2(b_1(t_0), t_0)$ since they are determined uniquely by the Riemann invariants (this hold even in the two layer case under the mapping (3.61), provided that a particular quadrant is chosen). A schematic of the characteristics in the $x - t$ plane is shown in figure 3.1.

In order to provides explicit solutions to system (3.46), we make use of a map [36, 47] relating it to system (3.45), allowing for the construction of explicit solutions with the type of singularities we have considered in the previous sections. This map is given by

$$\hat{u} = (1 - 2u)v, \qquad \hat{v} = (1 - v^2)(u - u^2) \tag{3.61}$$

sending solutions (u, v) of system (3.46) to solutions $(u, v) = (\hat{u}, \hat{v})$ of system (3.45). The map (3.61) is many-to-one with $1 \rightarrow 4$ inverses (see [15]) given by

$$u_{ij} = \frac{1}{2}\left(1 + (\operatorname{sgn} \hat{u})^{j+1}(-1)^i\sqrt{Q - (-1)^j\sqrt{Q^2 - \hat{u}^2}}\right) \tag{3.62}$$
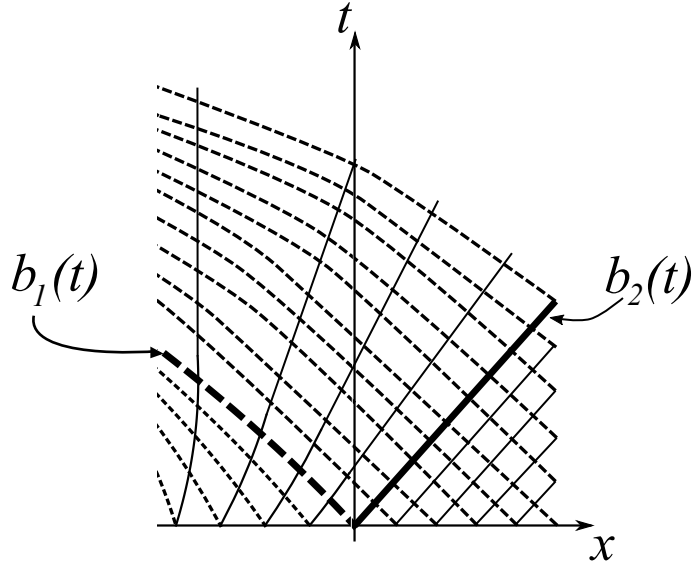
66

Figure 3.1: Characteristic diagram with the linear core solution for $x < b_1(t)$, the simple wave solution for $b_1(t) \le x \le b_2(t)$ and a constant state for $b_2(t) < x$. Dotted curves denote characteristics of the first family and solid curves denote characteristics of the second.

and

$$v_{ij} = -(\operatorname{sgn} \hat{u})^j (-1)^i \sqrt{Q + (-1)^j \sqrt{Q^2 - \hat{u}^2}} \tag{3.63}$$

where $j = 1, 2$ and

$$Q = \frac{\hat{u}^2 - 4\hat{v} + 1}{2} \tag{3.64}$$

(hereinafter we adorn the dependent variables with hats when they are obtained through the map (3.61)). Figure 3.2 shows the images of the four branches while figure 3.3 shows the image $\tilde{\Omega}$ of the hyperbolic region Ω of the two layer system (3.46) under the map (3.61) along with the singular curves

$$u = \frac{1}{2} \pm \frac{v}{2}. \tag{3.65}$$

Note that these are level curves of the Riemann invariants

$$R^j(\hat{u}, \hat{v}) = \hat{u} + 2(-1)^j \sqrt{\hat{v}} \tag{3.66}$$
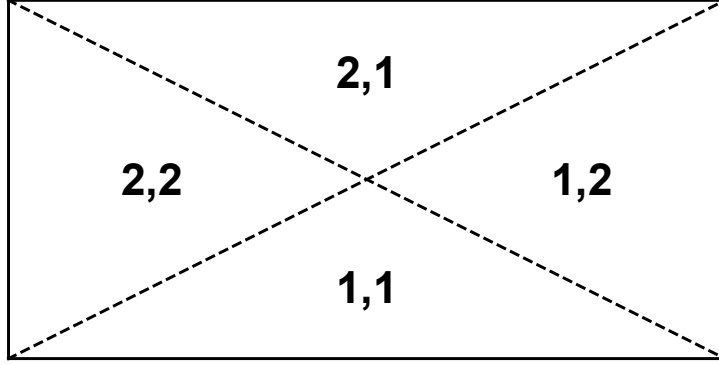
67

Figure 3.2: The i, j quadrant is the image of the curved triangle in figure 3.3 under $(\hat{u}_{ij}, \hat{v}_{ij})$ with v and u plotted on the horizontal and vertical axes respectively. The dotted lines are the singular curves of the map $(u, v) \to (\hat{u}, \hat{v})$.
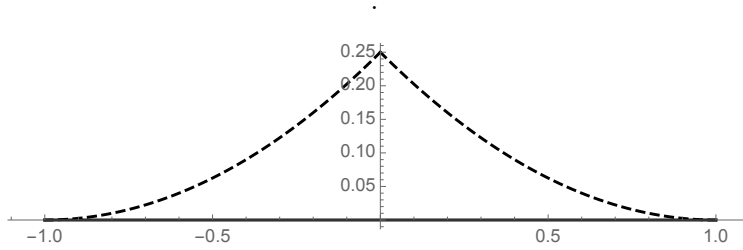
Figure 3.3: The image $\tilde{\Omega}$ of the hyperbolic region Ω under the map $(u, v) \to (\hat{u}, \hat{v})$, with $\hat{u}$ and $\hat{v}$ plotted on the horizontal and vertical axes respectively. The dotted curves are the image of the singular curves.

since

$$Q^2 - \hat{u}^2 = \frac{1}{16}(1 - 2\hat{u}^2 + \hat{u}^4 - 4\hat{v} - 4\hat{v}\hat{u}^2 + 16\hat{v}^2) \tag{3.67}$$

$$= \frac{1}{16}((R^1)^2 - 1)((R^2)^2 + 1). \tag{3.68}$$

3.5.2 Example 1: non-splitting corner in the Airy system

We use the linear core construction to present a solution which has a corner that does not split, corresponding to the lack of a jump in one of the Riemann invariants. We take initial conditions:

$$v_0(x) = \begin{cases} 1 + x, & x < 0 \\ 1, & 0 \le x \end{cases} \tag{3.69}$$

68

and

$$u_0(x) = \begin{cases} x, & x < 0 \\ 0, & 0 \le x \end{cases} \tag{3.70}$$

The initial Riemann invariants are then

$$R_0^k(x) = \begin{cases} x + 2(-1)^k\sqrt{1+x}, & x < 0 \\ 2(-1)^k, & 0 \le x. \end{cases} \tag{3.71}$$

The derivative jumps of the Riemann invariants for the initial corner at $x_0 = 0$ are given by

$$[R_0^{k'}] = -1 - (-1)^k \tag{3.72}$$

from which we may predict that the corner will not split given that only one of the Riemann invariants has a nonzero derivative jump using the conditions derived above. We have

$$\alpha_0 = \omega_0 = \zeta_0 = 1 \tag{3.73}$$

and

$$\beta_0 = 0 \tag{3.74}$$

so the linear core is given by

$$v(x,t) = \frac{x - \log(1+t) + 2t + 1}{(1+t)^2}, \tag{3.75}$$

$$u(x,t) = \frac{x - \log(1+t)}{1+t}, \tag{3.76}$$

and the leftmost characteristic bounding the core solution is given by

$$b_1(t) = -2t + \log(1+t). \tag{3.77}$$

Having computed the basic elements explicitly, we turn to show that no corner will propagate along $x = b_1(t_0)$. To achieve this we must take the spatial derivatives on the right side, i.e., in the simple wave region where u and v are defined implicitly via the method of characteristics, and

compare to the spatial derivatives defined by the linear core solution. The left derivatives are

$$u_x^l(b_1(t_0), t_0) = \alpha(t_0) = \frac{1}{1 + t_0} \tag{3.78}$$

and

$$v_x^l(b_1(t_0), t_0) = \omega(t_0) = \frac{1}{(1 + t_0)^2}. \tag{3.79}$$

Then the right spatial derivative of u is

$$u_x^r(b_1(t_0), t_0) = \lim_{t \to t_0} \frac{u(x(t_0, t), t) - u(b_1(t), t)}{x(t_0, t) - b_1(t)} \tag{3.80}$$

$$= \lim_{t \to t_0} \frac{u(b_1(t_0), t_0) - u(b_1(t), t)}{x(t_0, t) - b_1(t)} \tag{3.81}$$

where $x(t_0, t) = b_1(t_0) + (t - t_0)\lambda_2(b_1(t_0), t_0)$, and

$$u_x^r = \frac{\frac{d}{dt_0} u(b_1(t_0), t_0)}{\frac{\partial x}{\partial t_0}(t_0, t_0)} \tag{3.82}$$

$$= \frac{\frac{d}{dt_0} u(b_1(t_0), t_0)}{\lambda_1(b_1(t_0), t_0) - \lambda_2(b_1(t_0), t_0)}. \tag{3.83}$$

Identical manipulations yield

$$v_x^r = \frac{\frac{d}{dt_0} v(b_1(t_0), t_0)}{\lambda_2(b_1(t_0), t_0) - \lambda_1(b_1(t_0), t_0)}. \tag{3.84}$$

Thus we compute

$$\frac{d}{dt_0} u(b_1(t_0), t_0) = -\frac{2t_0}{(1 + t_0)^2}, \qquad \frac{d}{dt_0} v(b_1(t_0), t_0) = -\frac{2t_0}{(1 + t_0)^3}, \tag{3.85}$$

and

$$\lambda_1(b_1(t_0), t_0) - \lambda_2(b_1(t_0), t_0) = -\frac{2t_0}{(1 + t_0)}. \tag{3.86}$$

Plugging these into the formulae (3.82) and (3.84) for the right (simple-wave-side) derivatives yields the same results as those for the left (linear-core-side) derivatives (3.78) and (3.79), so there is no jump along this characteristic. The initial condition in figure 3.4 evolves into figure 3.5 illustrating
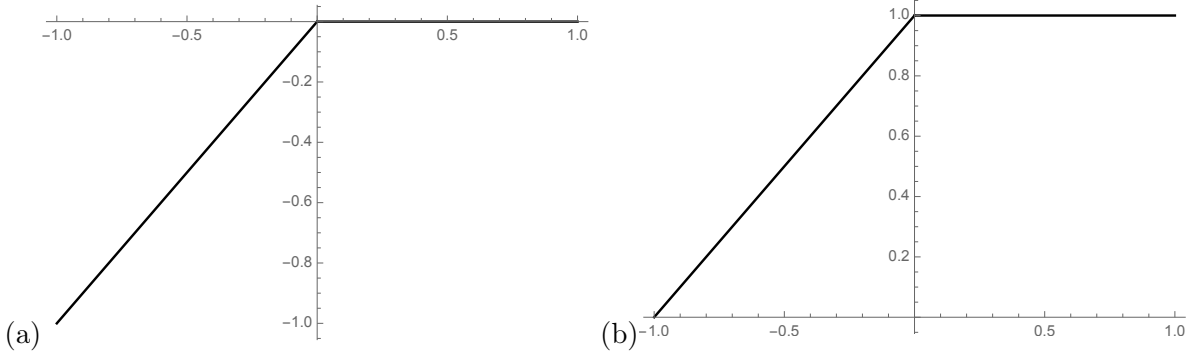
70

Figure 3.4: Initial conditions for which only one Riemann invariant has a corner: $u(x,0)$ is shown in (a) and $v(x,0)$ in (b).
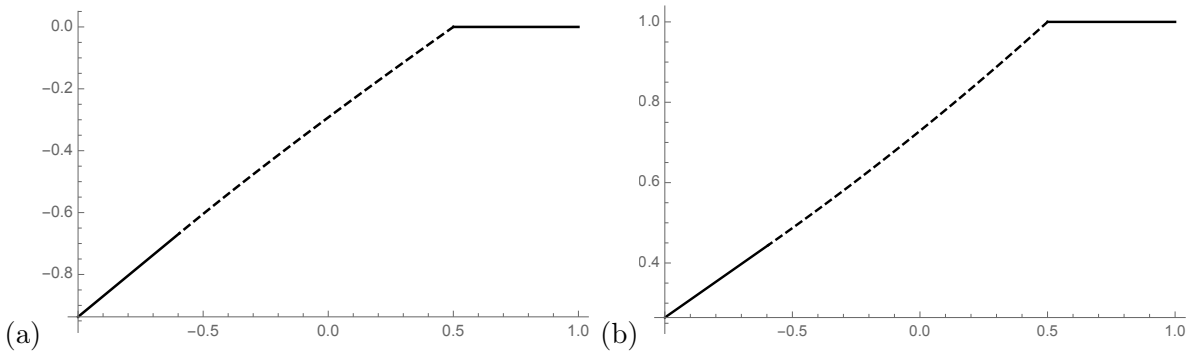

Figure 3.5: Evolution of a corner from the initial conditions in 3.4: $u(x,.5)$ is shown in (a) and $v(x,.5)$ in (b).

the non-splitting of the corner. This contrasts the generic case illustrated in figures 3.6 and 3.7 obtained by changing to $\alpha_0 = 1.6$, causing corners to occur in both Riemann invariants.

3.5.3   Example 2: non-splitting corner and singular Riemann invariant

In this subsection we consider a linear core solution[2] of the Airy system (3.45) which is tangent to the boundary of the domain of $(\hat{u}_{ij}, \hat{v}_{ij})$ and the images thereunder. That this property is maintained by evolution follows from the fact that this curve is a level surface of a Riemann invariant. An elementary computation shows that tangency can be achieved by setting

$$\beta_0 = \hat{u}_0, \qquad \omega_0 = \frac{\alpha_0}{2}(\hat{u}_0 - 1), \qquad \zeta_0 = \hat{v}_0 \tag{3.87}$$

---

[2]Since we are only concerned with local behavior at small time, we shall not, in this example, be concerned with splicing the linear core to a constant solution, shock formation at large time, or ellipticity away from points of interest.
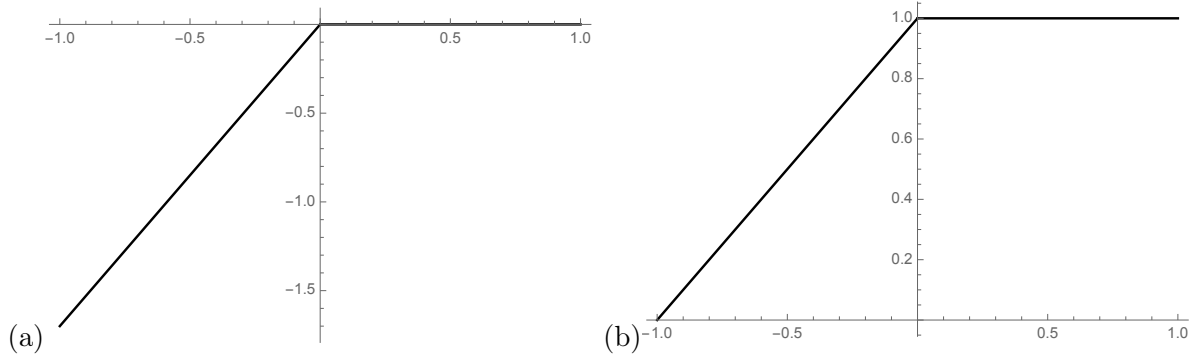
Figure 3.6: Initial conditions for which both Riemann invariants have corners: $u(x,0)$ is shown in (a) and $v(x,0)$ in (b).
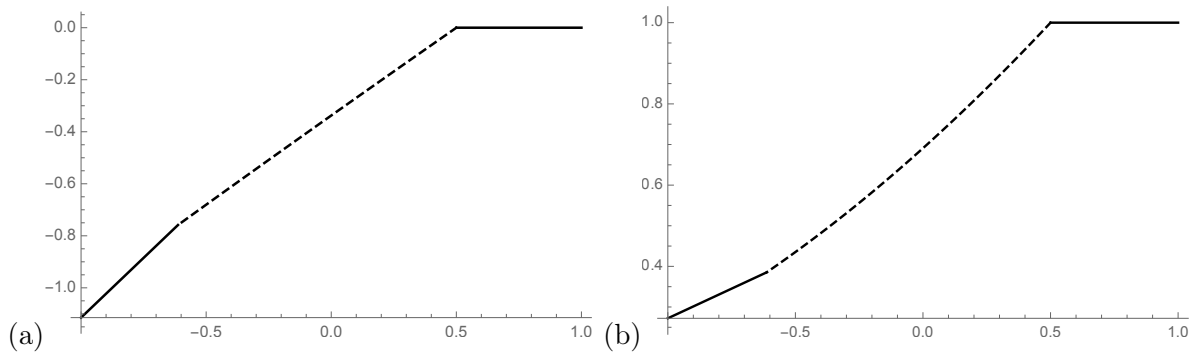

Figure 3.7: Evolution of a corner from the initial conditions in 3.6: $u(x,.5)$ is shown in (a) and $v(x,.5)$ in (b).
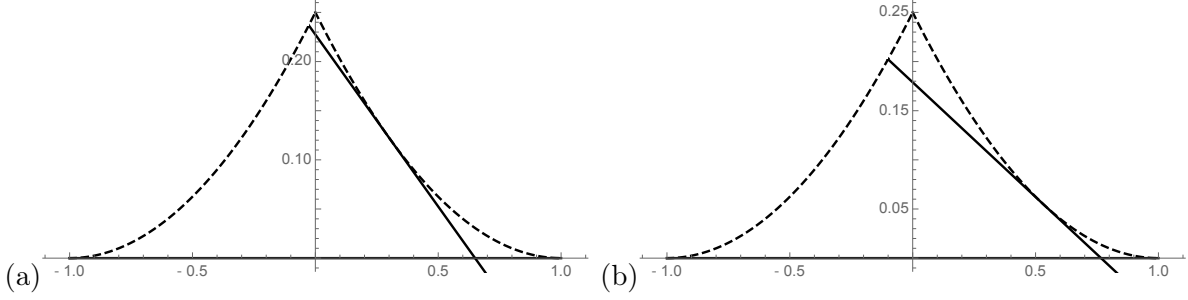
Figure 3.8: Linear core solutions tangent to the boundary of $\tilde{\Omega}$, (a) at time $t = 0$ and (b) at time $t = .5$.

where $(\hat{u}_0, \hat{v}_0) = (\hat{u}(0,0), \hat{v}(0,0))$ is the initial point of tangency and α_0 is a free parameter. For the present example we take $\beta_0 = .3$ and $\alpha_0 = 1$. The dependent variables in the $(\hat{u}, \hat{v})$ domain at time $t = 0$ and $t = .5$ are shown in figure 3.8.

Finally, we consider the solutions to (3.46) in the $1, 1$ quadrant by mapping the linear core solution:

$$u(x,t) = u_{11}(\hat{u}(x,t), \hat{v}(x,t)), \qquad v(x,t) = v_{11}(\hat{u}(x,t), \hat{v}(x,t)), \tag{3.88}$$

This solution is shown in the space of dependent variables at times $t = 0$ and $t = .5$ in figure 3.9 and the total pre-image of the linear core solution is shown in 3.10. The spatial dependence of u and v at fixed time are shown in figures 3.11 and 3.12.

We see that a single corner propagates in the solution (u, v), however the linear core solution is smooth by construction and the mapping from the system (3.45) to its Riemann invariants is also smooth in the hyperbolic region. Thus there are no corners in the initial Riemann invariants despite the fact that a single corner is achieved in the solution $(u(x,t), v(x,t))$. This is a consequence of the fact that the boundaries of the quadrants, i.e., the NGNL curves, are each vanishing loci for the gradients of the corresponding Riemann invariants.

3.5.4 Example 3: Infinite gradient in a scalar conservation law

We provide an example of an infinite gradient which is not constant on either side, in the scalar case of section 3.4.1. Since simple waves are, by definition, solutions to a scalar law, the present example qualitatively illustrates the general situation where two simple waves of the same family are glued together at the NGN point where the orientation of the curve reverses. This type of solution obviously leads to shocks at large enough time but we may track the evolution prior to
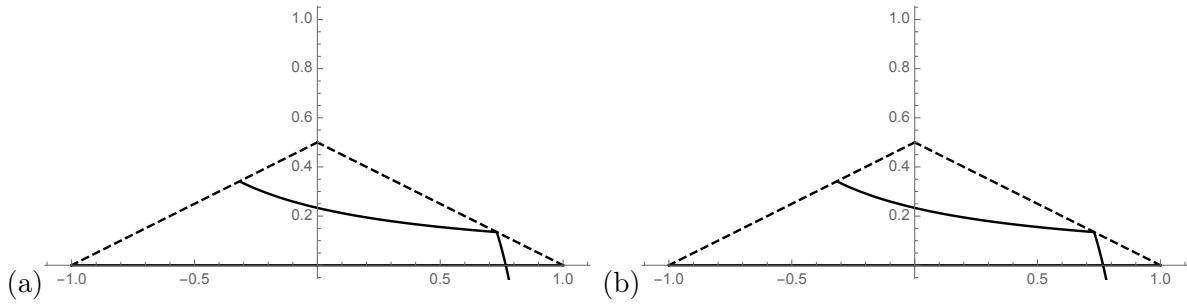
Figure 3.9: pre-image of linear core solutions in the $1, 1$ quadrant, (a) at time $t = 0$ and (b) at time $t = .5$.
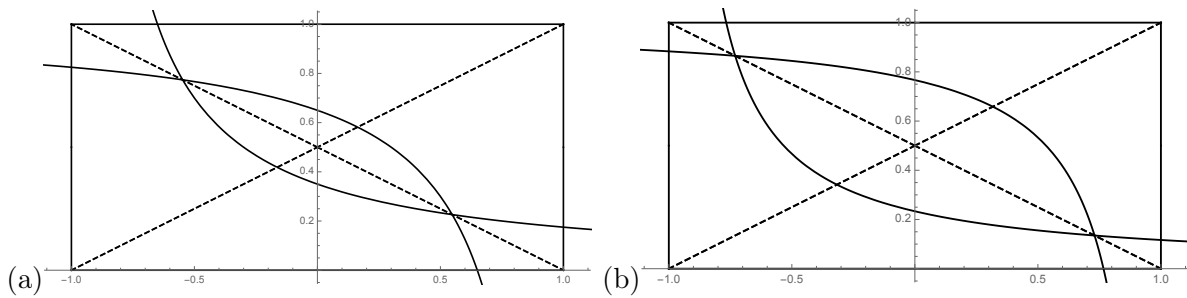
Figure 3.10: total pre-image of linear core solution in all quadrants, (a) at time $t = 0$ and (b) at time $t = .5$.
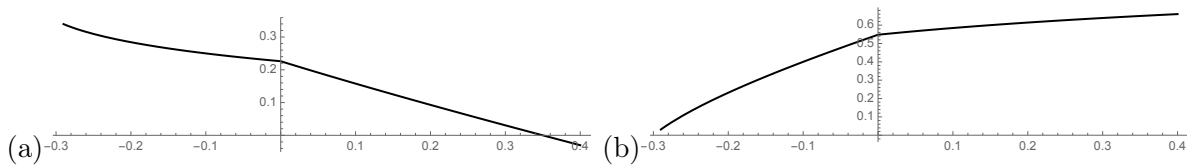
Figure 3.11: Initial conditions in the $1, 1$ quadrant: $u(x, 0)$ is shown in (a) and $v(x, 0)$ in (b).
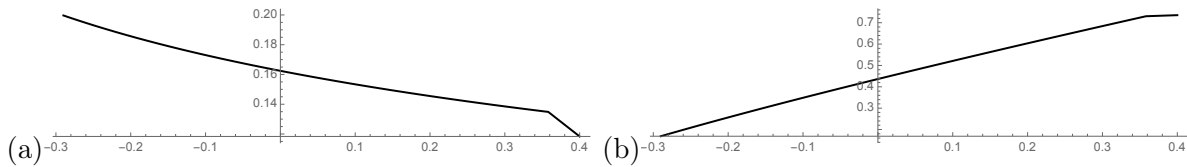
Figure 3.12: Evolution of the initial conditions in figure 3.11: $u(x, .5)$ is shown in (a) and $v(x, .5)$ in (b).

shock formation.

We consider the simplest possible scalar law: the cubic flux conservation law (3.47). With initial conditions $u(x,0) = u_0(x)$, the solution is given according to the method of characteristics:

$$u(x_0 + u_0(x_0)^2 t, t) = u_0(x_0). \tag{3.89}$$

In the case

$$u_0(x_0) = (\operatorname{sgn} x_0)\sqrt{|x_0|}, \tag{3.90}$$

we have

$$x = x_0(1 + (\operatorname{sgn} x_0)t) \tag{3.91}$$

which is single valued, having $\operatorname{sgn} x_0 = \operatorname{sgn} x$ when $t < 1$. Thus we may solve

$$x_0 = \frac{1}{1 + (\operatorname{sgn} x)t} x \tag{3.92}$$

yielding

$$u(x,t) = \frac{\operatorname{sgn} x}{1 + (\operatorname{sgn} x)t}\sqrt{|x|}. \tag{3.93}$$

The evolution of the solution before shock time is shown in figure 3.13. The same process may also be applied to the initial condition

$$u_0(x_0) = \sqrt{|x_0|}, \tag{3.94}$$

yielding the evolution

$$u(x,t) = \frac{1}{1 + (\operatorname{sgn} x)t}\sqrt{|x|}. \tag{3.95}$$

shown in 3.14.

(a)

(b)
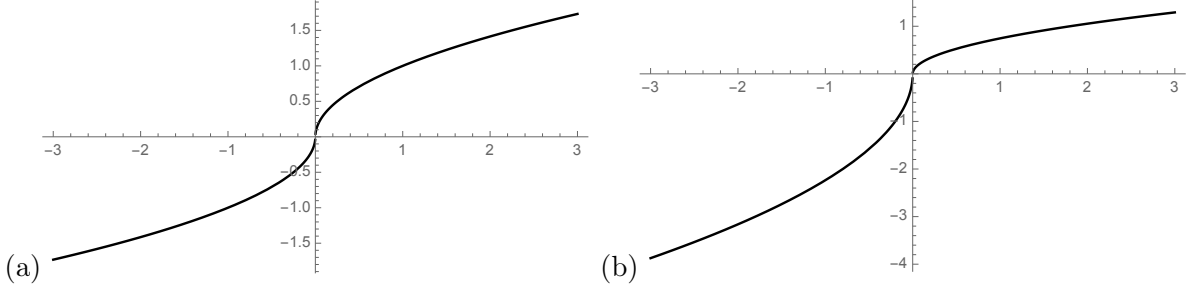
Figure 3.13: Evolution under the scalar law (3.47) of the initial condition (3.91), (a) at time $t = 0$ and (b) at time $t = .8$.

(a)

(b)
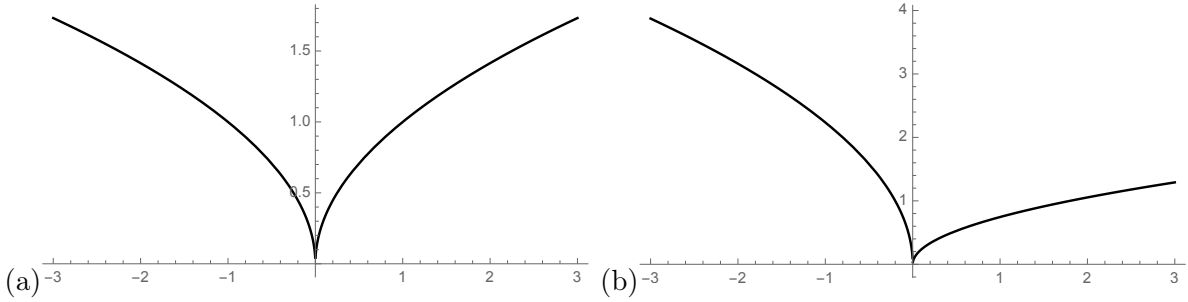
Figure 3.14: Evolution under the scalar law (3.47) with initial condition (3.94), (a) at time $t = 0$ and (b) at time $t = .8$.

3.5.5 Example 4: Infinite gradient in a centered simple wave

For the two layer system (3.46), the rarefaction curves (see Appendix for the setting) may be expressed explicitly. We take a centered simple wave solution in the $1, 1$ quadrant:

$$u(x,t) = \begin{cases} u_l, & x/t \le \lambda_2(u_l, v_l) \\ u_{11}(-\frac{1}{3}(2\frac{x}{t} + \frac{1}{2}), \frac{1}{36}(2\frac{x}{t} - 1)), & \lambda_2(u_l, v_l) < x/t < \lambda_2(u_r, v_r) \\ u_r, & x/t \ge \lambda_2(u_r, v_r) \end{cases} \tag{3.96}$$

and

$$v(x,t) = \begin{cases} v_l, & x/t \le \lambda_2(u_l, v_l) \\ v_{11}(-\frac{1}{3}(2\frac{x}{t} + \frac{1}{2}), \frac{1}{36}(2\frac{x}{t} - 1)), & \lambda_2(u_l, v_l) < x/t < \lambda_2(u_r, v_r) \\ v_r, & x/t \ge \lambda_2(u_r, v_r) \end{cases} \tag{3.97}$$

where

$$u_l = 0.15, \qquad v_l = 0.268466, \qquad u_r = 0.25, \qquad v_r = 0.5. \tag{3.98}$$

76
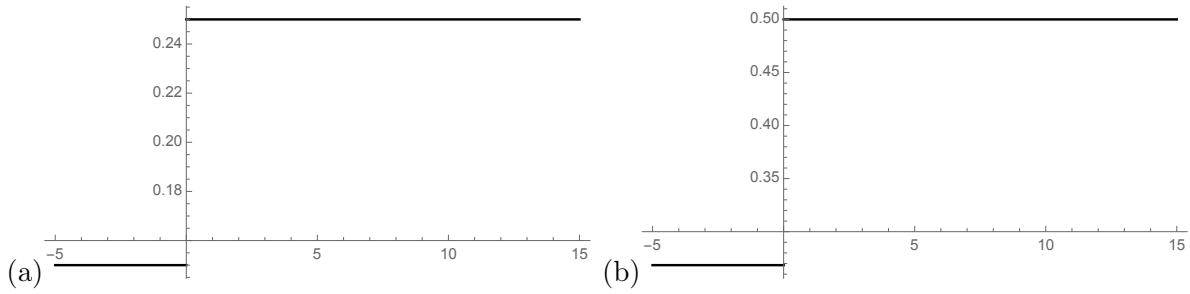
Figure 3.15: Initial conditions for the Riemann problem: $u(x,0)$ is shown in (a) and $v(x,0)$ in (b).
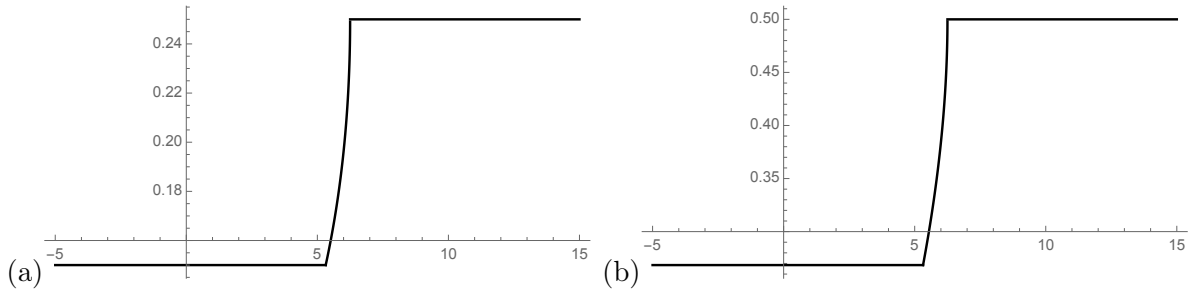
Figure 3.16: Evolution of the centered simple wave at time 10 is shown in (a) and $v(x,0)$ in (b).

The initial conditions in figure 3.15 are step functions. As time evolves in figures 3.16 and 3.17, the wave becomes less and less steep, except at the right state where the infinite gradient occurs. This is an NGNL point as can be seen in figure 3.18 where the simple wave segment is shown in the space of dependent variables.

3.5.6 Example 5: an infinite gradient spliced with a non-constant angle

In the previous infinite gradient examples the point in the space of dependent variables where an infinite gradient occurs remains constant in the evolution and, correspondingly, moving at a constant characteristic speed in the space-time half plane. This happens generically since the evolution along
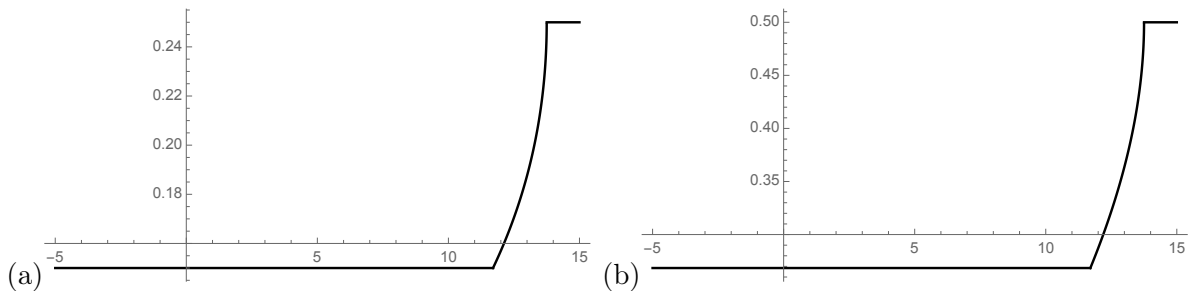
Figure 3.17: Evolution of the centered simple wave at time 22 is shown in (a) and $v(x,0)$ in (b).
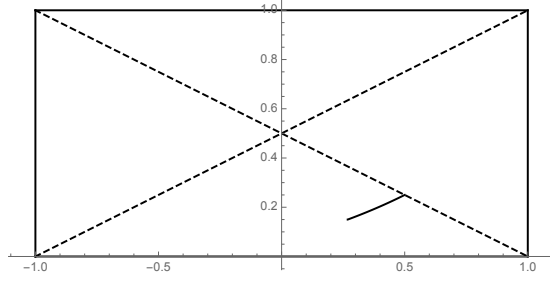
Figure 3.18: The simple wave segment shown in the space of dependent variables.

a characteristic for a hyperbolic system (3.1) occurs normally to the corresponding left eigenvector:

$$\boldsymbol{l}_k \cdot \frac{d}{dt}\boldsymbol{U}(\chi_k(t; x_0), t) = \boldsymbol{l}_k \cdot (\lambda_k I - D\boldsymbol{F}(\boldsymbol{U}))\boldsymbol{U}_x = 0, \tag{3.99}$$

whereas the NGNL manifold need not be normal to the left eigenvector. In the 2×2 case, non-constant evolution along a characteristic will remain on the NGNL curve if and only if the latter is a level set of a Riemann invariant. One particular instance where this is the case is the Boussinesq two layer system (3.46). We illustrate an explicit solution with an evolving infinite gradient point for this case. To accomplish this we consider the evolution obtained by connecting the linear core solution with initial parameters

$$\alpha_0 = \frac{1}{3}, \qquad \beta_0 = -\frac{1}{3}, \qquad \omega_0 = \frac{1}{3}, \qquad \zeta_0 = \frac{1}{9} \tag{3.100}$$

on the left of the origin with the constant state $(\hat{u}, \hat{v}) = (\beta, \zeta)$ on the right. Then a simple wave region will emerge between the rightmost characteristic $b_1(t)$ of the linear core and the leftmost characteristic $b_2(t)$ of the constant state. This simple wave coincides with the singular curve of the map (3.61) (see figure 3.19). The infinite gradient propagates along $b_1(t)$, with dependent variables evolving along the NGNL curve, as shown in figure 3.21 and 3.22. We note that, unlike previous examples, the angle formed between the tangent lines at the infinite gradient point is not $\pi/2$ (infinite gradient at the boundary of a constant state), π (front-like) or 0 (cusp) as it was in previous examples. This is apparent in figures 3.21 and 3.22 with the exact angle at a given time computable by the same method as in section 3.5.2.

(a)   (b)
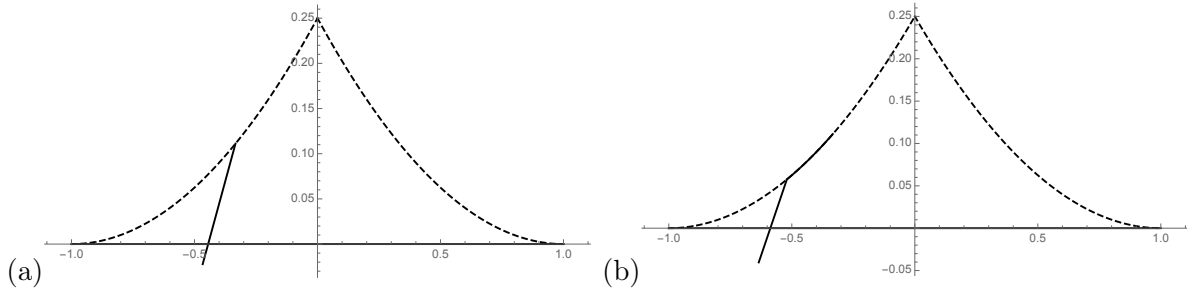
Figure 3.19: The solution in the $(\tilde{u}, \tilde{v})$ space (a) at time $t = 0$ and (b) at time $t = .5$.

(a)   (b)
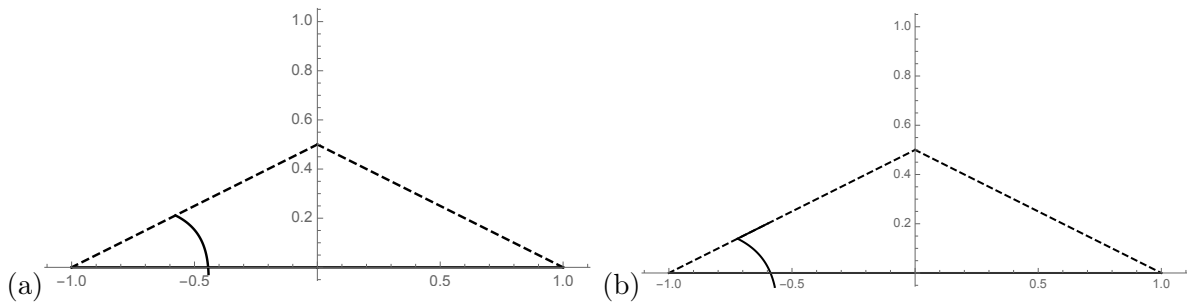
Figure 3.20: The solution to the two layer system, obtained from the $1, 1$ branch of the mapping applied to the solution in figure 3.19 (a) at time $t = 0$ and (b) at time $t = .5$.

(a)   (b)
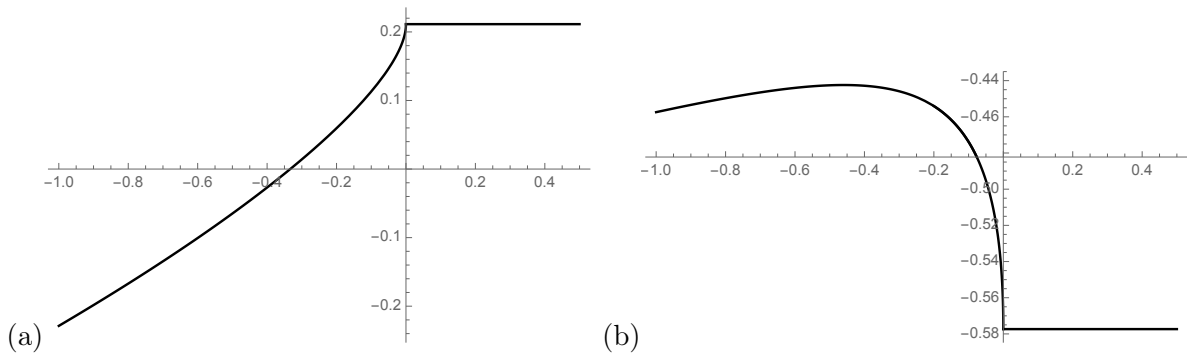
Figure 3.21: Initial conditions in the $1, 1$ quadrant: $u(x, 0)$ is shown in (a) and $v(x, 0)$ in (b).

(a)   (b)
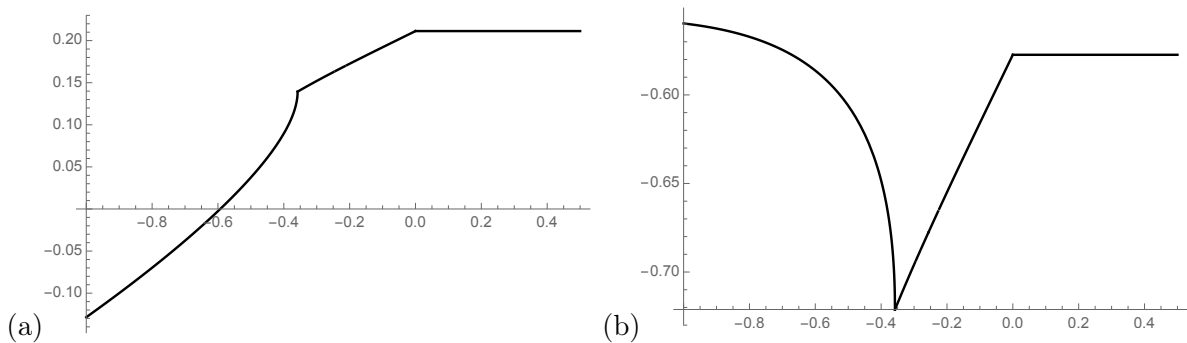
Figure 3.22: Evolution of the initial conditions in figure 3.21: $u(x, .5)$ is shown in (a) and $v(x, .5)$ in (b).

79

CHAPTER 4
Conclusions

In chapter 2, we developed a shock theory for quasilinear Hamiltonian systems where discontinuities are required to satisfy Rankine-Hugoniot conditions for all of the conservation laws naturally given by the Hamiltonian structure. This requires that the shocks be undercompressive and produce a map (or discrete set of maps), giving right states that can be joined to a given left state, in contrast to the one parameter family of the classical shock theory. The properties of this map were shown to determine key features of the system. It was shown,in particular that for a 2×2 system, preservation of simple waves by this map is a necessary condition for the satisfaction of Rankine-Hugoniot conditions for an infinitude of independent conservation laws across a Hamiltonian shock, and for the interaction of Hamiltonian shocks with continuous waves to be assured to proceed without the development of gradient catastrophe. The case where Hamiltonian shock solutions map to continuous solutions of an auxiliary system was used to explicitly compute interactions. These findings were compared to numerical simulations of dispersive systems, where gradient catastrophe signals the development of classical dispersive shocks, yielding agreement with the theory. Further tasks and questions emerge from this study which we now outline.

One direction for further research is stratified fluid flow with more than two layers. The three layer case was studied in the Hamiltonian setting in [57]. In the Boussinesq approximation with equal density gradients, a symmetry of the system exists [58] which was shown in [57] to be a Hamiltonian symmetry. It is not hard to show that this symmetry is a Hamiltonian shock map which thus produces conjugate states that produce continuity preserving Hamiltonian shock interactions. This map, however, does not exhaust the possible conjugate states of the system. In particular, these shocks are necessarily mode 1, whereas mode 2 conjugate states were studied in [59], wherein the existence of corresponding heteroclynic connections was argued for within the rich traveling wave dynamics of this system (recall that conjugate states are necessary but not sufficient for such a connection for arbitrary Hamiltonian perturbations).

Among two of the explicit examples we considered, the hyperbolic part of the Hamiltonian was given by a fourth order polynomial in two variables, one exhibiting simple wave preservation: $H = \frac{1}{2}(u(1-u)v^2 + u^2)$, and one not: $H = -\frac{1}{2}v^2 - u^4$. Further work will involve classifying the properties of Hamiltonian shocks for all polynomials of order at most four. In particular, it is not hard to see that if $H(u,v)$ is symmetric in u and v, the Hamiltonian shocks are obtained by switching the two and simple wave preservation holds.

A relationship could be sought between the simple wave preserving property to other paradigms in the study of dispersive perturbations of hyperbolic systems, e.g. solitonic modulation [18, 20] and N-integrability [29, 39]. Another further line of inquiry which we have not pursued is the interaction of two Hamiltonian shocks with one another. The possibility of such an interaction is based purely on algebraic properties of the various branches of the Hamiltonian shock map. In all of the cases we have studied, Hamiltonian shocks have given an accurate representations of kink-continuous wave interactions in a dispersive system. Further testing of the robustness of this representation against various different properties of the dispersive perturbations would require the inclusion of higher order dispersion, which is known to produce non-classical effects [35], or stronger non-linearities in the dispersion which could create asymmetric kink profiles.

Then in chapter 3, we described how initial discontinuities in derivatives evolve over time in hyperbolic systems and have shown that infinite derivatives may persist in a continuous solution if and only if genuine nonlinearity fails where the infinite derivative lies. The former development resolves a conjecture from [15] that a corner propagates along a characteristic if and only if the initial Riemann invariant of the corresponding family has a derivative jump. The resolution is in the affirmative except when $i.$ the corner point is also a critical point for the Riemann invariant and $ii.$ quantities arising from differentiating the eigenvectors are not Lipschitz continuous. In both cases a corner in the initial Riemann invariant is sufficient for corner propagation. A counterexample to the necessity of condition $i.$ was found: a corner which propogates along a characteristic despite the Riemann invariant of the corresponding family having no first derivative jump. In case $ii.$ on the other hand, further analysis would be required.

REFERENCES

[1] S. Zhang, M. H. Alford, and J. B. Mickett, "Characteristics, generation and mass transport of nonlinear internal waves on the w ashington continental shelf," *Journal of Geophysical Research: Oceans*, vol. 120, no. 2, pp. 741–758, 2015.

[2] A. Scotti, R. C. Beardsley, B. Butman, and J. Pineda, "Shoaling of nonlinear internal waves in massachusetts bay," *Journal of Geophysical Research: Oceans*, vol. 113, no. C8, 2008.

[3] A. Scotti and J. Pineda, "Observation of very large and steep internal waves of elevation near the massachusetts coast," *Geophysical Research Letters*, vol. 31, 2004.

[4] A. Bertrand, D. Grados, F. Colas, S. Bertrand, X. Capet, A. Chaigneau, G. Vargas, A. Mousseigne, and R. Fablet, "Broad impacts of fine-scale dynamics on seascape structure from zooplankton to seabirds," *Nature communications*, vol. 5, no. 1, pp. 1–9, 2014.

[5] M. Funakoshi and M. Oikawa, "Long internal waves of large amplitude in a two-layer fluid," *Journal of the Physical Society of Japan*, vol. 55, pp. 128–144, 1986.

[6] K. G. Lamb and B. Wan, "Conjugate flows and flat solitary waves for a continuously stratified fluid," *Physics of Fluids*, vol. 10, no. 8, pp. 2061–2079, 1998.

[7] W. Choi and R. Camassa, "Weakly nonlinear internal waves in a two-fluid system," *Journal of Fluid Mechanics*, vol. 313, pp. 83–103, 1996.

[8] A. Kluwick, S. Scheichl, and E. A. Cox, "Near-critical hydraulic flows in two-layer fluids," *Journal of Fluid Mechanics*, vol. 575, pp. 187–219, 2007.

[9] S. Benzoni-Gavage, "Linear stability of propagating phase boundaries in capillary fluids," *Physica D: Nonlinear Phenomena*, vol. 155, no. 3-4, pp. 235–273, 2001.

[10] P. LeFloch, *Hyperbolic Systems of Conservation Laws: The Theory of Classical and Nonclassical Shock Waves*. Lectures in Mathematics. ETH Zürich, Birkhäuser Basel, 2002.

[11] A. Gurevich and L. Pitayevsky, "Nonstationary structure of a collisionless shock wave," *Journal of Experimental and Theoretical Physics*, vol. 38, no. 3, pp. 291–297, 1973.

[12] G. Whitham and M. J. Lighthill, "Non-linear dispersive waves," *Proceedings of the Royal Society of London. Series A. Mathematical and Physical Sciences*, vol. 283, no. 1393, pp. 238–261, 1965.

[13] G. B. Whitham, *Linear and Nonlinear Waves*. John Wiley & Sons, Ltd, 1999.

[14] R. Camassa, G. Falqui, G. Ortenzi, M. Pedroni, and G. Pitton, "Singularity formation as a wetting mechanism in a dispersionless water wave model," *Nonlinearity*, vol. 32, pp. 4079–4116, sep 2019.

[15] R. Camassa, G. Falqui, G. Ortenzi, M. Pedroni, and C. Thomson, "Hydrodynamic Models and Confinement Effects by Horizontal Boundaries," *Journal of Nonlinear Science*, vol. 29, no. 4, pp. 1445–1498, 2019.

[16] R. Camassa, G. Falqui, G. Ortenzi, M. Pedroni, and G. Pitton, "On the "vacuum" dam-break problem: Exact solutions and their long time asymptotics," *SIAM J. Appl. Math.*, vol. 80, pp. 44–70, 2020.

[17] J. G. Esler and J. D. Pearce, "Dispersive dam-break and lock-exchange flows in a two-layer fluid," *Journal of Fluid Mechanics*, vol. 667, pp. 555–585, 2011.

[18] G. A. El, M. A. Hoefer, and M. Shearer, "Dispersive and diffusive-dispersive shock waves for nonconvex conservation laws," *SIAM Review*, vol. 59, no. 1, pp. 3–61, 2017.

[19] A. M. Kamchatnov, Y.-H. Kuo, T.-C. Lin, T.-L. Horng, S.-C. Gou, R. Clift, G. A. El, and R. H. J. Grimshaw, "Undular bore theory for the gardner equation," *Phys. Rev. E*, vol. 86, p. 036605, Sep 2012.

[20] K. van der Sande, G. A. El, and M. A. Hoefer, "Dynamic soliton–mean flow interaction with non-convex flux," *Journal of Fluid Mechanics*, vol. 928, p. A21, 2021.

[21] W. Melville and K. R. Helfrich, "Transcritical two-layer flow over topography," *Journal of Fluid Mechanics*, vol. 178, pp. 31–52, 1987.

[22] S. Benzoni-Gavage, R. Danchin, S. Descombes, and D. Jamet, "On korteweg models for fluids exhibiting phase changes," in *Proceedings of 10th International Conference on Hyperbolic Problems, Osaka, Yokohama Publishers*, 2004.

[23] M. Shearer, D. G. Schaeffer, D. Marchesin, and P. L. Paes-Leme, "Solution of the riemann problem for a prototype 2x2 system of non-strictly hyperbolic conservation laws," *Archive for Rational Mechanics and Analysis*, vol. 97, no. 4, pp. 299–320, 1987.

[24] M. R. Schulze and M. Shearer, "Undercompressive shocks for a system of hyperbolic conservation laws with cubic nonlinearity," *Journal of Mathematical Analysis and Applications*, vol. 229, p. 334, 1999.

[25] A. L. Bertozzi, A. Münch, and M. Shearer, "Undercompressive shocks in thin film flows," *Physica D: Nonlinear Phenomena*, vol. 134, no. 4, pp. 431–464, 1999.

[26] S. P. Tsarev, "The geometry of hamiltonian systems of hydrodynamic type. the generalized hodograph method," *Mathematics of the USSR-Izvestiya*, vol. 37, pp. 397–419, apr 1991.

[27] P. D. Lax, "Hyperbolic systems of conservation laws ii," *Communications on Pure and Applied Mathematics*, vol. 10, no. 4, pp. 537–566, 1957.

[28] P. D. Lax, *1. Hyperbolic Systems of Conservation Laws and the Mathematical Theory of Shock Waves*, pp. 1–48. Society for Industrial and Applied Mathematics, 1973.

[29] B. Dubrovin, "Hamiltonian pdes: deformations, integrability, solutions," *Journal of Physics A: Mathematical and Theoretical*, vol. 43, no. 43, p. 434002, 2010.

[30] S. Bianchini and A. Bressan, "Vanishing viscocity solutions to nonlinear hyperbolic systems," *Annals of mathematics*, vol. 161, no. 1, pp. 223–342, 2005.

[31] P. Le Floch, "Shock waves for nonlinear hyperbolic systems in nonconservative form." 1989.

[32] P. D. Lax and C. David Levermore, "The small dispersion limit of the korteweg-de vries equation. i," *Communications on Pure and Applied Mathematics*, vol. 36, no. 3, pp. 253–290, 1983.

[33] S. Venakides, "The zero dispersion limit of the korteweg-de vries equation for initial potentials with non-trivial reflection coefficient," *Communications on Pure and Applied Mathematics*, vol. 38, no. 2, pp. 125–155, 1985.

[34] G. A. El, "Resolution of a shock in hyperbolic systems modified by weak dispersion," *Chaos: An Interdisciplinary Journal of Nonlinear Science*, vol. 15, no. 3, p. 037103, 2005.

[35] M. A. Hoefer, N. F. Smyth, and P. Sprenger, "Modulation theory solution for nonlinearly resonant, fifth-order korteweg–de vries, nonclassical, traveling dispersive shock waves," *Studies in Applied Mathematics*, vol. 142, no. 3, pp. 219–240, 2019.

[36] L. V. Ovsyannikov, "Two-layer "Shallow water" model," *Journal of Applied Mechanics and Technical Physics*, vol. 20, no. 2, pp. 127–135, 1979.

[37] P. D. Lax, "Development of singularities of solutions of nonlinear hyperbolic partial differential equations," *Journal of Mathematical Physics*, vol. 5, no. 5, pp. 611–613, 1964.

[38] J. L. JOHNSON, *Global continuous solutions of hyperbolic systems of quasi-linear equations*. University of Michigan, 1967.

[39] B. Dubrovin, *Hamiltonian perturbations of hyperbolic PDEs: from classification results to the properties of solutions*, pp. 231–276. Springer, 2009.

[40] T. . B. . Benjamin and S. . Bowman, "Discontinuous solutions of one-dimensional hamiltonian systems," *Proceedings of the Royal Society of London*, vol. 413, no. 1845, pp. 263–295, 1987.

[41] F. Magri, "A simple model of the integrable hamiltonian equation," *Journal of Mathematical Physics*, vol. 19, no. 5, pp. 1156–1162, 1978.

[42] M. Slemrod, "Admissibility criteria for propagating phase boundaries in a van der Waals fluid," *Archive for Rational Mechanics and Analysis*, vol. 81, no. 4, pp. 301–315, 1983.

[43] R. D. James, "The propagation of phase boundaries in elastic bars," *Archive for Rational Mechanics and Analysis*, vol. 73, no. 2, pp. 125–158, 1980.

[44] C. Audiard, "Existence of multi-travelling waves in capillary fluids," *Proceedings.Section A, Mathematics - The Royal Society of Edinburgh*, vol. 150, pp. 2905–2936, 12 2020.

[45] R. Camassa, G. Falqui, and G. Ortenzi, "Two-layer interfacial flows beyond the Boussinesq approximation : a Hamiltonian approach," *Nonlinearity*, vol. 30, pp. 466–491, 2017.

[46] P. Milewski and E. Tabak, "Conservation law modelling of entrainment in layered hydrostatic flows," *Journal of Fluid Mechanics*, vol. 772, pp. 272–294, 2015.

[47] L. Chumakova, F. E. Menzaque, P. A. Milewski, R. R. Rosales, E. G. Tabak, and C. V. Turner, "Stability properties and nonlinear mappings of two and three-layer stratified flows," *Studies in Applied Mathematics*, vol. 122, no. 2, pp. 123–137, 2009.

[48] J. A. Gear and R. Grimshaw, "A second-order theory for solitary waves in shallow fluids," *The Physics of Fluids*, vol. 26, no. 1, pp. 14–29, 1983.

[49] A. Boonkasame and P. A. Milewski, "A model for strongly nonlinear long interfacial waves with background shear," *Studies in Applied Mathematics*, vol. 133, no. 2, pp. 182–213, 2014.

[50] B. Fornberg and G. B. Whitham, "A numerical and theoretical study of certain nonlinear wave phenomena," *Philosophical Transactions of the Royal Society of London. Series A, Mathematical and Physical Sciences*, vol. 289, no. 1361, pp. 373–404, 1978.

[51] J. A. Leach and D. J. Needham, "The large-time development of the solution to an initial-value problem for the korteweg–de vries equation: I. initial data has a discontinuous expansive step," *Nonlinearity*, vol. 21, pp. 2391–2408, sep 2008.

[52] T.-P. Liu, "The riemann problem for general 2x2 conservation laws," *Transactions of the American Mathematical Society*, vol. 199, pp. 89–112, 1974.

[53] T.-P. Liu, "The riemann problem for general systems of conservation laws," *Journal of Differential Equations*, vol. 18, no. 1, pp. 218–234, 1975.

[54] P. G. LeFloch and M. D. Thanh, "Nonclassical riemann solvers and kinetic relations i. a nonconvex hyperbolic model of phase transitions," *Zeitschrift für angewandte Mathematik und Physik ZAMP*, vol. 52, no. 4, pp. 597–619, 2001.

[55] C. M. Edwards, S. D. Howison, H. Ockendon, and J. R. Ockendon, "Non-classical shallow water flows," *IMA Journal of Applied Mathematics*, vol. 73, pp. 137–157, 12 2007.

[56] R. Camassa, G. Falqui, G. Ortenzi, M. Pedroni, and G. Pitton, "On the geometry of extended self-similar solutions of the airy shallow water equations," *Symmetry, Integrability and Geometry: Methods and Applications*, vol. 15, 2019.

[57] R. Camassa, G. Falqui, G. Ortenzi, M. Pedroni, and T. Ho, "Hamiltonian aspects of three-layer stratified fluids," *Journal of Nonlinear Science*, vol. 31, no. 4, pp. 1–32, 2021.

[58] F. de Melo Viríssimo and P. A. Milewski, "Three-layer flows in the shallow water limit," *Studies in Applied Mathematics*, vol. 142, no. 4, pp. 487–512, 2019.

[59] A. Doak, R. Barros, and P. A. Milewski, "Large mode-2 internal solitary waves in three-layer flows," *arXiv preprint arXiv:2205.00503*, 2022.

[60] J. A. Smoller and J. L. Johnson, "Global solutions for an extended class of hyperbolic systems of conservation laws," *Archive for Rational Mechanics and Analysis*, vol. 32, no. 3, pp. 169–189, 1969.

[61] J. A. Smoller, *Shock Waves and Reaction-Diffusion Equations*. Springer, 1983.

[62] L. Ding, R. Hunt, R. M. McLaughlin, and H. Woodie, "Enhanced diffusivity and skewness of a diffusing tracer in the presence of an oscillating wall," *Research in the Mathematical Sciences*, vol. 8, no. 3, pp. 1–29, 2021.

[63] L. Ding and R. M. McLaughlin, "Determinism and invariant measures for diffusing passive scalars advected by unsteady random shear flows," *Physical Review Fluids*, vol. 7, no. 7, p. 074502, 2022.

[64] L. Ding, *Scalar Transport and Mixing*. PhD thesis, University of North Carolina at Chapel Hill, 2022.

[65] J. P. Boyd, *Chebyshev and Fourier spectral methods*. Courier Corporation, 2001.

APPENDIX A

HYPERBOLIC QUASILINEAR SYSTEMS

We review the elements of the theory of quasilinear hyperbolic systems. A quasilinear hyperbolic system in one space dimension is a system of PDEs

$$\boldsymbol{U}_t + A(\boldsymbol{U})\boldsymbol{U}_x = 0 \tag{A.1}$$

where $\boldsymbol{U}$ is a vector valued function of one space variable x and time $t > 0$: $\boldsymbol{U} : \mathbb{R} \times \mathbb{R}^+ \to \mathbb{R}^n$, and A is an $n \times n$ matrix valued function of $\boldsymbol{U}$ which is assumed to have real and distinct eigenvalues $\lambda_1 < \lambda_2 < ... < \lambda_n$. In contrast, when $A(\boldsymbol{U})$ has real eigenvalues but is not diagonalizable (A.1) is referred to as parabolic, and when any of the eigenvalues are imaginary it is referred to as elliptic. When A is the differential of a vector valued function $\boldsymbol{F}$:

$$A_{ij} = \frac{\partial f_i}{\partial u_j}, \tag{A.2}$$

$$A(\boldsymbol{U}) = D\boldsymbol{F}(\boldsymbol{U}), \tag{A.3}$$

equation (A.1) can be written in *conservation form*

$$\partial_t \boldsymbol{U} + \partial_x\big(\boldsymbol{F}(\boldsymbol{U})\big) = 0. \tag{A.4}$$

In this case we may also consider weak solutions: possibly non-smooth or even discontinuous functions satisfying

$$-\int_0^\infty \int_{-\infty}^\infty (\partial_t \phi)\boldsymbol{U} + (\partial_x \phi)\big(\boldsymbol{F}(\boldsymbol{U})\big)dxdt - \int_{-\infty}^\infty \boldsymbol{U}(x,0)\phi(x,0)dx = 0 \tag{A.5}$$

for any ϕ infinitely differentiable and compactly supported. (A.5) reduces to (A.4) when $\boldsymbol{U}$ is differentiable.

A Riemann problem is an initial value problem for (A.5) with initial data of the form

$$\boldsymbol{U}(x,0) = \boldsymbol{U}_0(x) = \begin{cases} \boldsymbol{U}_l, & x < 0 \\ \boldsymbol{U}_r, & x > 0. \end{cases} \tag{A.6}$$

If $\boldsymbol{U}(x,t)$ is continuous except across a moving point $x = \mathfrak{s}(t)$, (A.5) is expressed at this point by the conditions

$$s(\boldsymbol{U}_r - \boldsymbol{U}_l) + (\boldsymbol{F}_r - \boldsymbol{F}_l) = 0, \tag{A.7}$$

$s = \mathfrak{s}'(t)$, known as the Rankine-Hugoniot conditions, where the subscripts r and l denote evaluation of the left and right limits of the quantities at $\mathfrak{s}(t)$:

$$\boldsymbol{U}_l = \lim_{x \to {}^-\mathfrak{s}(t)} \boldsymbol{U}(x,t), \tag{A.8}$$

$$\boldsymbol{U}_r = \lim_{x \to {}^+\mathfrak{s}(t)} \boldsymbol{U}(x,t). \tag{A.9}$$

Following [27], the building blocks of the solution to (A.6) are known as k-waves. These are a special set of curves $\boldsymbol{W}_k(\xi_k; \boldsymbol{U}_l)$ in the space of dependent variables defined as follows: for $\xi_k \geq \lambda_k(\boldsymbol{U}_l)$, $\boldsymbol{W}_k$ is an integral curve of $\boldsymbol{r}_k$, i.e.

$$\frac{d}{d\xi_k} \boldsymbol{W}_k(\xi_k; \boldsymbol{U}_l) = \boldsymbol{r}_k(\boldsymbol{W}_k(\xi_k; \boldsymbol{U}_l)), \tag{A.10}$$

with $\xi_k = \lambda_k(\boldsymbol{W}_k(\xi_k; \boldsymbol{U}_l))$, while for some $\delta_k > 0$, $\lambda_k(\boldsymbol{U}_l) - \delta_k < \xi_k < \lambda_k(\boldsymbol{U}_l)$, $\boldsymbol{W}_k$ is defined implicitly by (A.7):

$$\boldsymbol{F}(\boldsymbol{W}_k(\xi_k; \boldsymbol{U}_l)) - \boldsymbol{F}(\boldsymbol{U}_l) = s_k(\xi_k)(\boldsymbol{W}_k(\xi_k; \boldsymbol{U}_l) - \boldsymbol{U}_l). \tag{A.11}$$

The resulting singular 1-manifold is sometimes referred to as the Hugoniot locus. This also defines s_k implicitly and it is shown in [27] that the choice

$$s_k(\lambda_k(\boldsymbol{U}_l)) = \lambda_k(\boldsymbol{U}_l) \tag{A.12}$$

makes $\boldsymbol{W}_k(\xi_k; \boldsymbol{U}_l)$ twice differentiable at $\xi_k = \lambda_k$.

A solution to (A.5)-(A.6) with $\boldsymbol{U}_r = \boldsymbol{W}_k(\xi_k; \boldsymbol{U}_l)$ is, for $\xi_k > \lambda_k(\boldsymbol{U}_l)$:

$$\boldsymbol{U}_k(x,t; \boldsymbol{U}_l, \boldsymbol{U}_r) = \begin{cases} \boldsymbol{U}_l, & x/t \leq \lambda_k(\boldsymbol{U}_l) \\ \boldsymbol{W}_k(x/t; \boldsymbol{U}_l), & \lambda_k(\boldsymbol{U}_l) < x/t < \lambda_k(\boldsymbol{U}_r) \\ \boldsymbol{U}_r, & x/t \geq \lambda_k(\boldsymbol{U}_r), \end{cases} \tag{A.13}$$

or for $\xi_k < \lambda_k(\boldsymbol{U}_l)$:

$$\boldsymbol{U}_k(x,t;\boldsymbol{U}_l,\boldsymbol{U}_r) = \begin{cases} \boldsymbol{U}_l, & x/t < s_k(\xi_k) \\ \boldsymbol{U}_r, & x/t > s_k(\xi_k). \end{cases} \tag{A.14}$$

i.e. a discontinuous (shock) solution to (A.5)-(A.6).

In [27] a solution to (A.5)-(A.6) is constructed for any $\boldsymbol{U}_r$ that can be reached by gluing together consecutive $\boldsymbol{W}_k$ curves, $k = 1, 2, 3, ..., n$:

$$\boldsymbol{U}_r = \boldsymbol{W}_k(\xi_k; \boldsymbol{W}_{k-1}(\xi_{k-1}; (...(\boldsymbol{W}_1(\xi_1; \boldsymbol{U}_l))...))), \tag{A.15}$$

it is given by

$$\boldsymbol{U}(x,t) = \boldsymbol{U}_k(x,t;\boldsymbol{U}_r^{k-1},\boldsymbol{U}_r^k), \quad \zeta_{k-1}(\xi_{k-1}) \le \frac{x}{t} \le \zeta_k(\xi_k), \quad 1 \le k \le n \tag{A.16}$$

where

$$\boldsymbol{U}_r^0 = \boldsymbol{U}_l, \quad \boldsymbol{U}_r^j = \boldsymbol{W}_j(\xi_j; \boldsymbol{U}_r^{j-1}) \tag{A.17}$$

and

$$\zeta_j(\xi_j) = \begin{cases} \xi_j, & \xi_j \ge \lambda_j(\boldsymbol{U}_r^{j-1}) \\ s_j(\xi_j), & \xi_j < \lambda_j(\boldsymbol{U}_r^{j-1}). \end{cases} \tag{A.18}$$

Let Ω be the set $\boldsymbol{U}_r$ thus reachable from $\boldsymbol{U}_l$ (see [27]). Then $\boldsymbol{U}_l$ is an interior point of Ω so a solution to the Riemann problem (A.6) can be constructed for any $\boldsymbol{U}_r$ sufficiently close to $\boldsymbol{U}_l$. This solution is shown to be unique within the class satisfying the following inequalities for $\xi_k < \lambda_k(\boldsymbol{U}_l)$ (known as the Lax entropy inequalities)

$$\lambda_k(\boldsymbol{U}_r^k))) < s_k(\xi_k) < \lambda_k(\boldsymbol{U}_r^{k-1})), \tag{A.19}$$

and

$$\lambda_{k-1}(\boldsymbol{U}_r^{k-1})) < s_k(\xi_k) < \lambda_{k+1}(\boldsymbol{U}_r^k). \tag{A.20}$$

The first inequality holds for $\boldsymbol{W}_k$ by construction when ξ_k is close enough to λ_k and insisting that it hold on the full domain of $\boldsymbol{W}_k$ amounts to a restriction on δ_k. It also prevents the possibility that a k-shock and a k-rarefaction could coexist, i.e., that multiple admissible solutions could be found by

gluing together two $\boldsymbol{W}_k$ curves choosing the parameter ξ_k to have $\xi_k - \lambda_k$ first negative then positive or vice-versa to connect the same left and right states $\boldsymbol{U}_l$ and $\boldsymbol{U}_r$ by distinct centered solutions. The second set of inqualities ensures that the $\boldsymbol{U} = \boldsymbol{U}_{k-1}$ wedge of the solution falls to the left of the $\boldsymbol{U}_k$ segment which in turn falls to the left of the $\boldsymbol{U}_{k+1}$ wedge.

Some extensions of these results exist to larger neighborhoods from which $\boldsymbol{U}_r$ can be taken, see for [60] for a class of examples. This method of solution is also extended (see e.g. [61]) to the case of linear degeneracy, where

$$\nabla \lambda_k \cdot \boldsymbol{r}_k \equiv 0 \tag{A.21}$$

for some k and the result is a solution of (A.7) with $s_k = \lambda_k$, called a contact discontinuity.

Finally, we recall that a Riemann invariant (see e.g. [13]) is a function ϕ_k whose gradient is a left eigenvector $\boldsymbol{l}_k$ of $B\nabla^2 H$ corresponding to λ_k:

$$\nabla \phi_k(\boldsymbol{U})^T A(\boldsymbol{U}) = \lambda_k(\boldsymbol{U}) \nabla \phi_k(\boldsymbol{U}) \tag{A.22}$$

which are not guaranteed to exist for $n > 2$.

APPENDIX B

NUMERICAL METHODS (LINGYUN DING)

We document the details of the numerical methods. The (pseudo) Fourier spectral method is one of the efficient methods for the simulation the domains with regular geometries [17, 62, 63, 64]. In this method, all functions are approximated by the Fourier series. Therefore, the derivative acts as multiplication in the spectral space. The nonlinear terms are efficiently calculated by Fast Fourier transform (FFT) based convolution. We refer the reader to the textbook [65] for more details.

We approximate the infinite interval by the finite interval $x \in [L, L]$ with a large number L which depends on the traveling wave speed and the final time of the simulation. The solutions of equations discussed in this section usually tend to different constants at infinity. Applying Fourier series approximation to this non-periodic solution could yield a serious Gibbs phenomenon. To alleviate the approximation error, we consider an even extension of the computational domain.

We adopt the explicit 4th-order Runge-Kutta method as the time-marching scheme. In the dealiasing process at each time step, we apply the all-or-nothing filter with the two-thirds rule to the spectrum, that is, we set the upper one-third of the resolved spectrum to zero.

The inversion of the operator $\mathcal{L}$ provided in equation (2.255) is calculated via the generalized minimal residual method (GMRES). At each time step, we choose the solution value at the previous time step as the initial guess of GMRES.

The typical number of grid points is $2^{15} + 1$ before the even extension and 2^{16} after the even extension. The spatial grid size is around 0.0192, and the time step size is around 0.003. We verified that all numerical results were not sensitive to an increase in either spatial or temporal resolution. The relative error measured by the mesh refinement test is at the order of 10^{-4}.

APPENDIX C

UNDERCOMPRESSIVITY

we recall that the definition of an undercompressive shock, is a steplike solution (A.14) with left and right states satisfying (A.11) but failing to satisfy (A.19) and (A.20), and instead satisfying, for each characteristic family, either

$$\lambda_k(\boldsymbol{U}_l), \lambda_k(\boldsymbol{U}_r) < s_k \tag{C.1}$$

or

$$s_k < \lambda_k(\boldsymbol{U}_l), \lambda_k(\boldsymbol{U}_r). \tag{C.2}$$

Taking the determinant of (2.133) with $G = H$ gives

$$\det Y_r \det J\prod_{j=1}^{n}(\lambda_j^l - s) = \det Y_l\prod_{j=1}^{n}(\lambda_j^r - s). \tag{C.3}$$

We consider the case where J is negative. This holds in all the examples we have considered, thanks to the fact that the Hamiltonian shock map behaves like a reflection near a fixed curve in cast of a 2×2 system and likewise near a fixed point for a scalar equation. It can be seen by considering how Y_l and Y_r act by left multiplication on an orthonormal basis containing $\frac{[\boldsymbol{U}]^T}{\|[\boldsymbol{U}]\|}$, that both have eigenvalue $[\frac{1}{2}\boldsymbol{U}^T B^{-1}\boldsymbol{U}]$ with multiplicity $n - 1$ and the remaining eigenvalue is either $[\frac{1}{2}\boldsymbol{U}]^T B^{-1}[\boldsymbol{U}]$ or $-[\frac{1}{2}\boldsymbol{U}]^T B^{-1}[\boldsymbol{U}]$, respectively. The impulse $[\frac{1}{2}\boldsymbol{U}^T B^{-1}\boldsymbol{U}]$ can be assured not to vanish by making a constant shift (see section 2.3.2) and $\frac{1}{2}[\boldsymbol{U}]^T B^{-1}[\boldsymbol{U}] = \frac{1}{2s}[\boldsymbol{U}]^T[\nabla H]$, the vanishing of which violates convexity. To see this, we recall that convexity implies

$$H(\boldsymbol{U}_r) < H(\boldsymbol{U}_l) + \nabla H(U_l) \cdot (\boldsymbol{U}_r - \boldsymbol{U}_l), \tag{C.4}$$

$$H(\boldsymbol{U}_l) < H(\boldsymbol{U}_r) + \nabla H(U_r) \cdot (\boldsymbol{U}_l - \boldsymbol{U}_r) \tag{C.5}$$

and if $[\frac{1}{2}\boldsymbol{U}]^T[\nabla H] = 0$ we may substitute

$$\nabla H(U_r) \cdot (\boldsymbol{U}_l - \boldsymbol{U}_r) = -\nabla H(U_l) \cdot (\boldsymbol{U}_r - \boldsymbol{U}_l) \tag{C.6}$$

into (C.5) and add to (C.4) to obtain

$$H(\boldsymbol{U}_l) + H(\boldsymbol{U}_r) < H(\boldsymbol{U}_l) + H(\boldsymbol{U}_r) \tag{C.7}$$

which is a contradiction. Therefore

$$\frac{\det Y_r \det J}{\det Y_l} > 0 \tag{C.8}$$

which, together with (C.3), implies that

$$\mathrm{sgn}\,\Pi_{j=1}^n(\lambda_j^l - s) = \mathrm{sgn}\,\Pi_{j=1}^n(\lambda_j^r - s). \tag{C.9}$$

This shows that since $\lambda_k^l \leq s < \lambda_{k+1}^l$ and $\lambda_k^r \leq s < \lambda_{k+1}^r$ for some k at any point $\boldsymbol{U}_l = \boldsymbol{U}_0$ at a fixed point of $\tilde{\boldsymbol{U}}$, it must also hold on a neighborhood thereof.

APPENDIX D

CLASSICAL UNDERCOMPRESSIVE CASE

The construction of section 2.2.4 can be used to provide insight into solutions with evolving classical undercompressive shock fronts. The kinetic condition relating admissible pairs U_l and U_r is not symmetric in this case as it is for Hamiltonian shocks and thus the exact argument made above for loss of regularity following a failure of $\tilde{U}$ to preserve simple waves does not quite work. However, when the kinetic relation is a perturbation of $U_r = \tilde{U}(U_l)$ (see e.g. [10]), the regularity loss will carry over from the non-dissipative case, at least for small perturbations.

We give an explicit demonstration of the regularity maintenance for a classical undercompressive shock interacting with a continuous wave for a scalar law in the case of a cubic flux. The admissible undercompressive shocks are parametrized by β which controls the ratio of the dispersive terms to the dissipative terms: $\beta = \frac{\alpha}{\sqrt{54}}$, where the weakly dispersive-dissipative regularized system is given by

$$u_t + u^2 u - \epsilon \alpha u_{xx} - \epsilon^2 u_{xxx} = 0. \tag{D.1}$$

The parametrization of admissible undercompressive-shock-jumps is given by

$$u_r = \begin{cases} -u_l - \beta, & u_l \leq -2\beta \\ -u_l/2, & u_l \leq |2\beta| \\ -u_l + \beta, & u_l \geq 2\beta. \end{cases} \tag{D.2}$$

We consider the third case. Then the shock speed is given by

$$s = \frac{[u^3/3]}{[u]} = \frac{1}{3}(u_l^2 - \beta u_l + \beta^2). \tag{D.3}$$

Again, for a shock moving through a centered expansion wave, $u(x,t) = \sqrt{x/t}$, we have an ODE,

$$\mathfrak{s}'(t) = \frac{1}{3}(u(\mathfrak{s}(t),t)^2 - \beta u(\mathfrak{s}(t),t) + \beta^2) \tag{D.4}$$

and a convenient change of variable is to u, which has

$$u'(t) = \frac{-1}{2t}u(t) + \frac{1}{2}\sqrt{\frac{1}{t\mathfrak{s}(t)}}\mathfrak{s}'(t) \tag{D.5}$$

$$= \frac{1}{2t}\left(-u(t) + \frac{1}{u(t)}\mathfrak{s}'(t)\right) \tag{D.6}$$

$$= \frac{1}{6u(t)t}(-2u(t)^2 - \beta u(t) + \beta^2). \tag{D.7}$$

We may separate variables:

$$C_1 - \frac{1}{3}\log t = \int \frac{u\,du}{(u+\beta)(u-\beta/2)} \tag{D.8}$$

$$= \frac{1}{3}\int \frac{1}{u-\beta/2} + \frac{2}{u+\beta}du \tag{D.9}$$

for some constant C_1 and we ultimately obtain

$$\frac{C_2}{t} = (u+\beta)^2(u-\beta/2) \tag{D.10}$$

which yields an implicit expression for $\mathfrak{s}(t)$:

$$C_2\sqrt{t} = (\sqrt{\mathfrak{s}(t)} + \beta\sqrt{t})^2(\sqrt{\mathfrak{s}(t)} - \beta/2\sqrt{t}). \tag{D.11}$$

As before, we may fit this into a simple wave solution with constant states on the left and right. Figure D.1 shows this for $\alpha = \frac{1}{2}$, $u_l = 1.1$, $u_m = 2$ which together imply that $u_r = -\frac{3}{2}$. We observe that as the left state approaches the boundary of the piecewise definition (D.2) of an admissible undercompressive shock, $u_l \to 2\beta$, the leftmost characteristic emanating from $\mathfrak{s}(t)$ approaches the outgoing shock curve.

As in the non-dissipative case, the slope of the characteristics exiting from the undercompressive
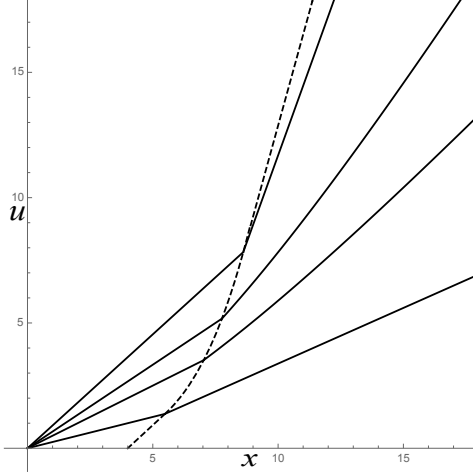
94

Figure D.1: Characteristic diagram for an undercompressive shock moving through a simple wave with $\alpha = \frac{1}{2}$, $u_l = 1.1$, $u_m = 2$.

shock may be computed:

$$\frac{d}{dt}\lambda(u_r) = \frac{d\lambda_r}{du_r}\frac{du_r}{du_l}(\mathfrak{s}'(t)(u_l)_x + (u_l)_t) \tag{D.12}$$

$$= \frac{d\lambda_r}{du_r}\frac{du_r}{du_l}(s - \lambda_l)(u_l)_x \tag{D.13}$$

$$= \frac{d\lambda_r}{du_r}\frac{du_r}{du_l}(s - \lambda_l)\frac{u_0^{c\,\prime}}{1 + t\lambda''(u_0^c)u_0^{c\,\prime}} \tag{D.14}$$

where as before, u_0^c denotes the continuous initial condition before interaction with the undercompressive shock. The same sign considerations apply, namely the continuity of the solution after interacting with the undercompressive shock is ensured by the negativity of $\frac{du_r}{du_l}$ and the property that $\frac{d\lambda_r}{du_r}$ has the opposite sign of $\frac{d\lambda_l}{du_l}$.